NUREG/CR–4819
ORNL/TM–12038
Vol. 2

Aging and Service Wear of Solenoid-Operated Valves Used in Safety Systems of Nuclear Power Plants

Evaluation of Monitoring Methods

Prepared by
R. C. Kryter

Oak Ridge National Laboratory

Prepared for
U.S. Nuclear Regulatory Commission

AVAILABILITY NOTICE

Availability of Reference Materials Cited in NRC Publications

Most documents cited in NRC publications will be available from one of the following sources:

1. The NRC Public Document Room, 2120 L Street, NW., Lower Level, Washington, DC 20555

2. The Superintendent of Documents, U.S. Government Printing Office, P.O. Box 37082, Washington, DC 20013-7082

3. The National Technical Information Service, Springfield, VA 22161

Although the listing that follows represents the majority of documents cited in NRC publications, it is not intended to be exhaustive.

Referenced documents available for inspection and copying for a fee from the NRC Public Document Room include NRC correspondence and internal NRC memoranda; NRC bulletins, circulars, information notices, inspection and investigation notices; licensee event reports; vendor reports and correspondence; Commission papers; and applicant and licensee documents and correspondence.

The following documents in the NUREG series are available for purchase from the GPO Sales Program: formal NRC staff and contractor reports, NRC-sponsored conference proceedings, international agreement reports, grant publications, and NRC booklets and brochures. Also available are regulatory guides, NRC regulations in the *Code of Federal Regulations*, and *Nuclear Regulatory Commission Issuances*.

Documents available from the National Technical Information Service include NUREG-series reports and technical reports prepared by other Federal agencies and reports prepared by the Atomic Energy Commission, forerunner agency to the Nuclear Regulatory Commission.

Documents available from public and special technical libraries include all open literature items, such as books, journal articles, and transactions. *Federal Register* notices, Federal and State legislation, and congressional reports can usually be obtained from these libraries.

Documents such as theses, dissertations, foreign reports and translations, and non-NRC conference proceedings are available for purchase from the organization sponsoring the publication cited.

Single copies of NRC draft reports are available free, to the extent of supply, upon written request to the Office of Administration, Distribution and Mail Services Section, U.S. Nuclear Regulatory Commission, Washington, DC 20555.

Copies of industry codes and standards used in a substantive manner in the NRC regulatory process are maintained at the NRC Library, 7920 Norfolk Avenue, Bethesda, Maryland, for use by the public. Codes and standards are usually copyrighted and may be purchased from the originating organization or, if they are American National Standards, from the American National Standards Institute, 1430 Broadway, New York, NY 10018.

DISCLAIMER NOTICE

NUREG/CR–4819
ORNL/TM–12038
Vol. 2
RV

Aging and Service Wear of Solenoid-Operated Valves Used in Safety Systems of Nuclear Power Plants

Evaluation of Monitoring Methods

Manuscript Completed: September 1991
Date Published: July 1992

Prepared by
R. C. Kryter

Oak Ridge National Laboratory
Managed by Martin Marietta Energy Systems, Inc.

Oak Ridge National Laboratory
Oak Ridge, TN 37831–6285

Prepared for
Division of Engineering
Office of Nuclear Regulatory Research
U.S. Nuclear Regulatory Commission
Washington, DC 20555
NRC FIN B0828
Under Contract No. DE–AC05–84OR21400

ABSTRACT

Solenoid-operated valves (SOVs) were studied at Oak Ridge National Laboratory as part of the U.S. Nuclear Regulatory Commission Nuclear Plant Aging Research (NPAR) Program. The primary objective of the study was to identify, evaluate, and recommend methods for inspection, surveillance, monitoring, and maintenance of SOVs that can help ensure their operational readiness—that is, their ability to perform required safety functions under all anticipated operating conditions—because, under certain circumstances, failure of one of these small and relatively inexpensive devices could have serious consequences.

An earlier (Phase I) NPAR Program study described SOV failure modes and causes and identified measurable parameters thought to be linked to the progress of degradations that may ultimately result in functional failure of the valve. Using this earlier work as a guide, the present (Phase II) study focuses on devising and then demonstrating the effectiveness of performance-measuring techniques and equipment that show promise for detecting and trending the progress of such degradations before they reach a critical stage.

Intrusive techniques requiring the addition of magnetic or acoustic sensors or the application of special test signals were investigated briefly, but major emphasis was placed on the examination of condition-indicating techniques that can be applied with minimal cost and impact on plant operation. These include monitoring coil mean temperature remotely by means of coil dc resistance or ac impedance, determining valve plunger position by means of coil ac impedance, verifying unrestricted SOV plunger movement by measuring current and voltage at their critical bistable (pull-in and dropout) values, and detecting the presence of shorted turns or insulation breakdown within the solenoid coil using interrupted-current test methods. The first of these techniques, though perhaps the simplest conceptually, will probably benefit the nuclear industry most because SOVs have a history of failure in service as a result of unwitting operation at excessive temperatures.

Experimental results are presented that demonstrate the technical feasibility and practicality of the monitoring techniques assessed in the study, and recommendations for further work are provided.

CONTENTS

FIGURES

TABLES

ACKNOWLEDGMENTS

The author wishes to acknowledge the contributions of the following people and organizations, without whose assistance and cooperation this study could not have been done:

- John Shank and Frank Fry of Automatic Switch Company, Florham Park, New Jersey, for helpful discussions regarding solenoid-operated valve (SOV) testing techniques, the loan of two new nuclear-grade SOVs for testing, and the loan of solenoid coils that had developed shorted turns as a result of environmental qualification testing at extreme conditions of temperature and humidity.

- Guy Vacca of Franklin Research Center, Philadelphia, Pennsylvania, for the loan of two naturally aged SOVs.

- Jack McElroy of Philadelphia Electric Company, Conshohocken, Pennsylvania, for helpful discussions regarding acoustic means for verifying proper opening and closing of SOVs and the application of this principle to the monitoring of boiling-water reactor control-rod-drive scram pilot valves.

- Dave Eissenberg of Oak Ridge National Laboratory (ORNL) for encouragement and technical guidance throughout the study, and for constructive criticism of the various technical papers generated as a result of the work.

- Howard Haynes of ORNL for his generous assistance and loan of equipment necessary to acquire and process portions of the data, and for his comradeship throughout the study.

- John Anderson of ORNL for many elucidative discussions concerning measurement and interpretation of the electromagnetic properties of SOV solenoids.

- Bob Shepard of ORNL for the long-term loan of the high-quality impedance analyzer used to ascertain the basic electrical properties of the solenoid coils under study.

- Kathy Sharp, Kathy McIntyre, and Maria Williams of ORNL for expert typing and editing of the manuscript.

Finally, the financial support provided by the Division of Engineering, Office of Nuclear Regulatory Research, U.S. Nuclear Regulatory Commission (NRC), is gratefully acknowledged, along with the patience and personal encouragement of the NRC Technical Monitor, Bill Farmer, throughout the Phase II investigation.

ACRONYMS

AEOD	(Office for) Analysis and Evaluation of Operational Data
ASCO	Automatic Switch Company
BWR	boiling-water reactor
EQ	environmental qualification (test)
IEEE	Institute of Electrical and Electronics Engineers
LWR	light-water reactor
MOV	metal-oxide varistor
NASA	National Aeronautics and Space Administration
NPAR	Nuclear Plant Aging Research (Program)
NPP	nuclear power plant
NRC	Nuclear Regulatory Commission
ORNL	Oak Ridge National Laboratory
PWR	pressurized-water reactor
SOV	solenoid-operated valve

1. BACKGROUND

In the context of this report, "aging" is defined as degradation that occurs with the passage of time. This degradation is associated with the alteration of physical properties brought about by the action of environmental and operational stressors. Aging affects all reactor structures, systems, and components to some degree and may potentially increase the risk to the public health and safety if its effects are not recognized and controlled. Therefore, to ensure continuous safe operation of a nuclear power plant as it ages, measures must be taken to monitor its systems, components, and interfaces in order to detect the presence of degradation and, if necessary, to restore integrity through maintenance, repair, or replacement.

Solenoid-operated valves (SOVs) were studied at Oak Ridge National Laboratory (ORNL) as part of the U.S. Nuclear Regulatory Commission (NRC) Nuclear Plant Aging Research (NPAR) Program, which was established to help resolve technical safety issues related to the aging of electrical and mechanical components, safety systems, support systems, and civil structures used in commercial nuclear power plants. Specifically, the NPAR Program is designed

- to identify and characterize aging effects that, if unchecked, could cause degradation of components, systems, and civil structures and thereby impair plant safety;
- to identify methods of inspection, surveillance, and monitoring that will ensure timely detection of significant aging effects before loss of safety function and also evaluate residual life of components, systems, and civil structures; and
- to evaluate the effectiveness of storage, maintenance, repair, and replacement practices in mitigating the rate and extent of degradation caused by aging.

The current Phase II report is intended to satisfy the second of these three goals.

1.1 Identification of the SOV as a Component for Study

In accordance with NPAR Program strategy, a component, system, or structure is identified for study by considering information from several sources. Criteria used in the selection process include

- the potential risk from failures of components, systems, and structures;
- experience obtained from operating plants;
- surveys of expert opinion; and
- user needs (including the resolution of generic issues, plant performance indicators, and plant maintenance and surveillance).

Information relevant to the selection of the SOV as a component meriting study on the basis of these criteria was developed and is documented in an NPAR Phase I report authored by Bacanskas et al.[1] A short summary of the findings of the Phase I work is given in Subsect. 1.2, but prior to addressing the directions provided by the Phase I study, additional background may be beneficial to the reader.

An SOV is a valve that is opened and closed by an electrically actuated solenoid coil that, in most designs, lifts a plunger to open or close the valve port(s). The process fluid that is thus controlled is most often instrument air, but nitrogen or process water may be encountered in some plant systems. SOVs may be direct-acting (where the solenoid coil provides the motive force for opening and closing the valve) or may be pilot-assisted (where the solenoid coil causes the opening of a pilot orifice, thereby allowing the process fluid to force the main orifice open). Only the direct-acting variety was employed in this study.

SOVs are available in a variety of sizes and constructions, both with and without nuclear qualification, from a number of different manufacturers. SOVs are found throughout nuclear power plants in relatively large numbers, often as a subcomponent of larger, more complex, and clearly safety-related systems such as containment isolation valve actuators, boiling-water-reactor (BWR) control-rod scram systems, and pressurized-water-reactor (PWR) safety injection systems.* A listing of safety- and

*Reference 1 estimates that the population of SOVs used in safety-related systems at U.S. light-water reactors (LWRs) lies between 1000 and 3000 per plant. BWRs generally employ a greater number of SOVs than PWRs.

non-safety-related systems that use SOVs at U.S. light-water reactors includes

- BWR scram;
- reactor coolant pump seal;
- safety injection;
- auxiliary feedwater;
- primary containment isolation;
- high-pressure coolant injection and reactor core isolation cooling;
- high-pressure injection;
- automatic depressurization;
- emergency diesel generator;
- instrument air;
- chemical volume control, charging and letdown, and boration;
- pressurizer control;
- steam generator relief (power-operated relief valves and atmospheric dump valves);
- low-temperature overpressurization protection;
- decay heat removal and residual heat removal;
- component cooling water;
- service water;
- reactor head vent;
- reactor cavity, spent fuel, and fuel handling;
- torus, drywell, vent, and vacuum;
- emergency dc power;
- main steam (main steam isolation valves and auxiliary boiler);
- reactor building and auxiliary building (ventilation and isolation);
- main feedwater; and
- condensate.[2]

They are relatively simple devices (Figure 1.1), with a long history of satisfactory operation in a variety of both nuclear and nonnuclear industrial applications. However, their presence in systems important to safety requires an especially high degree of assurance that they are ready to perform their required function under all anticipated operating conditions, because failure of one of these small and relatively inexpensive devices could have serious consequences under certain circumstances.[3]

For this reason the NRC Office for Analysis and Evaluation of Operational Data (AEOD) has had a continuing interest in SOV performance and failure characteristics and mechanisms and has documented its assessment of the vulnerability of safety-related equipment to common-mode failures or degradations of SOVs in a recently published operating experience feedback report.[2] This study cites over 20 representative operational events in which SOV failures or degradations affected or had the potential to affect multiple safety systems or multiple trains of individual safety systems. Although such common-mode SOV failures and degradations are often beyond the conditions analyzed in plant final safety analysis reports and are not ordinarily modeled explicitly in present-day probabilistic risk assessments, operating experience indicates that such failures and degradations have indeed compromised front-line safety systems in the past[2] and will probably continue to do so in the future. Events in which safety systems have been adversely affected by degradations or failures of SOVs are considered "legitimate precursors to more significant events" by AEOD. The operating experience feedback report notes that SOV problems permeate almost all U.S. nuclear power plants and that they encompass many aspects of the SOV's design, maintenance, and operation. AEOD analysis of operating data indicates that the underlying cause of many SOV failures is the licensees' lack of information or understanding of SOV requirements and capabilities. Compounding the problem is the fact that some SOV manufacturers fail to provide users with adequate guidance regarding proper SOV selection and maintenance.[2] Moreover, most plant technical specifications do not require periodic testing of SOVs per se, although the valves' performances may come into play in the regular exercise of systems and devices covered by technical specification testing requirements.

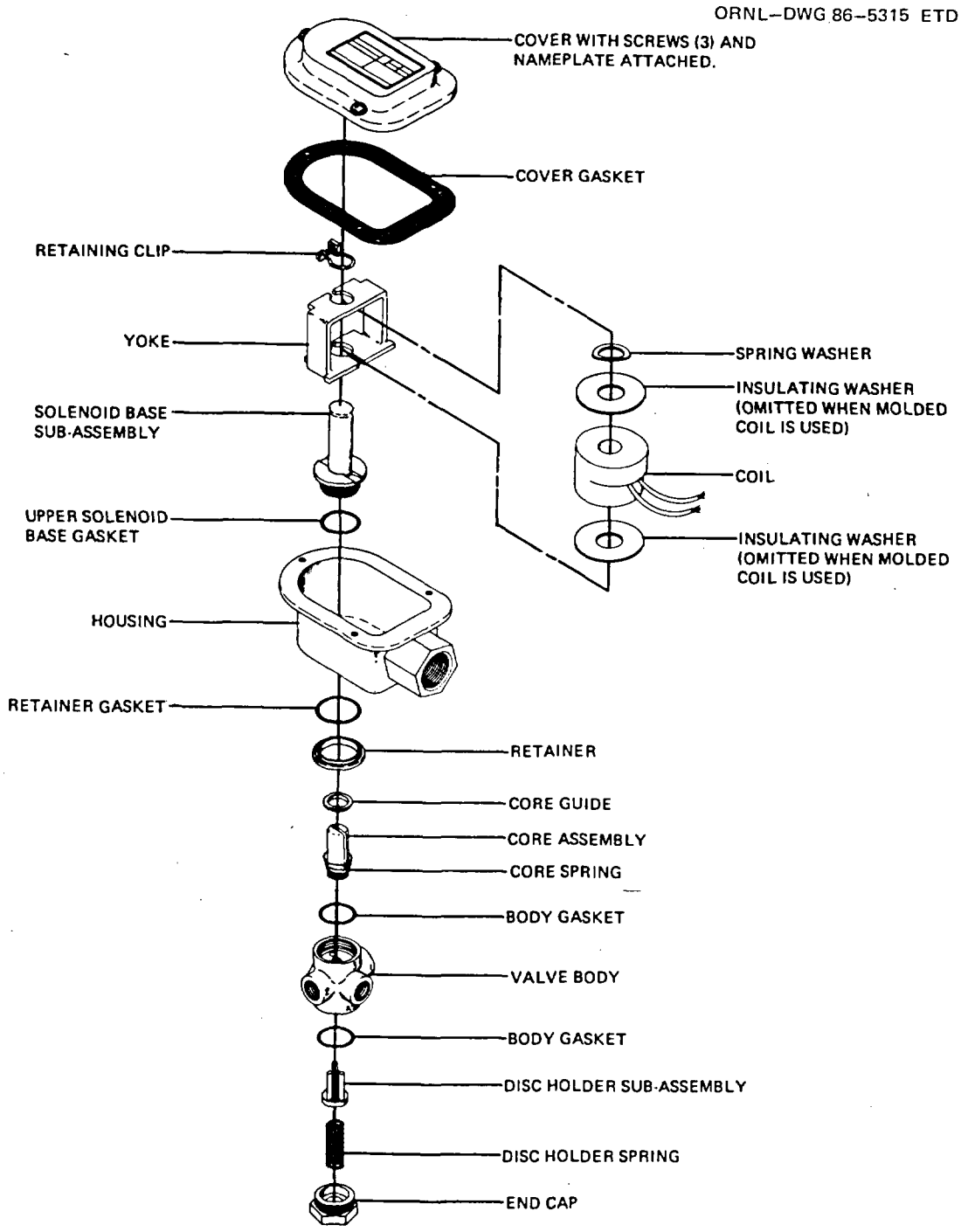

Figure 1.1 Exploded view of a typical enclosed-type, direct-acting, three-way SOV, illustrating relationships of internal parts and positions of the solenoid coil and elastomeric components (i.e., degradation sites). Source: Reprinted with permission from Automatic Switch Company, Bulletin 8320, Florham Park, New Jersey, 1978.

The AEOD report concludes that "... SOV problems represent a significant safety concern," and that "... the SOV problems outlined in this report need to be addressed to ensure that the margins of safety for U.S. LWRs remain at the levels perceived during original plant licensing. Generic and plant-specific actions are needed to correct the SOV problems in order to restore the plants' safety margins to their original perceived values."[4]

The findings and conclusions summarized above—plus continuing occurrences at plants resulting in the issuance over the past few years of some 36 NRC communications alerting licensees to generic problems with SOVs[3]—justify the inclusion of SOVs in the list of components to be studied by the NPAR Program.

1.2 Research Directions and Ideas Drawn from Preceding Reports

The previously referenced Phase I NPAR study described proximate and root causes of SOV failure or malfunction, recognized SOV-aging mechanisms, and listed principal SOV degradation sites (Table 1.1, Figure 1.1).[1] The study also identified measurable indicators of performance (Table 1.2) as well as nonquantitative testing and surveillance methods that might be used to detect the presence of or monitor the progression of various degradations that could ultimately lead to functional failure of the valve.* Those findings and suggestions provided valuable insight and direction for the ensuing Phase II studies reported here. Listed here is a summary of the conclusions of the Phase I study:

- The reported incidence of SOV failure in safety-related applications has been reasonably low.
- The most prevalent causes of SOV failure have been open-circuited coils, short-circuited coils, worn or degraded mechanical parts, and contamination by foreign materials.
- Review of technical literature did not reveal any degradation-monitoring techniques, either in use or under development, that are oriented specifically to SOVs. However, several potentially useful methods were identified.
- SOV failures caused by air system contamination and high dc voltages result from stressors that need to be addressed at the system level rather than at the component (i.e., SOV) level.
- Emphasis should be placed on development of degradation-monitoring techniques for the solenoid coil.
- Considering the large number of SOVs used in nuclear power plants and the low incidence of failure, degradation monitoring on a sampling basis should be considered.
- As required to maintain environmental qualification of safety-related SOVs, periodic replacement of elastomers and solenoid coils also aids in minimizing the incidence of SOV failure.
- Because of the importance of SOVs in controlling equipment such as control-rod drives (in BWRs) and isolation valves (in BWRs and PWRs), SOV failures can initiate unwanted challenges to plant safety systems and can be responsible for unanticipated transients. Development of a methodology for detection of incipient failures will reduce the frequency of these challenges and thereby enhance plant safety and operability.

The second, fourth, and fifth conclusions provided the driving force and direction of the present research, while the third conclusion dictated that the Phase II study would probably be inventive or developmental in nature rather than evaluative.

Specific recommendations of the Bacanskas report were to "... [conduct] research and development to devise test methods suitable for evaluation of the electrical and mechanical portions of SOVs" and to "... test the proposed monitoring techniques with new and used SOVs to evaluate the suitability, cost effectiveness, and practicality of the techniques."[1] Within the budgetary and sponsor-imposed limitations of this segment of the NPAR Program, we have attempted to carry out these two recommendations.*

*The findings summarized in Tables 1.1 and 1.2 are reinforced by similar conclusions reported by an Institute of Electrical and Electronics Engineers (IEEE) task group composed of representatives from utility, consulting, and manufacturing sectors of the nuclear power industry.[5]

*Several naturally aged SOVs were obtained, with the help of Pacific Northwest Laboratory, from the now-decommissioned Shippingport Atomic Power Station (operational from 1957 to 1982), but they were found to be radioactively contaminated to a degree that made their use in this study impractical.

Table 1.1. Aging and malfunction of SOVs—Phase I study findings

Topics of study	Findings
Proximate causes of malfunction	Electrical failure (open- or short-circuited coil) Mechanical failure (valve will not change state) Mechanical binding (sluggish operation)
Root causes of malfunction	Prolonged operation at excessive temperatures High-voltage transients produced by solenoid turnoff Improper choice of valve for operating environment Improper valve installation Lack of maintenance; incorrect replacement of parts Chemical attack of elastomers by oil Contamination by dirt, thread sealant, polymerized lubricants
Degradation sites	Elastomeric components (core seat, seals) Solenoid coil (insulation) Core spring Sliding surfaces
Aging mechanisms	Changes in mechanical and electrical properties of materials Conductor burnout

Source: NUREG/CR–4819, Vol. 1.

Table 1.2. Measurable performance parameters, testing, and surveillance methods identified as potentially useful by the Phase I study

Type	Performance indicators
Quantitative measures	Coil resistance Coil power consumption SOV temperature Valve actuation time Valve flow coefficient, C_v Internal (through-valve) leakage rate Relative level of hum or chattering
Nonquantitative indicators	Visual check: • General appearance of valve exterior • No evidence of accumulated moisture, burned paint, cracked or frayed wiring Aural check: • Absence of buzzing or rattling while in energized state Operational check: • For rapid, smooth change of state • Should be performed at extremes of rated valve pressure range Inspection of internal components: • Not recommended on a periodic basis • Necessary to establish replacement intervals for limited-life components

Source: NUREG/CR–4819, Vol. 1.

2. EVALUATION OF DIAGNOSTIC METHODS APPLICABLE TO SOVs

2.1 General Considerations; Hardware Studied

Any proposal for implementation of surveillance and diagnostics in nuclear power plants must address the issues of practicality and cost-effectiveness. For example, it must be recognized that the SOVs installed in present-day nuclear power plants are uninstrumented and that backfitting them with instrumentation would probably be quite expensive. It is also necessary to understand that many SOVs important to plant safety are inaccessible during plant operation and that some requiring verification of operational readiness will change state only rarely during normal operations, thereby offering little opportunity for measuring SOV dynamic performance parameters. Because of these circumstances, many utilities have elected to periodically replace degradable components or subassemblies within SOVs that are embodied in safety-related systems—that is, to use preventive maintenance—rather than to attempt to practice predictive maintenance using one or more of the approaches listed in Table 1.2.[1] In the extreme, some utilities replace the entire SOV as a precautionary measure at predetermined intervals based on lifetime expectations derived from environmental qualification (EQ) tests, even though no malfunction has been observed.[1,2]

In carrying out these Phase II studies, we chose to view the practical implementation considerations discussed previously as challenges rather than insurmountable obstacles. Therefore, while acknowledging that implementation of diagnostic capabilities must be cost-effective relative to the alternative of SOV replacement, we continued to search for techniques and equipment with which to measure some of the performance parameters identified in the Phase I study and thereby detect and trend the progress of any degradation that might eventually compromise the ability of an SOV to perform its intended function. In recognition of the cost-effectiveness issue, attention was focused on remotely applied, completely nonintrusive techniques (i.e., ones that do not require physical access to the SOV, the addition of sensors or signal wires, the removal of power to the solenoid, or application of a special test signal). However, we found it necessary to depart from these restrictions in order to be able to detect some well-recognized modes of SOV degradation. Clearly, tradeoffs must usually be made between the degree of disruptiveness to plant operations and the amount of information obtained, and this aspect of the surveillance and diagnostic methods investigated here is in need of further attention.

Nine small enclosed-type SOVs from various manufacturers were obtained for use in the study (see Table 2.1 and Figures 2.1–2.3). Three were nuclear-grade valves; one of these ("C") was used, and the others were new. All of the remaining six valves except one ("I") were new. The valve pressure ratings (60 to 2200 psi) are indicative of valve wall thickness and material of construction (i.e., brass or stainless steel), while electrical ratings (115 to 120 Vac or 125 Vdc) are established by solenoid coil construction (i.e., wire gage and number of turns). The nominal power consumption for all nine valves was in the range of 10 to 20 W at rated voltage.

The study began with measurement of every conceivably useful electrical property of an SOV because, in many nuclear plant applications, the solenoid lead wires provide the only available link to the outside world where measurements can be performed. Full details of these fundamental electrical measurements, along with the conclusions and possibilities for monitoring schemes that resulted from thoughtful consideration of each measurable property, are documented in Appendices A through E. However, for the sake of brevity, only a few representative examples are extracted for presentation in the main body of the report, with occasional reference to the appendices for additional detail.

The surveillance or diagnostic techniques studied (summarized in Table 2.2 and described in the following five subsections) were a natural outgrowth of the investigations of fundamental electrical properties of SOVs just described. Each technique was proposed to be specifically responsive to one or more of the proximate or root causes of SOV failure or malfunction cited in Table 1.1. The strengths and weaknesses of each technique as a means for detecting or tracking the progression of age-related degradation were then evaluated. The four techniques receiving the most attention were

- measurement of coil mean temperature during operation by means of in situ measurement of coil electrical dc resistance or ac impedance, combined with an experimentally established temperature coefficient of resistivity for the copper winding (i.e., the same principle as a resistance thermometer);

Table 2.1. Solenoid-operated valves used in this study

Designation	Manufacturer: valve identification	Design power	Comments
A	ASCO NP8320A 185V S/N S14	125 Vdc	Nuclear grade, rated for 115 psi
B	ASCO NP8320A 185V S/N S15	125 Vdc	Nuclear grade, rated for 115 psi
C	ASCO NP8314C29E S/N K-62	125 Vdc	Used; nuclear grade; rated for 60 psi air
D	Skinner V5H30650 CTN	120 Vac	Rated for 150 psi
E	Skinner V5H38880	120 Vac	Rated for 100 psi
F	Skinner (no type number available)	120 Vac	
G	ASCO 8262A214 S/N S94804	115 Vac	Rated for 2200 psi
H	ASCO 8210B26 S/N 91634S	115 Vac	Rated for 350 psi air
I	ASCO HTX831429 S/N 2445A	125 Vdc	Used; rated for 70 psi air

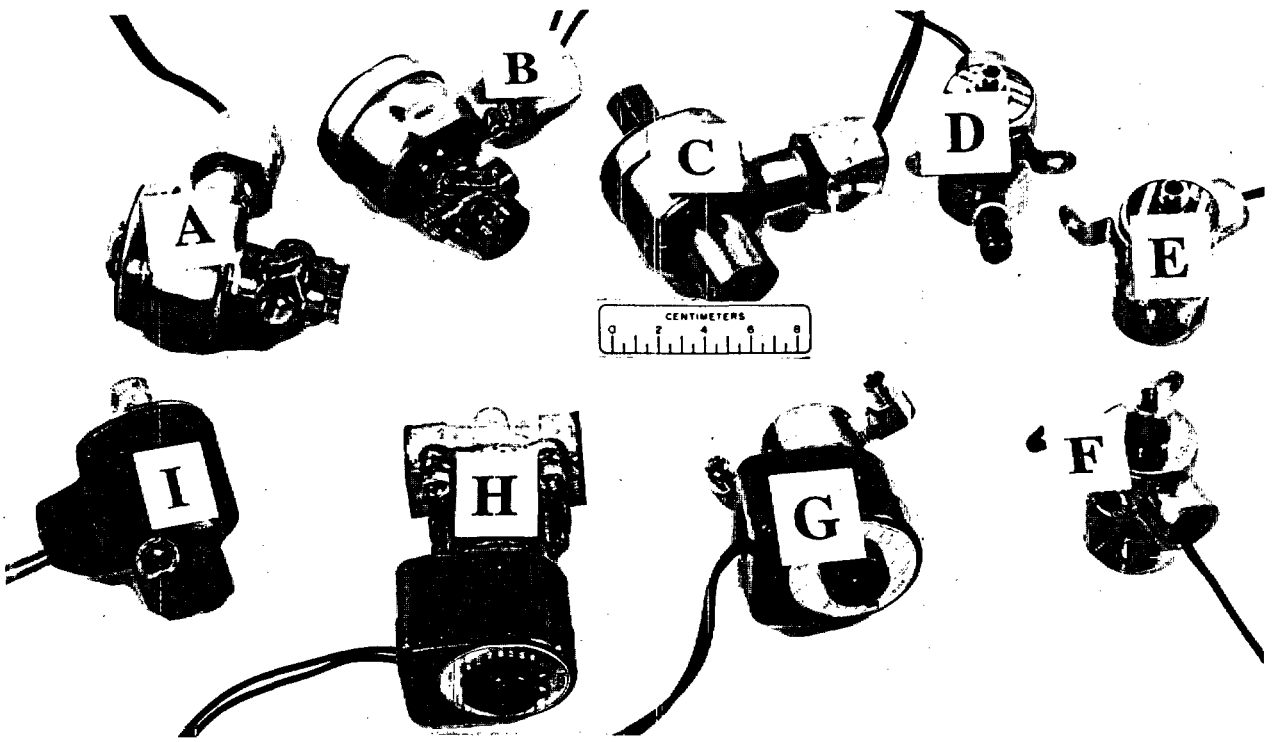

Figure 2.1 The nine SOVs used in this study, fully assembled. (See Table 2.1 for manufacturer and type.)

- indication of plunger movement upon application of ac power, plunger static position within the solenoid coil, and freedom of plunger movement within the guide tube by means of measurement of coil ac impedance (inductance) changes resulting from movement of the iron plunger relative to the coil;
- indication of mechanical binding by tracking changes in the electric current (or voltage) at the SOV critical bistable (pull-in and dropout) points, because these define conditions of balance between electrical (magnetic), spring (restoring), and friction forces within the SOV assembly;

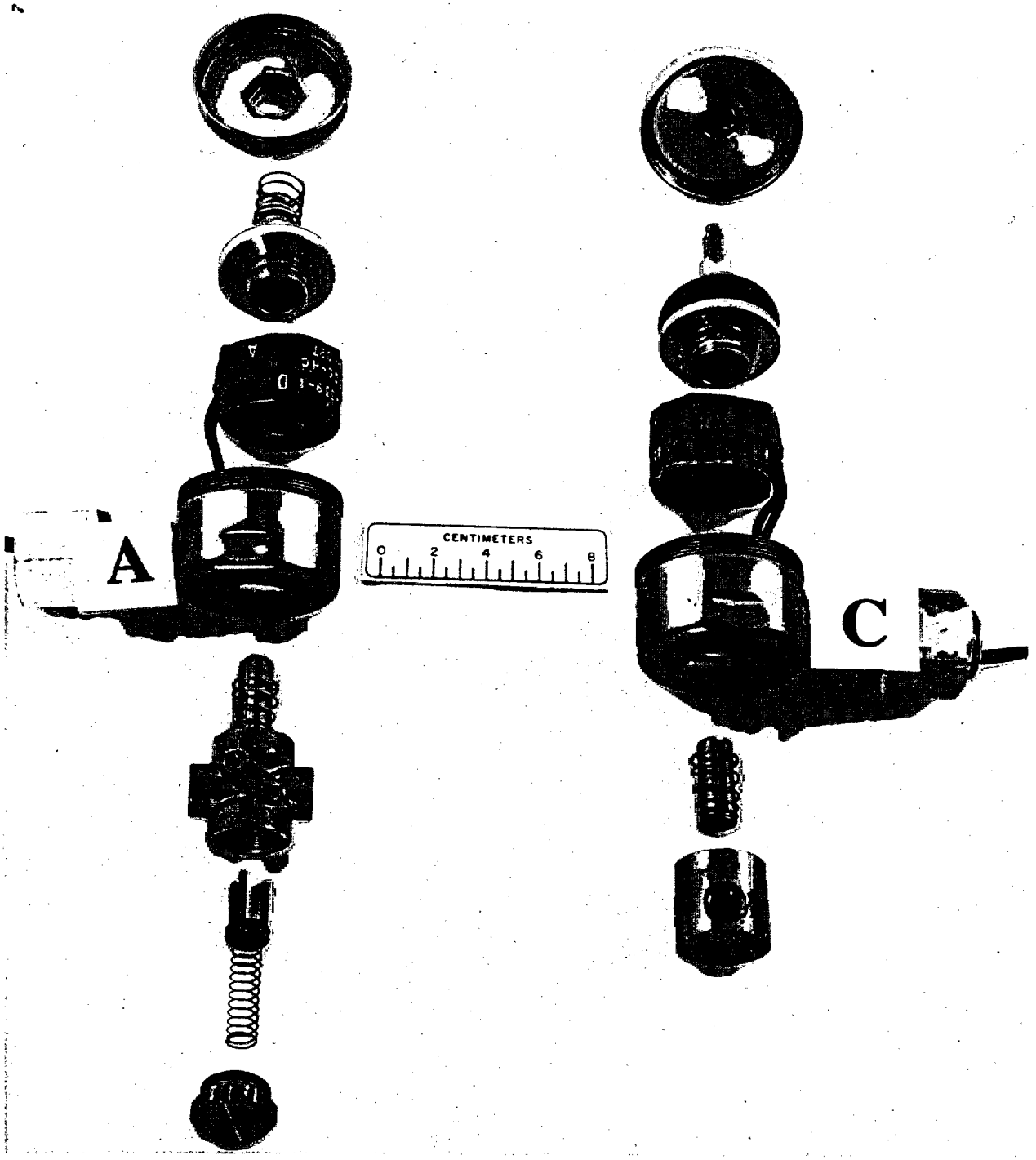

Figure 2.2 Photograph of disassembled SOVs "A" and "C" showing interior parts and differing construction details. (Both are three-way valves, but the placement of the third port is different.)

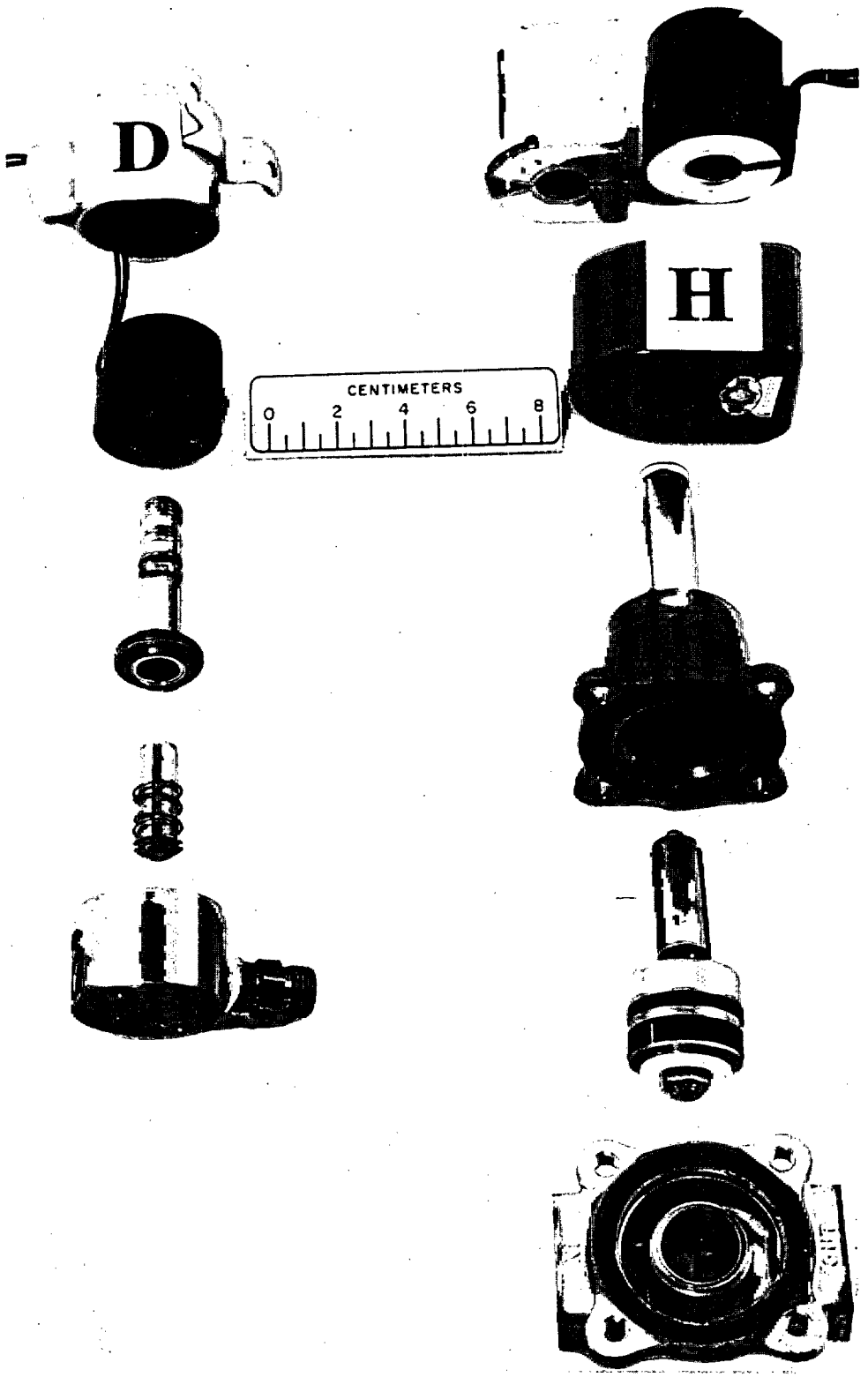

Figure 2.3 Photograph of disassembled SOVs "D" and "H." (These are three-way and two-way valves, respectively.)

Table 2.2. Solenoid-operated valve monitoring methods evaluated in this study

Method	Degradation(s) or malfunction(s) addressed	Strengths	Weaknesses	Promise for in-plant use
Measurement of SOV temperature via coil resistance or impedance	Electrical failure of coil and degradation of elastomers resulting from prolonged operation at excessively high temperatures	• Nonperturbative to plant operations • No new sensors or signal cables are required • No permanent instrumentation required; can be applied as needed from a remote location • Applicable to ac- and dc-powered SOVs	• Measures mean coil temperature, not coil hot spot or valve body temperature	High; ready for immediate use
Indication of valve position and change of state upon application of power, via change in coil impedance	Mechanical binding, sluggishness, or failure to shift as a result of worn or improper parts or the presence of foreign materials inside the valve	• No need for add-on sensors or signal cables • Valve position readout is obtained from a remote location • Static method does not disturb SOV	• Dynamic method requires introduction of special ramp-voltage power supply • Applicable only to ac-powered valves	High; some additional developmental work required
Indication of mechanical binding by tracking changes in current/voltage at SOV pull-in and dropout points	Mechanical binding and sluggish shifting caused by worn, swollen, or improper parts or the presence of foreign materials inside the valve	• Simultaneously detects degradation of magnetic and spring forces, increase in frictional forces • No need for add-on sensors or cables or access to SOV • Applicable to ac- and dc-powered SOVs	• Requires introduction of a special variable-voltage power supply • Adequate sensitivity to degraded valve condition is presently undemonstrated	Medium; further testing needed to ascertain cause of poor repeatability of test results
Indication of shorted coil turns or insulation breakdown based on characteristics of the electrical transient generated upon deenergizing a dc SOV	Electrical failure of solenoid coil, caused by high-voltage turn-off transients in combination with insulation weakened by prolonged operation at high temperatures	• Detects presence of defects within coil that cannot be revealed by other means	• Requires access to coil leads at the SOV and removal of normal valve-control electrical cable • Installation of transient suppression devices effectively removes threat of insulation puncture	Low; useful for laboratory postmortem tests
Indication of mechanical binding by analyzing the time-varying characteristics of the inrush current accompanying application of electrical power to the SOV	Mechanical binding and sluggish shifting caused by worn, swollen, or improper parts or the presence of foreign materials inside the valve	• No need for add-on sensors, signal cables, or access to SOV • Information could be obtained as a result of everyday valve operation	• Apparent lack of sensitivity to valve degradations • Short stroke time of small SOVs creates instrumentation problems for ac-powered valves	Minimal; investigation of method abandoned early in the study
Indication of mechanical looseness within ac-powered valves via electrical detection of humming or chattering of the plunger assembly (frequency decomposition of steady-state coil current)	Wear of internal valve parts, improper assembly, or replacement with incorrect parts	• No need for add-on sensors, signal cables, or access to SOV • Nonperturbative to plant operations	• Apparent lack of sensitivity to valve degradations • Requires sophisticated signal analysis equipment	Minimal; investigation of method abandoned early in the study. Addition of miniature acoustic sensor to SOV might prove worthwhile

- indication of shorted turns and/or insulation breakdown within the solenoid coil based on the characteristics of the "flyback" transient generated when a dc SOV is deenergized abruptly.

Two other techniques were examined briefly and then abandoned because initial results showed little promise for eventual development into effective degradation detection and diagnosis tools. These were

- indication of mechanical binding by analysis of the detailed time "signature" of inrushing current that accompanies initial plunger movement upon application of electrical power to the SOV; and

- indication of mechanical looseness (resulting from wear of internal valve parts, improper assembly, or replacement with incorrect internal parts) by electrical detection of the presence of humming or wear-producing chattering of the plunger assembly within ac-powered SOVs, using frequency-domain analysis of the coil current signal.

The operational principles, selected test results, and perceived merits and shortcomings of each of these techniques are described in the following subsections. For most techniques, additional details are available in the appendices.

2.2 Nonintrusive Measurement of Solenoid-Coil Operating Temperature

[Malfunctions addressed: electrical failure of coil and degradation of elastomers, caused by prolonged operation at excessive temperatures]

As a result of the strong temperature dependence of chemical reactions (Arrhenius theory[6]) that are constantly in progress and that tend to break down organic compounds, excessive operating temperature can be expected to shorten the service life of both the solenoid coil insulation and critical elastomeric parts (O-ring seals and valve seats, in particular) within the valve. Arrhenius theory is widely used in extrapolating results obtained in equipment qualification tests performed to industry standards[7,8] to more realistic (as well as abnormal) plant conditions in order to obtain an estimate of qualified service life for the component. To be meaningful, the Arrhenius calculations must employ correct time and temperature profiles, especially the temperatures actually encountered during plant operation. Measurement of true coil temperature using the method described here may help to improve the accuracy of such qualified service life predictions.

Undesirably high operating temperatures may be caused by a number of circumstances such as an application of higher-than-normal voltage to the solenoid coil (as when station batteries are being charged), restricted air flow or an elevated ambient air temperature at the valve location, elevated temperature of the fluid being controlled by the valve, or an insulation breakdown within the solenoid coil winding (resulting in shorted turns, hence lowered electrical resistance and increased power consumption). Therefore, one major cause of premature valve failure might be vastly curtailed if a simple, reliable, and inexpensive means were available to monitor (at will) the actual operating temperatures* of critical SOVs that may be inaccessible and thereby unmonitorable by traditional methods such as infrared pyrometry.

The test results presented below indicate that a promising means of fulfilling this need is to use the copper winding of the solenoid as a self-indicating, permanently available resistance thermometer. To do so requires only in situ measurement of coil dc resistance (or ac impedance) combined with prior knowledge of the temperature coefficient of resistivity for the copper winding and the coil resistance (or impedance) at a single known temperature (most conveniently, normal room temperature).** The dc resistance or ac impedance may be obtained nonperturbatively by measuring voltage applied to and current drawn by the solenoid coil, the former by a voltmeter and the latter by a clamp-on current transformer or a Hall-effect probe (neither of which requires disturbance of the valve control circuitry). The resistance of the electrical leads connecting the SOV to the power source (and the possible variation of this lead resistance

*Monitoring actual SOV operating temperature is, of course, only one approach to increasing life; others are to increase heat dissipation capability (e.g., by the addition of cooling fins) or to curtail heat generation within the solenoid. Devices are available to automatically reduce solenoid operating voltage to a "holding" level (~70 V) once the solenoid has achieved pull-in on full voltage (125 V), the reduction taking place ~5 s after valve actuation. One manufacturer of such devices is Enertech Sollex of Brea, California; the availability of nuclear-qualified units is unknown to the author.

**The temperature inferred by this method will be an average value for the volume occupied by the copper winding rather than for the hottest spot within the solenoid coil. However, unless the coil has a localized fault (such as a shorted turn), this difference may not be very large: measurements by Bacanskas et al. indicate that the "hot spot increment" is in the range of 3 to 5°C.[9]

with changes in ambient temperature) is normally so small relative to the resistance of the solenoid coil that it can be ignored, but it could be measured separately and subtracted from the field-acquired data if such correction is thought to be warranted.

2.2.1 Principles of Operation

To serve as an accurate and a remote sensor of local temperature, some electrical property of the copper solenoid coil must be demonstrated to have a stable dependence on temperature. Though not essential, it is desirable that the relationship of the electrical property and temperature be linear. It is also desirable that the relationship not be affected by changes in other conditions that may not be controllable in a real plant environment. As the data of Appendices A, B, and C illustrate, several candidate parameters exist, each having advantages and disadvantages both in theory and in practice. Because SOVs are designed for two fundamentally distinct electrical environments, alternating current (ac) and direct current (dc), the two types are treated separately below.

2.2.1.1 Dc-Powered SOVs

Coil dc resistance is an easily measured quantity satisfying the given criteria. Similar to platinum (widely used as a resistance thermometer), copper has a stable and sufficiently large temperature coefficient of resistance (~0.2 to 0.3% of value per °C, depending on copper purity[10]) to permit its use as the resistance element of a practical industrial thermometer. Figure 2.4 shows the resistance-temperature relationships obtained for two SOV coils having quite different dc resistances as a result of differences in wire size and in the number of turns employed in their construction. These data, which are typical of results measured on nine separate valves designed for both ac and dc operation and produced by different manufacturers (see Appendix A), were obtained by placing all nine valves in a thermostatically controlled oven and measuring their dc resistances at selected elevated temperatures. For each of the nine valves an extremely linear relationship (correlation coefficient 0.9997) was obtained over the temperature range of interest (20 to 170°C). It must be stressed that, regardless of the actual numerical value of the coil resistance, the temperature coefficient of resistance (expressed as a percentage of value) is sufficiently large (~0.3% per °C) to permit temperature measurement with better than ±10°C accuracy using resistance measurement equipment of only modest (2 to 3%) accuracy. Temperature measurement accuracy of this order is surely adequate for indicating coil temperatures that exceed accepted operating limits established by qualification tests[7,8] or service life prediction curves based on Arrhenius reaction rate theory. In this context it should also be recognized that the trend of indicated coil temperature over a time span of months may be as important to assessing the impact of operating environment on SOV condition and operability as a highly accurate measurement of the coil's temperature would be.

Figure 2.5 provides a laboratory demonstration of this technique. When the 125-Vdc SOV was first energized at the start of the test (when ambient temperature was known to be 25°C), a coil resistance of 793.9 Ω was established by means of Ohm's law from applied electrical potential and current readings. This single calibration point, in conjunction with the empirically determined slope of the resistance-vs-temperature relationship for the copper wire used in this solenoid (3.41 Ω/°C), allows establishment of a temperature scale for the right-hand ordinate of the graph that exactly matches the directly measured resistance scale on the left-hand ordinate; namely,

$$T(°C) = \frac{R(\Omega) - 793.9}{3.41\ \Omega/°C} + 25.0\ . \qquad (1)$$

Once established, this linear scaling relationship permits direct interpretation of changes in SOV coil resistance accompanying altered test conditions in terms of their temperature equivalents. (Such dual scales are used in figures throughout this section as a reminder that resistance or impedance is the quantity directly measured.)

Placed inside a 2-ft^3 open-ended enclosure with only natural convection for cooling and with no instrument air flowing through it, the SOV was first allowed to approach thermal equilibrium at a dc excitation voltage of 117 V. The coil temperature inferred from periodic measurement of dc resistance (Figure 2.5) reached about 113°C (as a result of the deposition of about 14 W of resistive heat within the coil) 65 min after initial power-up, whereas the temperature indicated at this time by a mercury-in-glass stem thermometer placed in contact with the periphery of the potted solenoid coil was only ~70°C (Figure 2.5). This rather large (>40°C) difference is not indicative of a calibration problem but, as has been shown by data acquired under more nearly isothermal conditions (see Appendix F), results from a combination of high thermal resistance at the thermometer-coil contact point and the existence of a large temperature gradient between the center and the outer periphery of the coil, which is encapsulated in a material having poor thermal conductivity. The point here is that, despite the

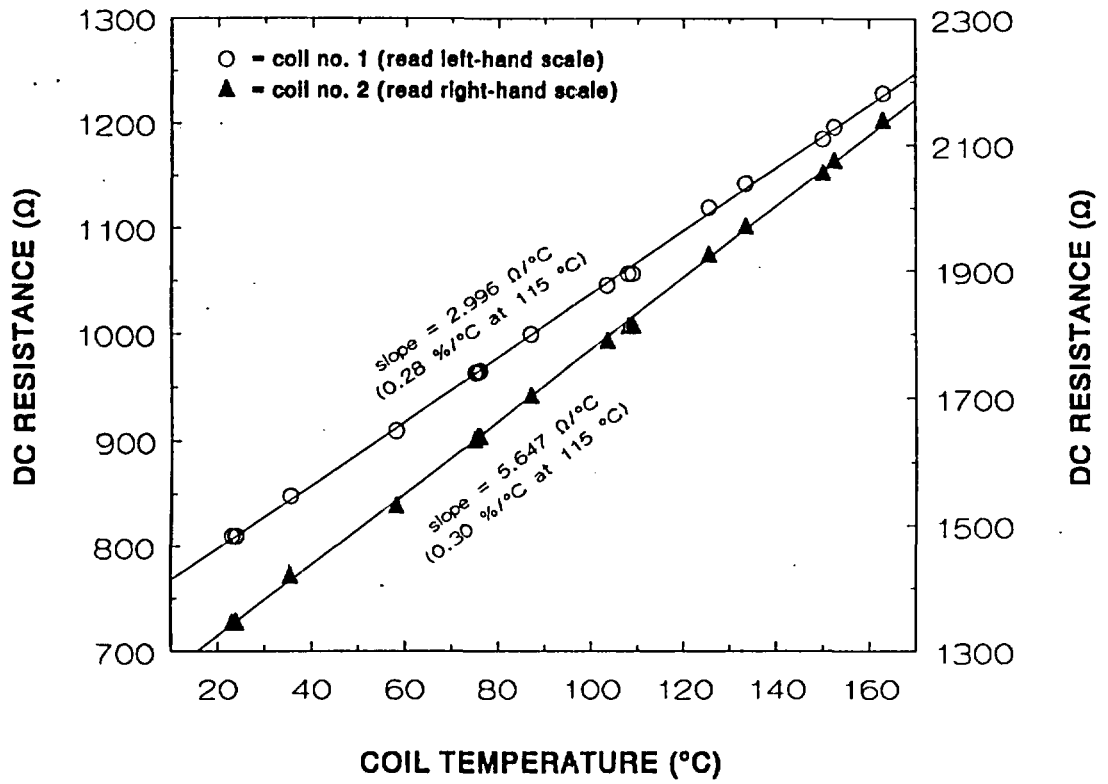

Figure 2.4 Linear variation of coil dc resistance with temperature for two different solenoid coils.

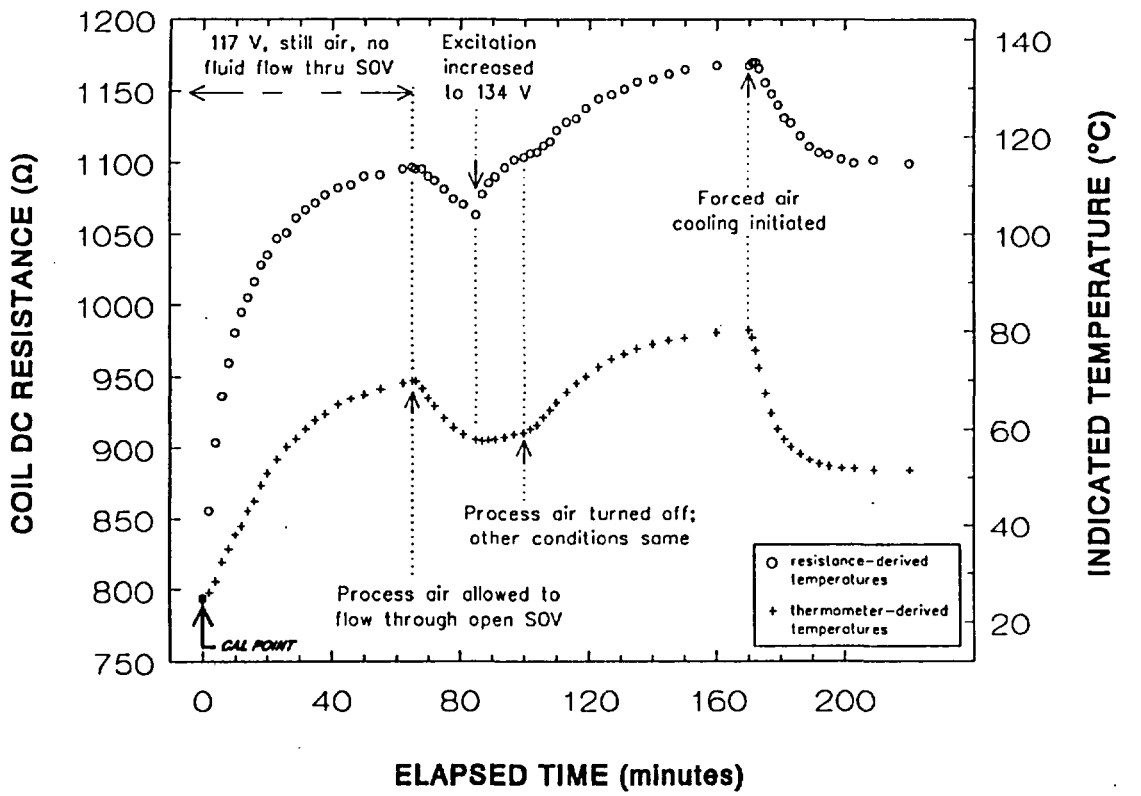

Figure 2.5 Changes in solenoid coil temperature as inferred from coil dc resistance, brought about by altered electrical excitation, fluid flow, and environmental conditions.

considerable differences in the absolute temperatures indicated by the coil resistance and the mercury bulb, the two curves in Figure 2.5 clearly track each other in detail throughout the 220-min duration of the test.

At $t = 65$ minutes instrument air was allowed to flow through the already-open SOV. The cooling effect of room-temperature air flowing through the brass valve body is evident in both curves—somewhat more so for the mercury bulb than for the coil, which is understandable since the bulb was positioned closer to the valve body than is the bulk of the coil. At $t = 85$ minutes the dc supply voltage driving the solenoid was increased to 134 V to simulate a condition that might be encountered on a nominal 125-Vdc power bus during times when station batteries are being charged. Note that the resulting temperature increase was immediate in the coil but slower to appear at the mercury bulb; this phenomenon results because the additional heat produced by the increased excitation voltage is generated instantaneously within the wire of the coil, whereas it must be transported to the coil periphery (where the mercury thermometer was located) by the relatively slow process of thermal conduction.

The 20-psi instrument air was turned off at $t = 100$ min, but the SOV remained powered at 134 Vdc and cooled only by natural convection within its enclosure. Over the next 70 min the indicated coil temperature rose to an asymptotic value of about 135°C,* and a commensurate rise was recorded on the mercury bulb thermometer. At $t = 170$ min a muffin fan positioned below the enclosure surrounding the SOV was turned on to draw air down past the valve at low velocity. The effect of this forced-air cooling was seen to be a prompt reduction of both indicated temperatures—somewhat more rapid for the bulb thermometer than for the coil, which is explainable by the same reasoning offered for the difference in time response of the two curves when the electrical excitation was increased at $t = 70$ min (i.e., time lag due to conductive heat transport). However, the effect on the curve is in the opposite direction because, in the experiment, heat was being removed from the outside of the coil rather than added from the inside.

In summary, the results of the test described previously and depicted in Figure 2.5 illustrate that using the copper winding of a dc-powered SOV as a resistance thermometer can provide meaningful real-time indication of altered excitation, environmental, and fluid flow conditions likely to occur in power plants from time to time that could result in unacceptably high SOV operating temperatures and therefore in shortened service life. Moreover, the temperatures so obtained are better indicators of temperature stress imposed on the coil materials than might be obtained from conventional, externally applied temperature-indicating devices such as thermocouples or thermistors.

2.2.1.2 Ac-Powered SOVs

Ac-powered valves offer many more electrical measurement possibilities, some of which may be useful for the inference of coil temperature. These include inductance, quality factor, and impedance (expressed either as a vector magnitude or in terms of its real and imaginary orthogonal components). However, some measurable parameters prove more suitable than others: take for example inductance and quality factor,* whose variations with temperature are shown in Figure 2.6 for a typical ac SOV excited at two widely separated frequencies, 60 and 500 Hz. (See Appendix C for additional data.) As a measure of temperature, quality factor is easily dismissed, owing to the poor quality of the correlation at 60 Hz (as evidenced by the considerable data scatter) and almost zero slope at 500-Hz excitation frequency. Inductance is not so easily dismissed: its relationship to temperature is quite linear and its temperature coefficient (somewhat less than 0.1% of value per °C), although not large, is sufficient to be useful, especially at 500-Hz excitation frequency. However, application of a 500-Hz test signal for the purpose of temperature measurement would require removal of normal of 60-Hz power from the SOV, thereby making the measurement perturbative. Moreover, the measurement of inductance requires fairly sophisticated electronic circuitry. For all these reasons, temperature inference via inductance and quality factor was not pursued further; instead, attention was turned to the obvious analog of dc resistance: ac impedance.

*Even this relatively high temperature, representing an increase relative to ambient of about 110°C, is still well below what is considered acceptable for the Class H coil insulation that has been used in recent years in nuclear-grade SOVs. (Class H insulation is rated for continuous operation at 160°C; the newer Class N is rated for 175°C.) However, had the ambient been 50°C—a condition that might be encountered in some areas within containment—Class H insulation would be at its operational limit.

*Quality factor—often designated Q in electrical engineering texts—is a dimensionless attribute of an inductor or a capacitor that quantifies its ability to *store* power (as inductance or capacitance) as opposed to its ability to *dissipate* power (as resistance); that is, it is the ratio (volt-amps stored)/(watts dissipated) = reactance/resistance.[11] Therefore, the greater Q is, the more nearly the inductor or capacitor approaches an ideal, purely reactive (zero-resistance) device.

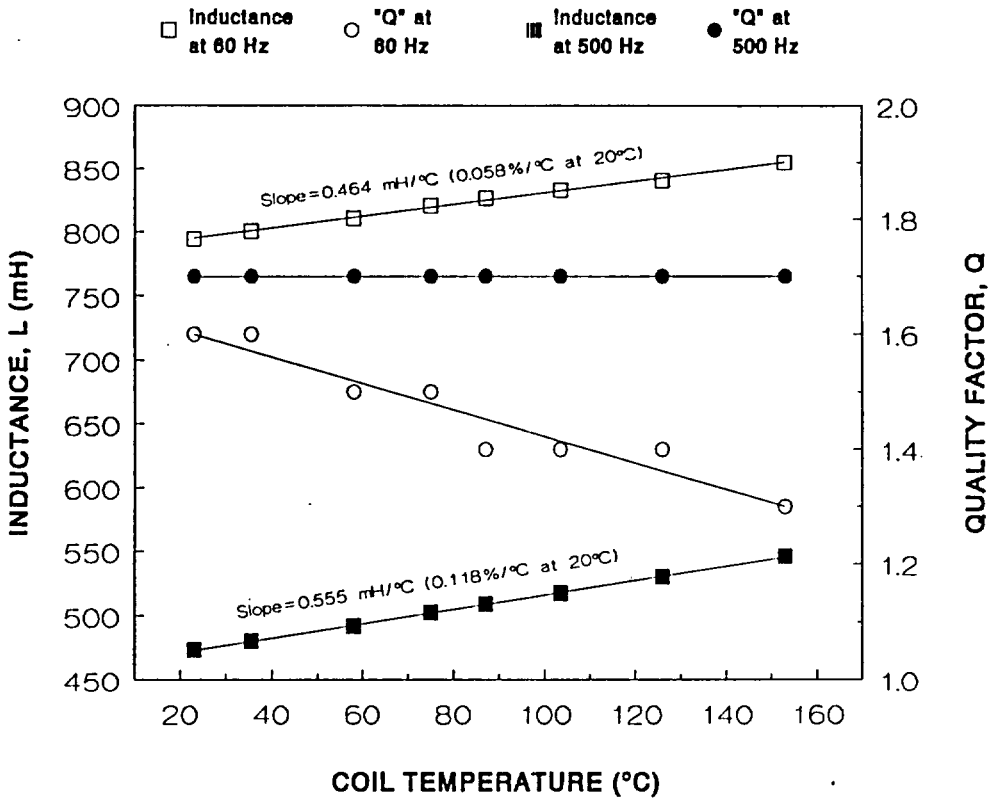

Figure 2.6 Approximately linear variation of solenoid inductance and quality factor with temperature for a typical SOV excited at 60 and 500 Hz. (Data for other coils and excitation frequencies are given in Appendix C.)

By analogy to the measurement procedure previously illustrated for a dc-powered SOV, the inference of operating temperature for an ac-powered SOV would follow the same path except that impedance (measured at the power line frequency of 60 Hz in the United States but often 50 Hz abroad) would replace resistance as the quantity obtained by applying Ohm's Law to the root-mean-square (rms) voltage and current measured at the SOV's electrical leads. However, two complicating factors arise that were not troublesome when dealing with dc valves. While neither poses an insurmountable obstacle to temperature inference, these troublesome factors need to be appreciated and so will be described in some detail in the following two subsections.

Diminished Temperature Coefficient

Figure 2.7 illustrates the manner in which the magnitude of a typical solenoid's electrical impedance, $|Z|$, varies with temperature for a power line frequency of 60 Hz. (Data for five of the nine valves at three different frequencies are given in Appendix B for the interested reader.) The orthogonal components of the vector Z—Re(Z) and Im(Z)—are also shown, along with the dc resistance, *R*, for comparison. Note that, like *R*, each of the representations of ac impedance shows a highly linear variation with temperature and that, with the exception of Im(Z), they all display approximately the same absolute slope, expressed in the figure as ohms/°C. The linear relationship is, of course, highly desirable, and shows that in principle any of these quantities might be used as a measure of temperature. However, because the absolute magnitudes of the measured quantities increase substantially as one moves from dc resistance through Re(Z) and Im(Z) to $|Z|$ while retaining essentially the same slope, the temperature coefficients for these four measurable quantities, expressed as percentage of value, decrease markedly as one moves from the bottom to the top of the graph. The practical implication of this observation is that because the temperature coefficient of $|Z|$ (0.118%/°C) is only about 30% as large as the temperature coefficient of *R* (0.396%/°C), the accuracy of $|Z|$ measurements would have to be three times greater than the accuracy of *R* measurements to achieve an equally accurate inference of temperature. Given a typical field-instrumentation accuracy of ±2%, the above numbers suggest that coil temperatures inferred from dc resistance measurements may be expected to be accurate to within perhaps ±5°C, whereas ac impedance measurements of comparable accuracy could not be expected to yield coil temperatures more accurate than within ±17°C.

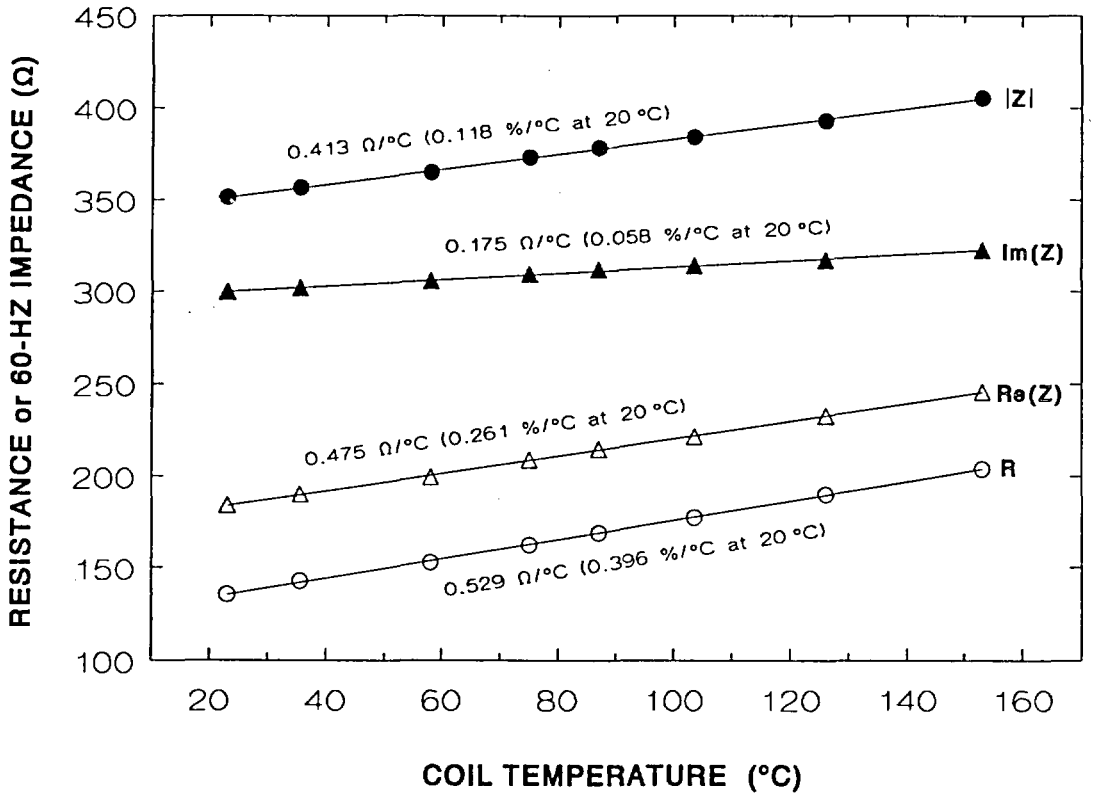

Figure 2.7 Linear variation of coil dc resistance and 60-Hz ac impedance with temperature for a typical ac-powered SOV.

One apparent solution to this problem would be to measure Re(Z) rather than $|Z|$, since the temperature coefficient of the former (0.261%/°C) is only 35% smaller than that of *R*. The difficulty in doing so is the more complex and therefore costly instrumentation necessary to measure Re(Z) as opposed to $|Z|$.

Variation of Impedance with Excitation

In contrast to the dc resistance, which for all practical purposes does not change with the amount of voltage applied to the coil, the measured ac impedance of a solenoid *in its actuated state* is strongly dependent on the level of electrical excitation. This is illustrated in Figure 2.8, which shows the manner in which the 60-Hz impedance of a typical ac-powered SOV held at constant temperature changes with impressed voltage (see also Appendix E). Although it is true that the solenoid impedance is very nearly constant at excitation levels between 20 and 60 V_{rms} (i.e., at voltages insufficient to make the valve shift), once the solenoid changes state, the impedance drops by approximately 40% as impressed voltage is further increased from 70 to 135 V_{rms}.

Of course, this variation of impedance with level of excitation occurs simultaneously with (and is indistinguishable from) the variation of impedance with temperature that is the basis for its intended use as an impedance thermometer, and must therefore be accounted for when translating the measured impedances into temperatures. Unfortunately, the excitation dependency of impedance (–6.5 Ω/V at the operating point of 117 V_{rms} for the SOV whose characteristics are shown in Figure 2.8) may be even stronger than the temperature dependency (+0.72 Ω/°C for this same SOV). Therefore, if the voltage applied to the solenoid is not reasonably constant over time, corrections for excitation changes may be quite large and obviously would introduce additional uncertainty into the inferred temperatures. (This will be illustrated in a later figure).

Four possible solutions to this problem come to mind: (1) perform temperature inference measurements at a low impressed voltage where the impedance is invariant with respect to excitation level, (2) power the SOV from a constant-voltage power supply, (3) make the temperature-determining measurement with dc rather than ac excitation, or (4) correct for the change in impedance introduced by varying excitation voltage. Assuming that the SOV is normally energized, the first solution requires that the valve be allowed to change state momentarily, which may or may not be permissible depending on the plant situation. The second option is completely

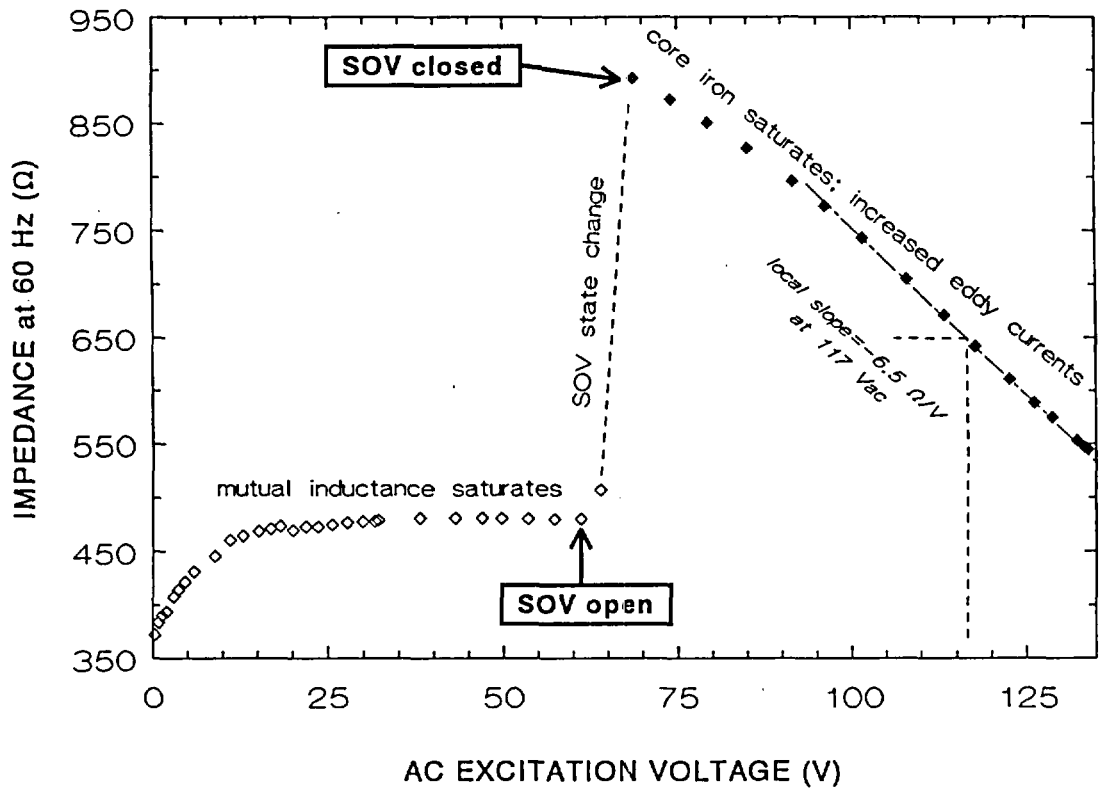

Figure 2.8 Variation of ac impedance with impressed voltage for an SOV held at a constant temperature of 25°C, showing the abrupt impedance change accompanying valve state change.

straightforward but may be difficult to backfit into an existing plant. The third solution, though technically most attractive (because it solves both of the problems cited), may be hardest to implement because special circuitry would be needed either to switch the SOV momentarily from ac to dc power or to superimpose a dc resistance interrogation signal on the normal ac valve actuation voltage. The fourth option, though inherently inexact because of the large corrections required, is perhaps the easiest to implement. Its workability is illustrated in the laboratory demonstration described next.

Using a test sequence very similar to that described in detail for a dc-powered SOV (Figure 2.5), the temperature response of an ac-powered SOV to changes in fluid flow through the valve, excitation level, and air flow in the vicinity of the valve was demonstrated (Figure 2.9). The same general features are present here as in the test previously presented (including a difference in temperatures indicated by the coil impedance vs the mercury bulb thermometer reading that approaches 40°C) except that the scatter of the coil temperatures inferred from ac impedance is noticeably larger than was observed from the dc-derived data. This is understandable in view of the preceding discussion regarding the reduced magnitude of the temperature coefficient for ac impedance and the necessity of large corrections to the data.

The magnitude of the corrections applied for excitation voltage changes (specifically the changes at $t = 70$ and 115 min) can be seen by comparing the crosses and the filled circles in Figure 2.9. The corrections were performed by using a third-order polynomial fit to the postclosure impedance data of Figure 2.8 to estimate the impedance that might have been measured had the excitation been exactly 117 V_{rms} (the excitation used at the calibration point for this valve) via the relation

$$|Z|^{T}_{corr} = |Z|^{T,V}_{meas} \cdot \frac{|Z|^{25°C,117}_{fit}}{|Z|^{25°C,V}_{fit}} , \qquad (2)$$

where $|Z|^{T}_{corr}$ represents the impedance appropriate to temperature T, corrected to standard excitation; $|Z|^{T,V}_{meas}$ represents the impedance actually measured at temperature T and impressed voltage V; and the remaining quantities represent impedances that would be obtained at standard (117 V_{rms}) and nonstandard (V) excitation voltages at a temperature of 25°C, as determined from the polynomial fit to the data of Figure 2.8. Despite the large corrections, for the purpose of detecting far-off-normal operating temperatures that pose a serious problem in regard to accelerated aging of coil insulation and valve

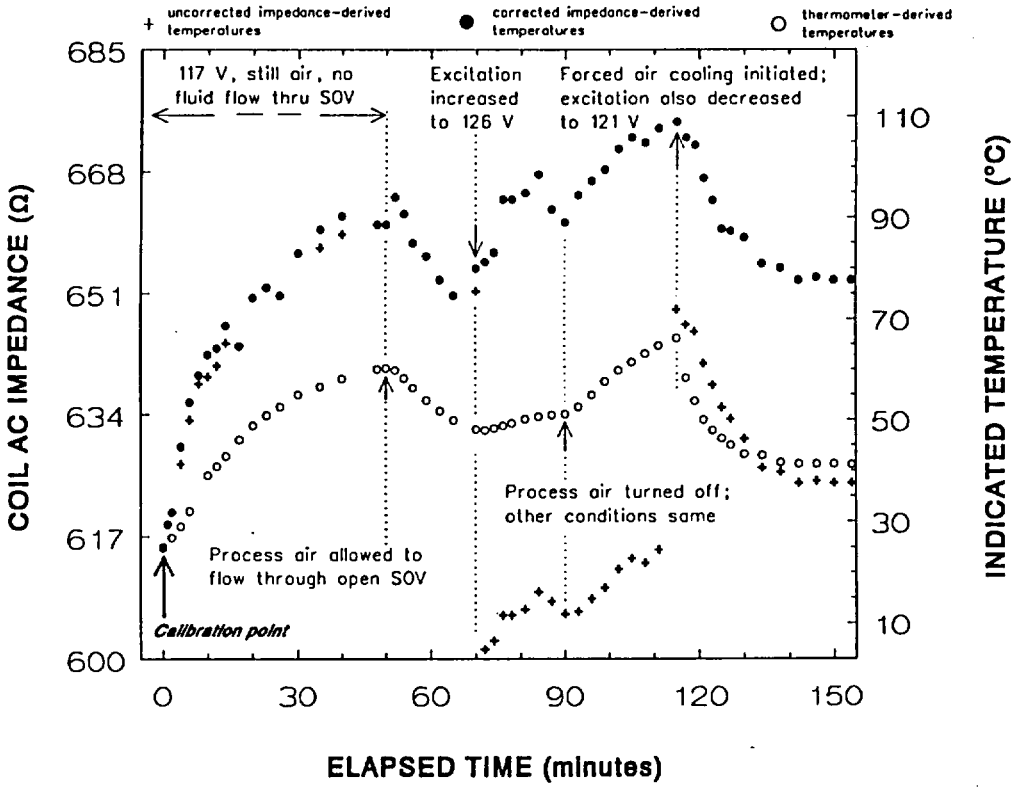

Figure 2.9 Changes in solenoid coil temperature as inferred from coil ac impedance, brought about by altered electrical excitation, fluid flow, and environmental conditions.

elastomerics, the level of accuracy implied by the results of Figure 2.9 is probably acceptable.

2.2.2 Practical Field Application

To illustrate the workability of this coil resistance/ impedance method of SOV operating temperature inference in a true field environment, the rms voltage impressed upon and the rms current drawn by an ac SOV controlling the flow of refrigerant in a large chilled-water air-conditioning system were recorded at 100-s intervals over a 55-h period of system operation. The recorded voltages were divided point by point by the recorded currents to yield a curve of $|Z|$ vs time. Knowing the 60-Hz $|Z|$ of the solenoid at a known temperature (593.9 Ω at 25.5°C) and assuming a value of 0.115% /°C (the median value for the five ac-powered SOVs tested) for the temperature coefficient of impedance, an equivalent temperature scale was affixed to the data plot; namely,

$$T(°C) = \frac{|Z|(\Omega) - 593.9}{(0.00115)(593.9)} + 25.5 \ . \qquad (3)$$

Since the impressed voltage changed very little over the duration of the test, no corrections of the form given by Eq. (2) were required for impedance change caused by altered excitation level.

The test results, split into two roughly 27-h time periods for clarity, are presented in Figure 2.10 and Figure 2.11(a) and (b). The entire 55-h time period encompassed in these data was characterized by generally rising outside air temperatures (necessitating continuous compressor operation to maintain the chilled-water temperature setpoint during the initial 28 h of the test) as well as by rising ambient temperature at the SOV location (which is near the compressor, the essentially continuous operation of which caused the entire equipment room in which it is located to heat up). These weather and local environment temperature trends explain the generally rising SOV temperatures seen in the two figures. An environmental perturbation was introduced 24 h into the test just to see its effect: a blower that had been aiding the cooling of the finned SOV was turned off. This change resulted in a prompt rise in SOV coil temperature (by about 10°C), followed by a slow fall as nighttime brought cooler temperatures to the equipment room.

The second 27 h of operation [Figure 2.11(a) and (b)] illustrate a new data feature; namely, cyclic compressor operation. At first glance, the inferred temperatures during these periods appear to have a great deal of scatter

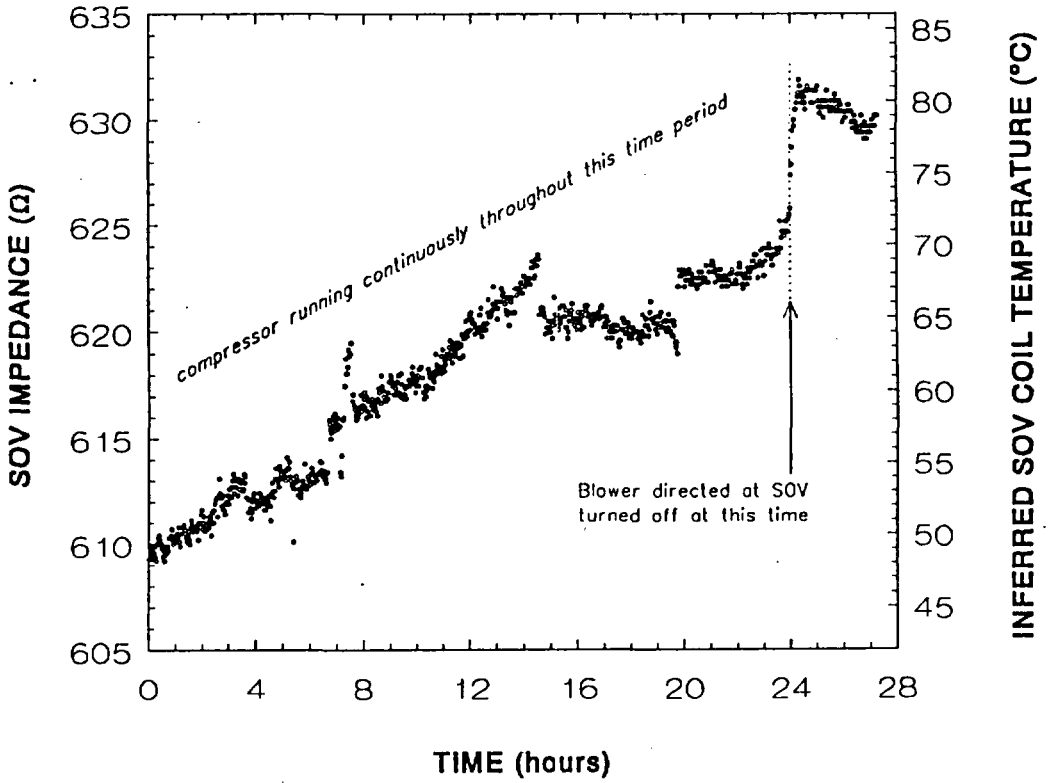

Figure 2.10 Weekend performance of an ac-powered SOV in a refrigeration system (first 27 h).

[Figure 2.11(a)], but when examined on an expanded time scale [Figure 2.11(b)], what had appeared to be data scatter is revealed as repeated SOV heat-up during each cycle of compressor operation followed by cool-down after each compressor shutoff.

The temperatures inferred for the SOV installed on the chilled-water system during the monitored period were never so high as to pose a threat to its continued operation. However, the data illustrate that, had some operational anomaly occurred that would have resulted in a dangerous rise in SOV temperature, it almost certainly would have been detected by this relatively simple, nonintrusive temperature-measurement technique, which required only the connection of a voltmeter and a clamp-on current transformer.

In conclusion, laboratory- and field-acquired test data illustrate that the true operating temperature of an SOV can be inferred simply, nondisruptively, and with satisfactory accuracy for detecting temperature conditions that exceed accepted operating limits by using the copper winding of the solenoid coil as a self-indicating, permanently available resistance thermometer. This approach to monitoring the temperatures actually "seen" by SOVs during the course of plant operation and the temperature changes introduced by altered environmental or process conditions might be used to advantage by those concerned with prediction of qualified life. The method has a number of merits, among which are the following: (1) there is no need for an add-on temperature sensor, (2) the true volume-averaged temperature of a critical—and probably the hottest—part of the SOV (i.e., the electrical coil) is measured directly, (3) temperature readout can be provided at any location at which the SOV electrical lead wires are accessible (even though remote from the valve), (4) the SOV need not be disturbed (whether normally energized or deenergized) to measure its temperature in situ, and (5) the method is applicable to all types of SOVs—large and small, ac- and dc-powered. From a standpoint of prediction of qualified life, the principal shortcoming of the method is that the coil's volume-averaged temperature—rather than its peak temperature—is the quantity measured, although this difference may not be substantial.[9]

This method is usable in its current form, although additional developmental work could improve the accuracy of temperature indications derived from impedance measurements on ac-powered SOVs. The hardware implementation would depend on plant needs but could take the form of a permanently installed, computerized data logger or hand-held, walk-around instrumentation for use on an as-needed basis.

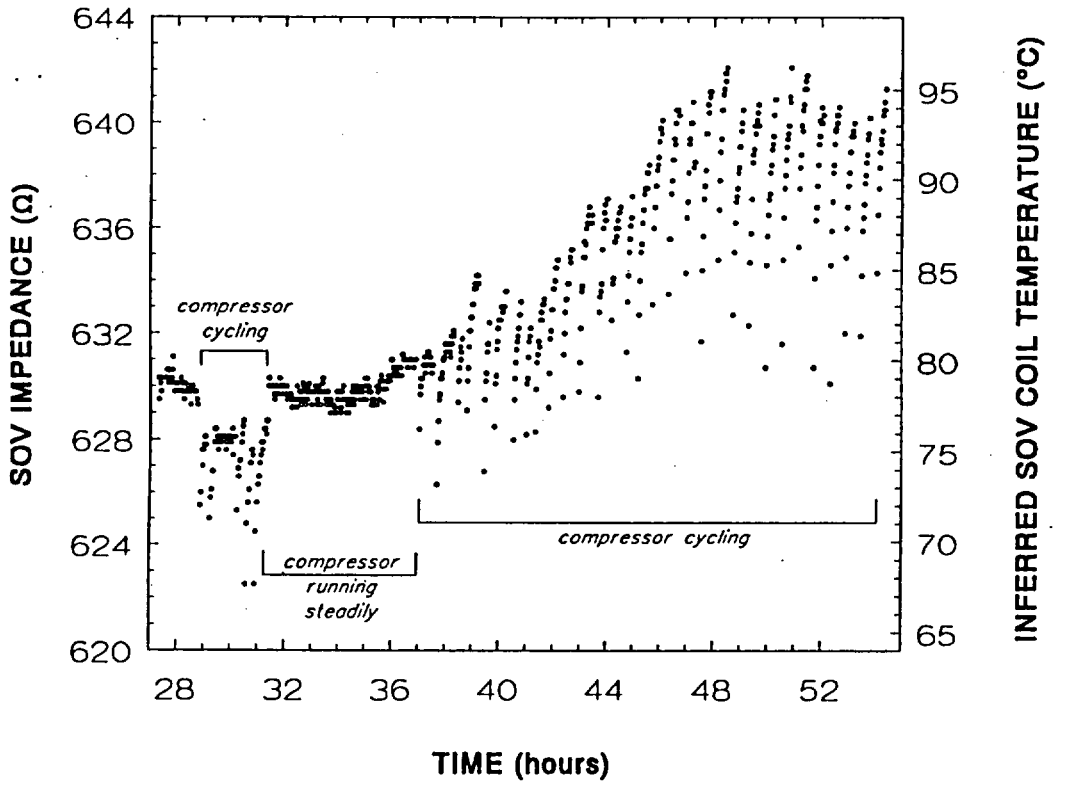

Figure 2.11(a) Weekend performance of an ac-powered SOV in a refrigeration system (second 27 h).

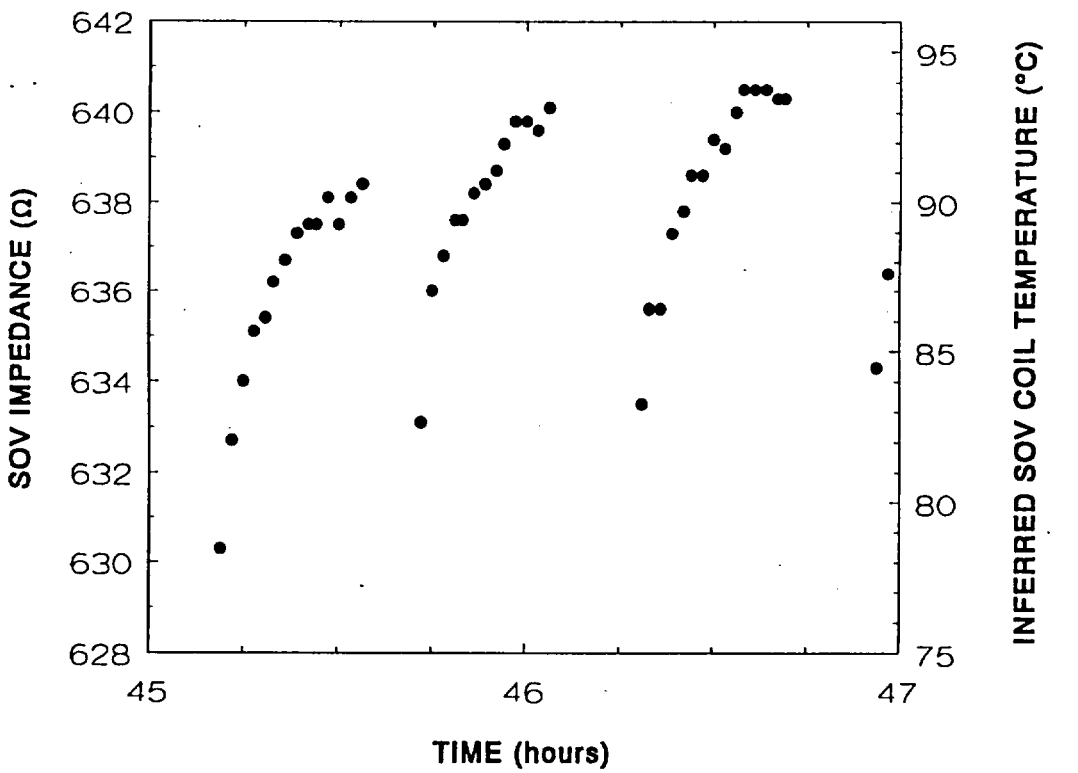

Figure 2.11(b) Expanded view of a typical 2-h period from Fig. 2.11(a) during which the compressor was cycling.

2.3 Indication of Valve Position and Change of State

[Malfunctions addressed: mechanical binding, sluggishness, or failure to shift caused by worn or improper parts or the presence of foreign materials inside the valve]

The technique presented in the preceding section addresses the issue of reduced solenoid coil and elastomer life resulting from prolonged operation at excessive temperature, an acknowledged problem in the nuclear industry. Here we address another well-known problem, that of the solenoid plunger (core) "frozen" in position so that it refuses to move when the SOV is called upon to change states, whether normally energized or normally deenergized. Such a condition may arise from age-related changes in the physical properties of the elastomeric seats (the seat material may become sticky, thus holding the plunger fast), thermally degraded and deformed shaft seal O-rings, faulty valve assembly, the use of incorrect replacement parts, or the presence of internal contaminants such as metal chips, dirt, paint, thread sealant, desiccant, and hardened lubricant that can interfere with free movement of the core within the core tube.[1,3,12] Depending on the nature of the information to be obtained, this general technique can be implemented either as a nonintrusive static measurement of coil impedance or as a dynamic measurement, the latter requiring application of a special voltage profile to the SOV. The two types of tests are treated in separate subsections below.

2.3.1 Static Tests (Nonintrusive to Plant Operations)

Absolute plunger position within the solenoid coil or simple indication of plunger movement upon application of ac power can be obtained in situ by measuring the ac impedance presented by the SOV electrical lead wires. As shown in Figure 2.8, if SOV terminal impedance at 60 Hz is plotted as a function of excitation level, it is found first to increase about 30% as turn-to-turn flux linkages within the coil saturate in the current region of 0 to 50 mA, then to remain about constant until 130 mA is reached, at which point the plunger shifts position, and is drawn abruptly into the solenoid. This change of valve state is seen to produce a near doubling of the coil's electrical impedance, which then decreases fairly rapidly as excitation is further increased, owing to increased eddy current losses and magnetic saturation of the core iron. Accordingly, if the temperature of the SOV is known (at least approximately), a simple rms voltmeter/ammeter measurement of ac impedance of the powered SOV (or an impedance meter measurement of the unpowered SOV) will provide a good indication of whether the valve is truly open or closed.

Carrying this idea one step further, one can try to quantify the absolute position of the core within the solenoid coil. This might be important if internal contamination by foreign objects or substances were suspected of holding the plunger slightly off its seat, thus causing the valve to leak.[1,12] Static measurements were performed by placing movement-restricting shims of various thicknesses between one or the other valve orifice and the corresponding elastomer seat. Referring to Table 2.3, an impedance sensitivity figure of $\delta|Z|/\delta d \approx 7\ \Omega$/mil of plunger displacement (1.4% change in $|Z|$/mil) was obtained for small movements of the valve core in the vicinity of the valve's unenergized seat position. This implies that an impedance measurement performed on an SOV at a known temperature and electrical excitation level could provide indication of plunger position in the vicinity of the valve's unenergized seat to within a few thousandths of an inch, making detection of anomalous conditions causing displacement of the plunger from its unenergized, spring-assisted rest point a relatively simple matter. However, as Table 2.3 also illustrates, a corresponding sensitivity to plunger displacement in the vicinity of the other (energized) seat was not found, probably because after the iron core is drawn substantially into the solenoid—thus becoming a part of the magnetic circuit—further movement within the coil has little or no effect on the resulting coil inductance (and hence the impedance).

It must be clearly understood that the preceding discussion applies only to SOVs powered—permanently or temporarily—by ac. Dc-powered valves show no corresponding change in their terminal resistance as the plunger changes its position within the solenoid coil, as illustrated in Figure 2.12.

2.3.2 Dynamic Tests (Intrusive to Plant Operations)

For ac-powered SOVs, dynamic tests that verify both the presence of plunger movement upon application of power and also the absence of binding throughout the transition from an unpowered to a powered state, are also possible if one is able to temporarily remove the 117-V, 60-Hz ac power applied to the SOV and substitute an ac power supply capable of ramping up and down more or less uniformly with time. To see how this is possible, Figure 2.13 shows the manner in which the current drawn

Table 2.3 Variation of 60-Hz impedance with position of the plunger

SOV condition	|Z| (Ω)	δ|Z|/δd	
Normal assembly, unenergized state	483.37	(base condition)	
Shimmed 0.0035 in. off unenergized valve seat[a]	510.97	7.89 Ω/mil (1.6%/mil)	
Shimmed 0.0065 in. off unenergized valve seat	529.15	7.04 Ω/mil (1.4%/mil)	
Shimmed 0.0115 in. off unenergized valve seat	551.37	5.91 Ω/mil (1.2%/mil)	
Normal assembly, energized state	635.5	(base condition)	
Shimmed 0.0035 in. off energized valve seat[b]	635.2	−0.09 Ω/mil	NULL RESULT
Shimmed 0.0065 in. off energized valve seat	637.9	0.37 Ω/mil	NULL RESULT
Shimmed 0.0115 in. off energized valve seat	636.4	0.08 Ω/mil	NULL RESULT

[a]The seat position assumed by the plunger, with spring assistance, when the SOV coil is unenergized.
[b]The seat position assumed by the plunger when the SOV coil is energized.

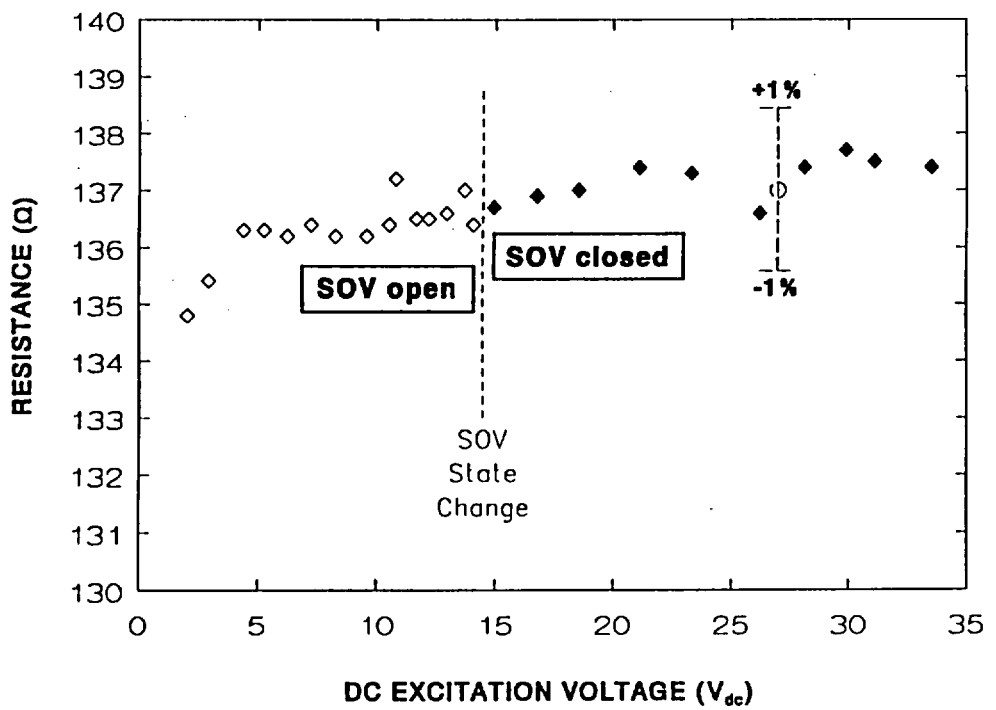

Figure 2.12 Dc resistance of SOV from open to closed state. Unlike ac impedance (Fig. 2.8), the dc resistance of an SOV does not change when the valve closes.

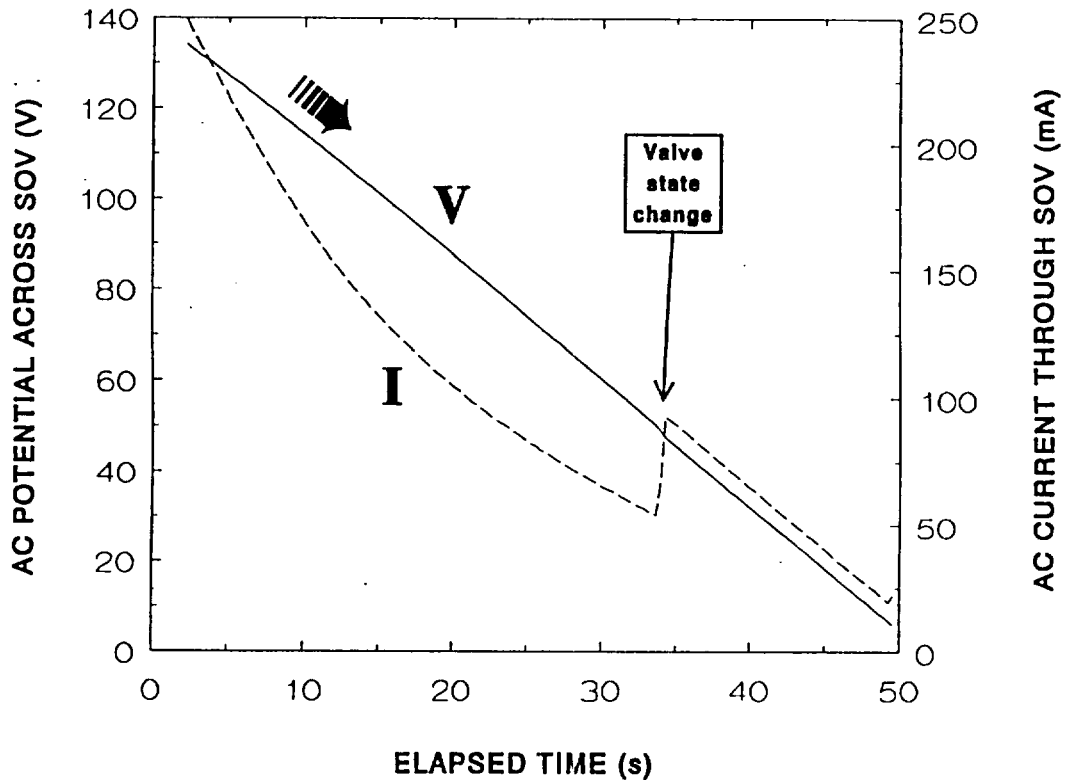

Figure 2.13 The nonlinear variation of SOV current during a linear rampdown of voltage over a 50-s period is a reflection of the solenoid's nonconstant impedance at all but low levels of excitation.

by the solenoid changes with time when the voltage applied to the coil leads is slowly ramped down in a linear fashion from about 135 V_{rms} to 5 V_{rms} over a period of 50 s.* The nonlinear behavior of the current seen in Figure 2.13 over the initial 33 s (equivalent to the right-hand side of Figure 2.8) reflects the variation of impedance caused by eddy current and hysteresis losses, whereas the behavior over the final 15 s (t = 35 to 50 s) reflects the approximately constant and much lower impedance produced by the plunger being somewhat outside the solenoid coil (equivalent to the left-hand side of Figure 2.8).

The shift of the plunger in its guide tube is clearly seen at about t = 33 s as an abrupt change in the current drawn by the SOV as a result of the change in impedance that accompanies plunger movement. It is the current/voltage (i.e., impedance) characteristics obtained during this brief time of transition that reveal not only the overall movement of the solenoid core but also any tendency it may have to bind within its guide tube during the valve state transition, as is illustrated at some length in Subsect. 2.4.

The ramp rate can be increased considerably in order to improve both time definition and thereby the capture of detail. For example, if we take an ac-powered SOV in good condition and make provision to ramp its excitation voltage over the full operational range (0 to 135 V) in a rather short time interval (200 ms) as shown in Figures 2.14 and 2.15, then a marked rise in impedance, $|Z|$, and a corresponding fall in current will be evident when the valve changes state (t = 125 ms in Figure 2.14). On the other hand, if the plunger is jammed in position and cannot move (the condition purposely created in Figure 2.15), the lack of impedance change and the continued monotonic rise of current throughout the ramp-up will clearly signal a lack of plunger movement.

If $|Z|$ can be measured on a time scale of 1 to 1.5 electrical cycles (from 17 to 25 ms for 60-Hz power) following contact closure, it might even be possible to obtain indication of plunger movement by using normal switch-on actuation rather than a ramp-up, thus obviating the need for electrical disconnections and a special power source. An attempt was made to do so (see Figure 2.16) but without much success, owing to the difficulty of calculating rms quantities over time periods as short as

*The downward voltage ramp was produced by driving the shaft of a Variac autotransformer at a constant rotational speed (1 rev/min) with the aid of a gear motor, thus producing a ramp rate of ~2.75 V/s. The gear motor's direction of rotation could be electrically reversed to produce an upward voltage ramp having the same rate of change with time.

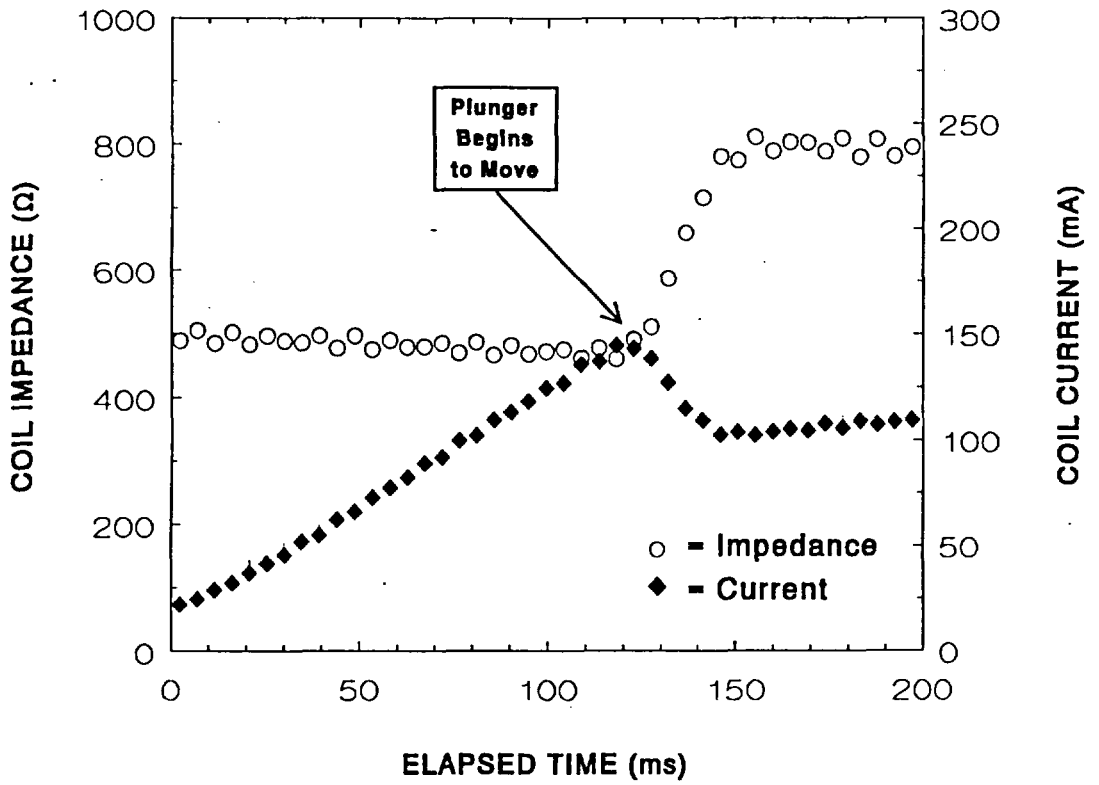

Figure 2.14 Current and impedance discontinuities during linear voltage ramp-up over a period of 0.2 s—an indication of plunger movement in a normally operating ac-powered SOV.

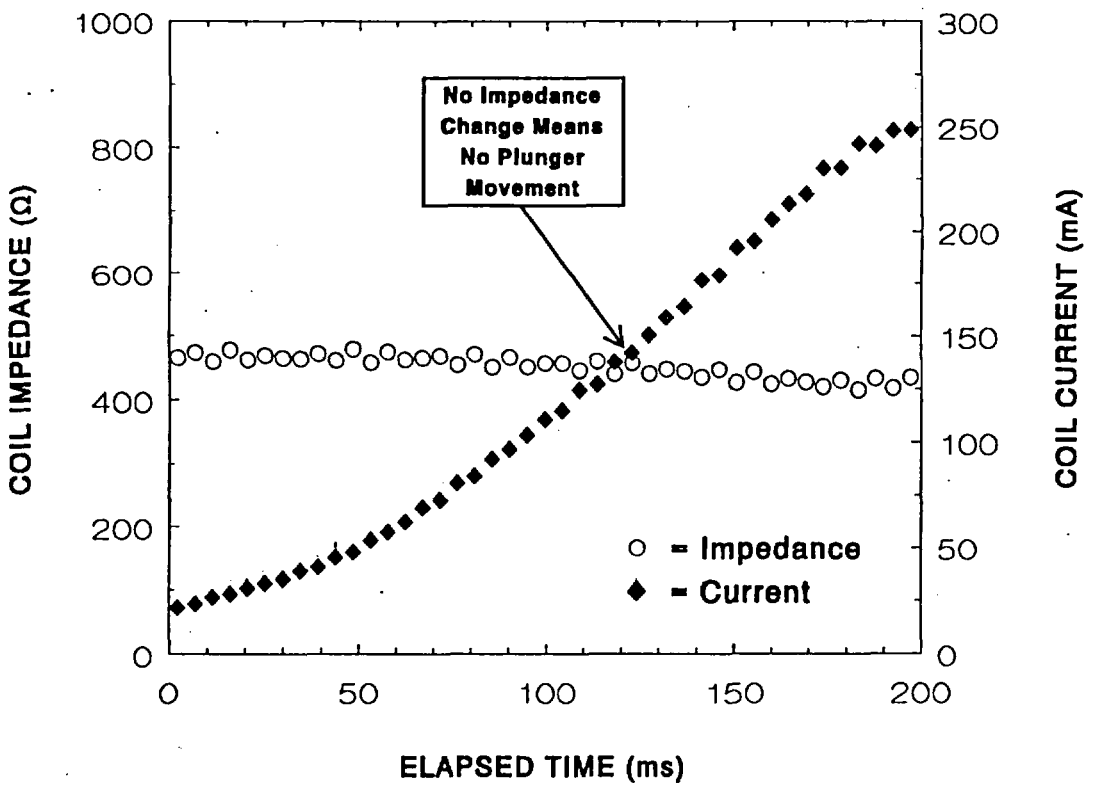

Figure 2.15 Lack of impedance change and current discontinuity during linear voltage ramp-up over a period of 0.2 s—an indication of lack of plunger movement in an ac-powered SOV in which the plunger was purposely jammed.

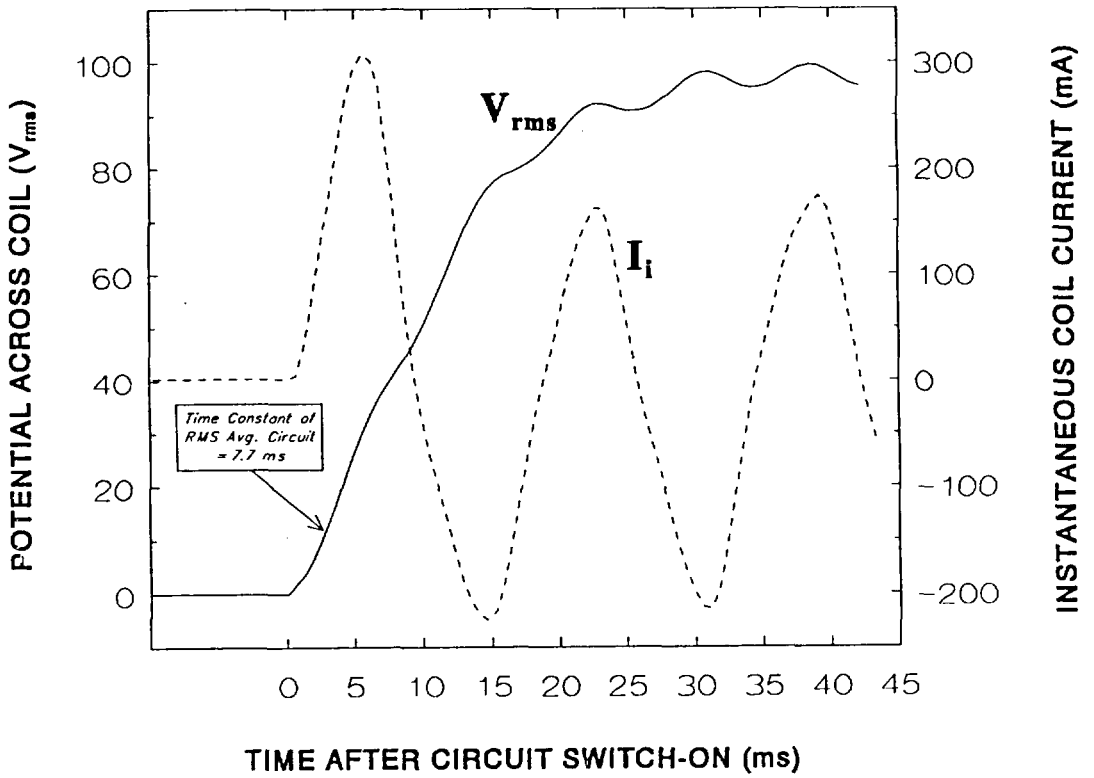

Figure 2.16 Instantaneous current through a solenoid coil immediately following application of 60-Hz ac power compared with rms voltage across the coil calculated by a true rms meter having an averaging time constant of 7.7 ms.

1 to 1.5 electrical cycles. As seen in the figure, the rms calculation simply cannot keep pace with the plunger's rapid movement, which appears to be complete about 20 ms after power is applied.

In conclusion, positive indication of current SOV state and ability to change state (as a dynamic response to an "open" or "close" command) is often possible using either static (nonintrusive) or dynamic (intrusive) ac measurement techniques. The merits are similar to those cited for temperature inference through coil resistance/impedance; namely, that (1) there is no need for an add-on sensor, (2) valve state readout can be provided at any location at which the SOV electrical lead wires are accessible (even though remote from the valve), and (3) the SOV need not be disturbed (whether normally energized or deenergized) if the static method is used. The shortcomings are that (1) the method is applicable only to ac-powered SOVs and (2) arrangements must be made to power the valve from a special ramp-voltage power supply if the dynamic method is used.

The methods, although useable in their present form, would need additional development to provide a means of obtaining desired dynamic information from instantaneous switch-on tests rather than from the 200-ms ramps described here. In any case, the preferred hardware implementation would be determined by plant needs.

2.4 Verification of Unrestricted Plunger Movement

[Malfunctions addressed: mechanical binding and sluggish shifting caused by worn, swollen, or improper parts or the presence of foreign materials inside the valve]

2.4.1 Sensitivity of Results to Presence of Internal Contamination

The ramp-up technique described in Subsect. 2.3.2 is also useful in diagnosing mechanical abnormalities less severe than a completely immobile plunger (e.g., a plunger whose movement within its guide tube is impeded by the presence of foreign substances such as dirt or oil).[3,12] Figure 2.17 illustrates the current/voltage relationship obtained for an ac-powered SOV when its excitation is ramped up over its full voltage range within a time period of a few tens of seconds. Curve A (solid) was obtained with a clean, normally assembled valve, whereas curve B (broken) was obtained from a valve of identical construction in which

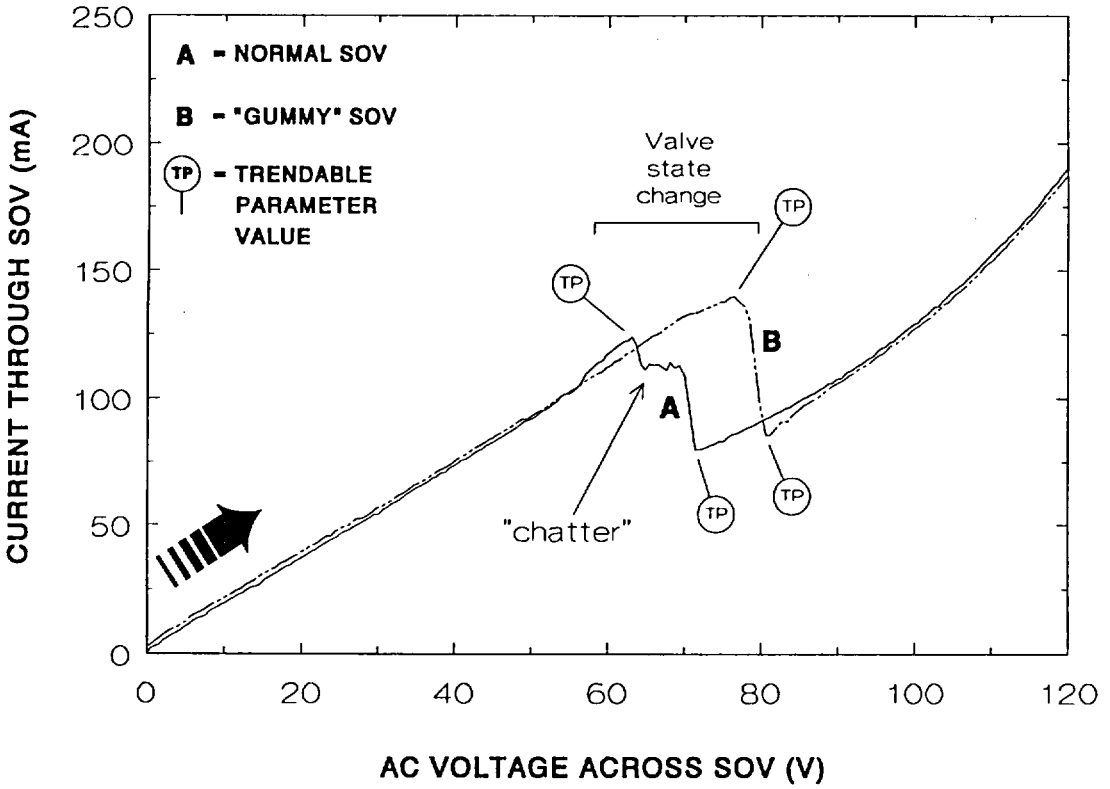

Figure 2.17 Ac current and voltage characteristics obtained during a slow excitation ramp-up, showing sensitivity to the presence of mechanical binding. (A: clean, normally assembled SOV; B: valve treated to produce binding.)

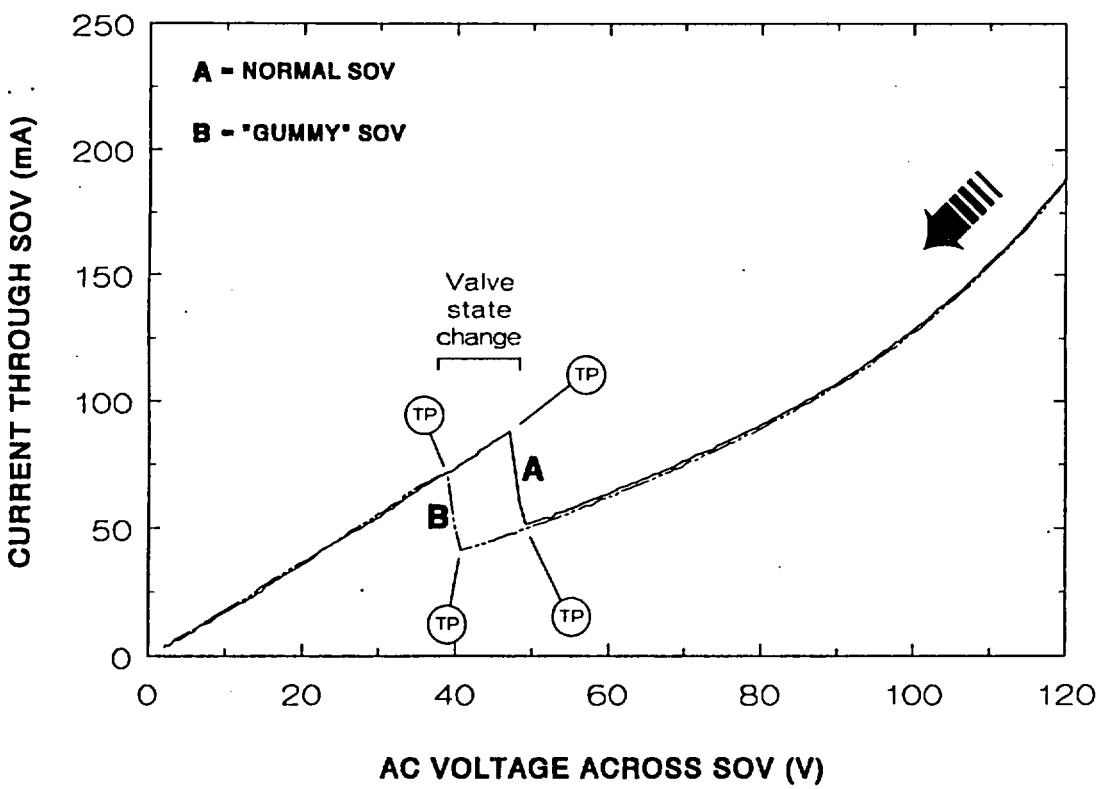

Figure 2.18 Ac current and voltage characteristics obtained during a slow excitation rampdown. (A: clean, normally assembled SOV; B: valve treated to produce binding.)

the core and the interior of the guide tube had been coated with a thin layer of thickened, sticky, liquid shellac during assembly to simulate the mechanical binding that has been found to result from polymerized lubricants, use of excessive thread sealant, or unfiltered air supplies.[1,3,12] The curves are seen to track each other extremely well in the low- and high-excitation regions that represent static plunger positions (i.e., the purely electrical properties are quite reproducible), but they differ markedly in the middle region of the graph at which the valve shifts its state. The "normal" SOV was seen not only to shift at a lower level of excitation than its "gummy" counterpart but also to exhibit some instability as it began to execute the change of state. (The valve was audibly buzzing at this time during the ramp-up.) However, the SOV having internal contamination exhibited a smoother (damped) transition after sufficient magnetic force was developed to overcome the resistance to movement produced by the sticky shellac.

Similar results are obtained if the excitation is ramped in the decreasing (Figure 2.18) rather than increasing direction—namely a pronounced difference between the voltage/current transition points for the normal and sluggish SOVs in addition to lower *V* and *I* critical values than were obtained for the ramp-up. Both upward and downward ramp tests thus establish a set of four pull-in and dropout critical points [identified by "TP" (trendable parameter) symbols in the figures] that can be trended over time to provide early indication of mechanical binding, should it occur.

2.4.2 Consistency of Results for Clean Valves in Good Operating Condition

The degree to which the pull-in and dropout voltages and currents provide reliable, consistent performance indicators was studied only briefly and with mixed results. The reproducibility of the voltages and currents first required to make the plunger draw into the solenoid (i.e., the pull-in point) and then to allow the spring to withdraw the plunger (i.e., the dropout point) was measured for both ac and dc SOVs, as illustrated in Figures 2.19 and 2.20 respectively.* For all these baseline tests the valves were clean and assembled normally. The test duration for the ac-powered valve "D" (Figure 2.19) was ~2 h for 17 trials; for the dc-powered valve "B" (Figure 2.20) the duration was 3 days, each day consisting of 10 trials subdivided into 2 sets of 5 consecutive actuations separated by ~1 h.

Despite careful and consistent test execution, the data scatter is seen to be rather large (±10%) for the ac-powered SOV. The gradual merging of the pull-in and dropout voltage data throughout the tests is thought to be the result of gradual heating of the valve assembly produced by repeated actuations over the relatively short testing period, even though power was applied during each trial only long enough to obtain an accurate measure of the transition points.

Data scatter is substantially reduced (±3%) for the dc-powered SOV, making possible the observation of deviant behavior at each occurrence of first valve operation following a period of inactivity. The anomalous data points in the pull-in voltage and current plots of Figure 2.20 at trial numbers 1, 11, and 21 each represent the first time that the valve was actuated on successive test days. Close examination of these data will reveal a much smaller but consistent aberration on each fifth trial, resulting from the 1-h pause between test sets.

To determine the reason for the more consistent performance of the dc-powered SOV, further tests were conducted on additional valves, yielding the statistical results summarized in Table 2.4. The data plotted in Figures 2.19 and 2.20 correspond to the first and third rows of the table respectively. (Figure 2.19 shows the trial-by-trial results for SOV "D," a valve intended for ac operation and powered by ac for this test, and Figure 2.20 displays corresponding results for SOV "B," a valve intended for dc operation and powered by dc for this test.) In order to sort out performance differences based on different valve constructions from those based on the use of ac vs dc power sources, cross-combination tests were also included in the test matrix (i.e., valves designed for ac operation were tested on dc power as well as on ac).*

The following conclusions may be drawn from the data of Table 2.4 (primarily from the mean values and the variabilities expressed as percent of mean value):

*Completion of the SOV stroke (i.e., the pull-in or dropout point) was ascertained by the sound produced by the core shifting its position. For dc-powered valves, the critical points were clearly audible as a distinct metallic click; for ac-powered valves, the critical points were less precisely determinable, owing to a continuous buzzing of the core in its guide tube as the transition point was approached from either direction (but especially for the upward-going ramp).

*It was not possible to power the SOVs designed for dc operation on ac, however, since their 60-Hz impedances (of about 3 to 5 kΩ) were much too high to permit currents sufficient to actuate the valves to be produced at reasonable applied voltages (<200 Vac). Likewise, SOVs intended for ac operation proved troublesome to test on dc using the motor-driven autotransformer because their coil dc resistances were so small that large currents flowed at quite low excitation voltages, thereby reducing the accuracy achievable with the relatively rapid ramp rate of 2.75 V/s.

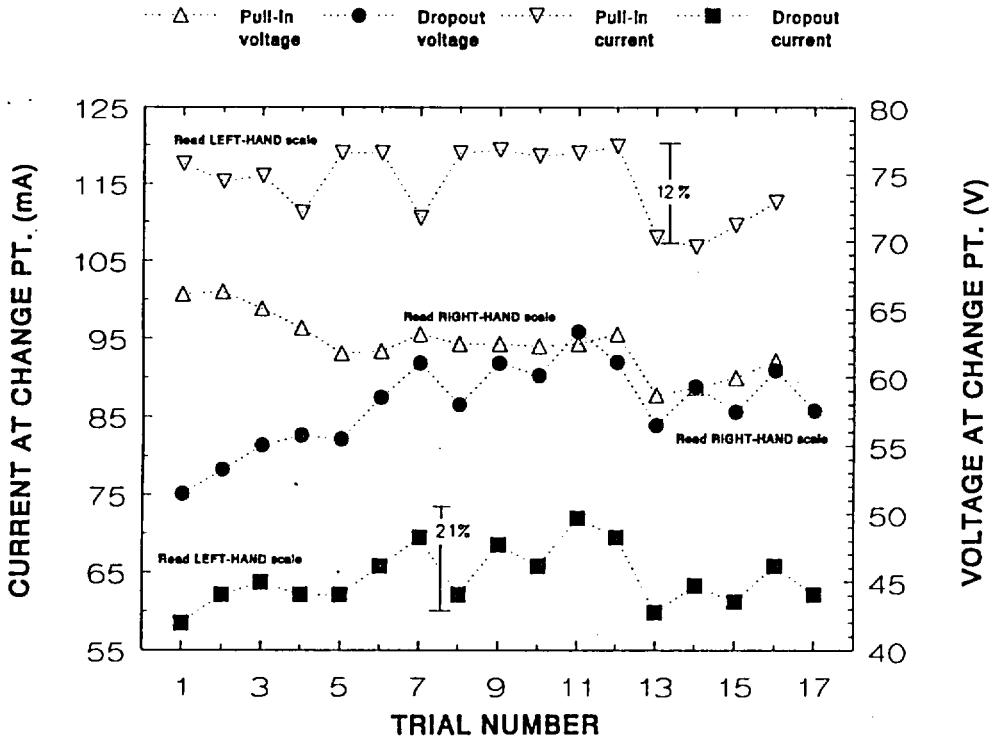

Figure 2.19 Short-term variability of pull-in and dropout voltages and currents for a clean and normally assembled ac-powered SOV. [The gradual merging of the pull-in and dropout voltages (middle curves) with trial number is associated with temperature rise of the SOV resulting from application of power over the testing period (~2 h).]

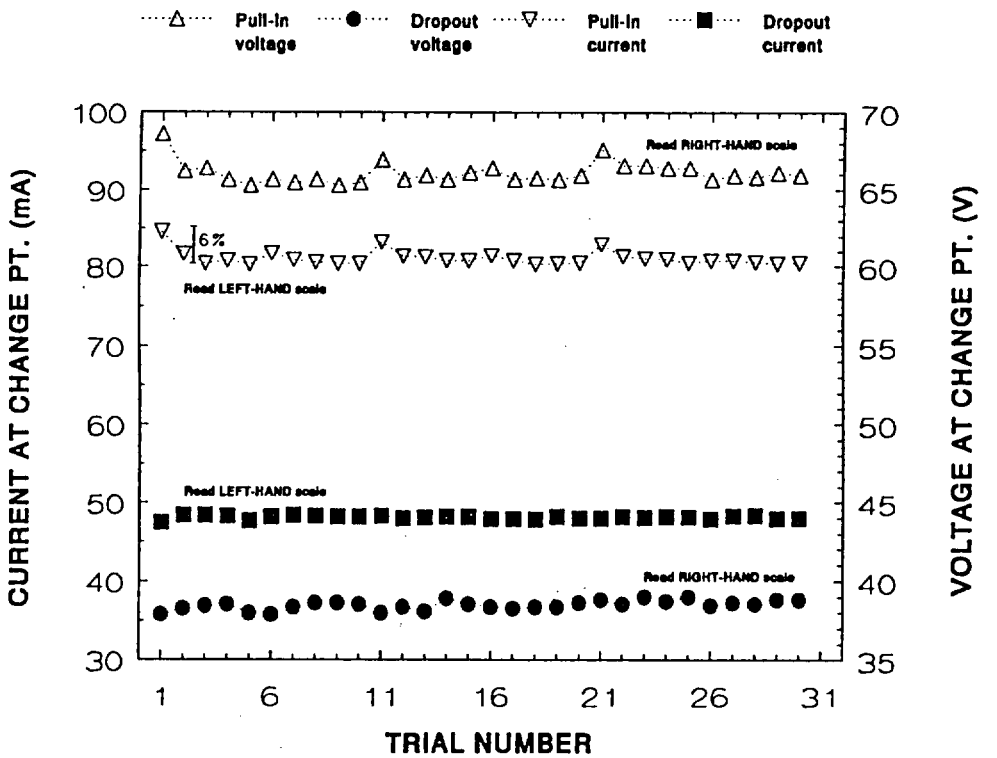

Figure 2.20 Short-term variability of pull-in and dropout voltages and currents for a clean and normally assembled dc-powered SOV. (The discontinuities at trials 1, 11, and 21 result from first operation after a period of inactivity.)

Table 2.4. Variability of SOV actuation levels (pull-in and dropout voltages and currents) and its relationship to solenoid design and power source (ac vs dc)

Valve ID (type)	Power source	Pull-in volts		Dropout volts		Pull-in mA		Dropout mA	
		Min Mean Max	No. of trials Std. dev. (% of mean)	Min Mean Max	No. of trials Std. dev. (% of mean)	Min Mean Max	No. of trials Std. dev. (% of mean)	Min Mean Max	No. of trials Std. dev. (% of mean)
D[a]	ac	58.7	16	51.5	17	106.8	16	58.5	17
(ac)		62.5	2.16	58.0	3.1	115.1	4.6	64.4	3.8
		66.3	(3.5)	63.4	(5.4)	119.9	(4.0)	72.0	(5.8)
A[b]	dc	71.5	31	37.3	31	84.8	31	45.2	31
(dc)		72.2	0.51	38.0	0.40	85.8	0.83	46.1	0.36
		73.4	(0.7)	38.7	(1.1)	88.1	(1.0)	46.7	(0.8)
B[b]	dc	65.3	31	37.9	31	80.2	31	47.5	31
(dc)		66.1	0.68	38.5	0.31	81.0	0.98	48.1	0.21
		68.6	(1.0)	39.0	(0.8)	84.6	(1.2)	48.4	(0.4)
C[b]	dc	48.7	31	6.2	31	60.1	31	7.5	31
(dc)		49.2	0.54	6.71	0.21	60.8	0.75	7.93	0.33
		51.7	(1.1)	7.2	(3.2)	64.5	(1.2)	8.7	(4.2)
D[c]	ac	65.9	28	46.7	28	83.5	28	53.2	28
(ac)		67.8	0.96	48.3	1.04	108	13	70.2	12
		69.9	(1.4)	50.5	(2.2)	123	(12.0)	93.2	(17.3)
E[c]	ac	72.1	28	50.4	28	81.6	28	53.9	28
(ac)		74.9	1.9	56.3	3.1	142.1	42	109.1	38
		78.9	(2.5)	62.4	(5.5)	191.8	(29.5)	155.1	(34.7)
H[c]	ac	64.5	28	37.3	28	116	28	67.9	28
(ac)		66.8	1.52	40.3	1.85	196	69	169	64
		69.0	(2.3)	43.9	(4.6)	304	(35.0)	229	(37.8)
D[c]	dc	20.6	28	2.37	28	150	28	19.8	28
(ac)		21.0	0.45	2.68	0.19	152	2.9	21.0	0.67
		23.1	(2.2)	3.03	(7.0)	166	(1.9)	22.4	(3.2)
E[c]	dc	30.0	28	2.66	28	214	28	21.4	28
(ac)		30.8	0.64	3.09	0.29	219	5.5	23.8	1.8
		33.3	(2.1)	3.68	(9.5)	245	(2.5)	26.6	(7.7)
H[c]	dc	16.3	28	1.10	28	296	28	26.1	28
(ac)		16.6	0.25	1.40	0.18	302	3.6	30.3	1.7
		17.2	(1.5)	1.67	(12.6)	310	(1.2)	32.8	(5.5)

[a]Data acquired 7/88 using instrumentation having 500-ms response (2 readings per second).
[b]Data acquired 2/89 using instrumentation having 500-ms response (2 readings per second).
[c]Data acquired 7/91 using instrumentation having 100-ms response (10 readings per second).

1. For ac SOVs powered on ac, pull-in and dropout voltages appear to be considerably more reproducible from test to test than pull-in and dropout currents.

2. For ac SOVs powered on dc, pull-in voltages and currents appear to be more reproducible than dropout voltages and currents. (This apparent difference may be attributable to imprecise measurement of small numerical values of current and voltage rather than to true valve performance differences, and so must be regarded with some skepticism.)

3. For dc SOVs powered on dc, pull-in and dropout voltages and currents appear to be about equally reproducible, provided that the dropout values are not so small in magnitude that least-count errors in the instrumentation artificially inflate the variance.

4. For the single SOV ("D") for which ac critical-point measurements were repeated after a considerable lapse of time (3 years), the repeatability was only as good as could be expected from the standard deviations estimated from the repeated trials: mean pull-in voltage increased over this period from 62.5 to 67.8 V, whereas

mean dropout voltage decreased from 58.0 to 48.3 V; mean pull-in current decreased from 115.1 to 108 mA, whereas mean dropout current increased from 64.4 to 70.2 mA. (These changes are not consistent with an assumption that valve "D" developed some degree of internal binding over the 3-year idle period because, as is demonstrated by Figures 2.17 and 2.18, binding would be characterized by simultaneous increases in pull-in voltage and current plus decreases in dropout voltage and current, and this is clearly not the case here.)

5. There is some evidence that the detailed properties of the measuring instruments may influence the results obtained. (Citing again the repeat measurements on SOV "D" in 1988 and 1991, it appears that—in the absence of other unknown factors—the use in 1991 of instrumentation having more rapid response caused the standard deviations of the voltage measurements to decrease but caused the standard deviations of the current measurements to increase. This may result from the manner in which the different meters used in 1988 and 1991 compute the rms value of a nonstationary, alternating-polarity voltage or current; this possibility was not investigated further.)

6. Critical voltage and current values are sensitive to valve construction details. For example, the electrical properties of SOVs "A" and "C" are virtually identical (see Appendices A and B), the coil housings look substantially the same (Figure 2.1), and the valve core assembly, core spring, and solenoid base subassembly* are of similar construction, although the actual valve bodies are noticeably different in shape and although two-way SOV "C" lacks the disc holder subassembly incorporated in three-way SOV "A" (see Figure 2.2). The pull-in voltages and currents are about 45% greater for SOV "A" than for "C" (Table 2.4), whereas the dropout voltages and currents are greater for SOV "A" than for "C" by a factor of almost 6. This leads to the conclusion that the magnetic attraction and spring restoration forces must be quite different for the two SOVs, perhaps as a result of different stroke lengths, degrees of core insertion into the solenoid, or materials.

Therefore, despite early results (Figures 2.19 and 2.20) which gave indication that the critical excitation levels were less repeatable for a particular ac-powered SOV than for a particular dc-powered SOV, further investigations with an increased number of samples revealed that a broad generalization of this initial finding cannot be supported because valve construction differences and greater measurement uncertainties for the ac SOVs were shown to affect experimental variance estimates.

Because we had no service-aged SOVs available for test nor any means by which to realistically simulate gradual valve degradation from the binding of internal parts, no data from a degraded SOV are available for comparison. This leaves unproven our contention that measurement of pull-in and dropout voltages and currents should provide reliable indicators of unrestricted plunger movement.

In summary, measurements performed on valves in which plunger movement had been somewhat impeded by artificial (but moderately realistic) means illustrate that measurements of coil voltage and current at valve transition points may be useful as early indicators of SOV contamination by foreign substances, inadvertent use of incorrect internal replacement parts, swollen elastomers, and other deteriorations that can cause sluggishness of the valve plunger. However, further testing will be required to establish the sensitivity and limitations of this performance-monitoring technique. Even though the technique is applicable to both ac and dc SOVs and has no need for add-on sensors or for physical access to the valve, it is also true that measurement of pull-in and dropout critical points is inherently intrusive, necessitating disconnection of the SOV from its normal source of excitation and temporary substitution of a variable-voltage power supply. There is also some indication that the critical points for ac-powered valves—even those in good operating condition—display greater variability than do dc-powered SOVs, which may limit the application of this technique.

2.5 Indication of Shorted Turns or Insulation Breakdown Within the Coil

[Malfunction addressed: electrical failure of solenoid coil, caused by high-voltage turnoff transients in combination with insulation weakened by prolonged operation at high temperatures]

On the basis of recorded operational experience and opinions cited in the Phase I study,[1] a considerable number of coil open- and short-circuit SOV failures may be attributable to high-voltage transients generated by the abrupt collapse of a dc solenoid's magnetic field as a result of circuit interruption. SOVs operating in elevated-

*Refer to Fig. 1.1 for terminology and location of parts.

temperature, high-humidity environments are particularly susceptible to failure from this stressor because the insulating properties of the coil varnish, encapsulating material, and electrical lead wires are weakened under these conditions. The phenomenon is quite similar to the generation of high-voltage pulses of short duration that feed the spark plugs in an automobile's ignition system. Such an ignition system is composed of an ignition coil whose primary winding current is turned on and off rapidly as a result of periodic closing and opening of the breaker points within the distributor. In both the automobile and the SOV, energy that is stored in the magnetic field of an inductor (i.e., the coil) as a result of being energized with dc current is converted at the instant of circuit interruption to an electrostatic potential (i.e., voltage) that appears across the distributed capacitance of the coil (and, in the case of the automobile, across the secondary winding).

It stands to reason that such high-voltage transients within the solenoid coil may produce damage by puncturing the insulation that covers the copper wire of the winding at any existing weak points. When this has happened, the area surrounding the point of puncture becomes carbonized, thereby lowering the insulation resistance and so assuring that the same spot will be the site of electrical arcs upon future valve deexcitations. Once begun, this process produces rapid degradation of the insulation, which will ultimately burn away and leave a permanent turn-to-turn or layer-to-layer short circuit. According to industry sources* the consequences of such a short circuit within the coil are not especially serious for dc solenoids, which will continue to function normally with a considerable number of shorted turns. However, ac solenoids are not so tolerant in this regard because, in effect, a step-down transformer is created by the shorted turn. The result is a large current flow through the shorted turn, intense localized heating, and eventual thermal destruction (followed by electrical destruction) of adjacent portions of the coil (i.e., coil burnout).

An example will serve to illustrate that very high voltages can be generated at the coil terminals at power turnoff, provided that the energy transfer from electromagnetic field to electrostatic potential is accomplished efficiently.** The energy stored in the electromagnetic field of an inductor of inductance L whose field is being sustained by a continuous current I is given[13] by

$$E_{em} = \tfrac{1}{2} L I^2 \ ; \qquad (4)$$

taking $L = 6.5$ H for a typical dc-powered SOV (Appendix C) whose 800-Ω resistance will draw ~155 mA at the rated excitation voltage of 125 Vdc, we obtain $E_{em} = 78$ mJ. Likewise, the energy stored in the electrostatic field of a capacitor of capacitance C charged to a voltage V is given[13] by

$$E_{es} = \tfrac{1}{2} C V^2 \ ; \qquad (5)$$

therefore, if all the energy stored in the inductor were to be transferred to the capacitor, it would charge to a voltage

$$V_c = \sqrt{2E_{em}/C} \ . \qquad (6)$$

Substituting an approximate value of 45 pF for the distributed capacitance of a typical fully assembled SOV yields an estimate for V_c of ~59 kV.

This estimated "flyback" voltage is clearly an upper bound since in practice the energy transfer between the electromagnetic and electrostatic fields cannot be achieved without loss. Nonetheless, as illustrated in Figure 2.21, it is indeed possible to generate large inductive surges at the SOV coil terminals (in this example, almost 25 kV for a duration of ~100 μs) by abruptly deenergizing a 125-Vdc solenoid using a relay having mercury-wetted contacts (Figure 2.22) so as to obtain an extremely rapid interruption of current flow (because the magnitude of the flyback voltage is in large measure controlled by the time derivative of the current, dI/dt). Despite this finding we do not believe that inductive surge need be a major problem in connection with SOV service life, for the following reasons:

- **Coil insulation is tough.** Hundreds of transients of the magnitude shown in Figure 2.21 were produced during the course of this study, but they failed to cause any shorted turns in a variety of coil types having Class H insulation. (It must be acknowledged, however, that our tests were performed in a mild operating environment rather than under loss-of-coolant accident conditions.) The new Class N insulation is claimed to have electrical properties superior to Class H, particularly in high humidity.* Its temperature rating for continuous operation is also 15°C higher than for Class H.

*Telephone discussion, John Shank and Frank Fry, Automatic Switch Company (ASCO), with Robert Kryter (ORNL), November 17, 1988.

**Without going into detail, the rapidity with which the current interruption takes place, dI/dt, is a major determining factor.

*Telephone discussion, John Shank and Frank Fry (ASCO) with Robert Kryter (ORNL), November 17, 1988.

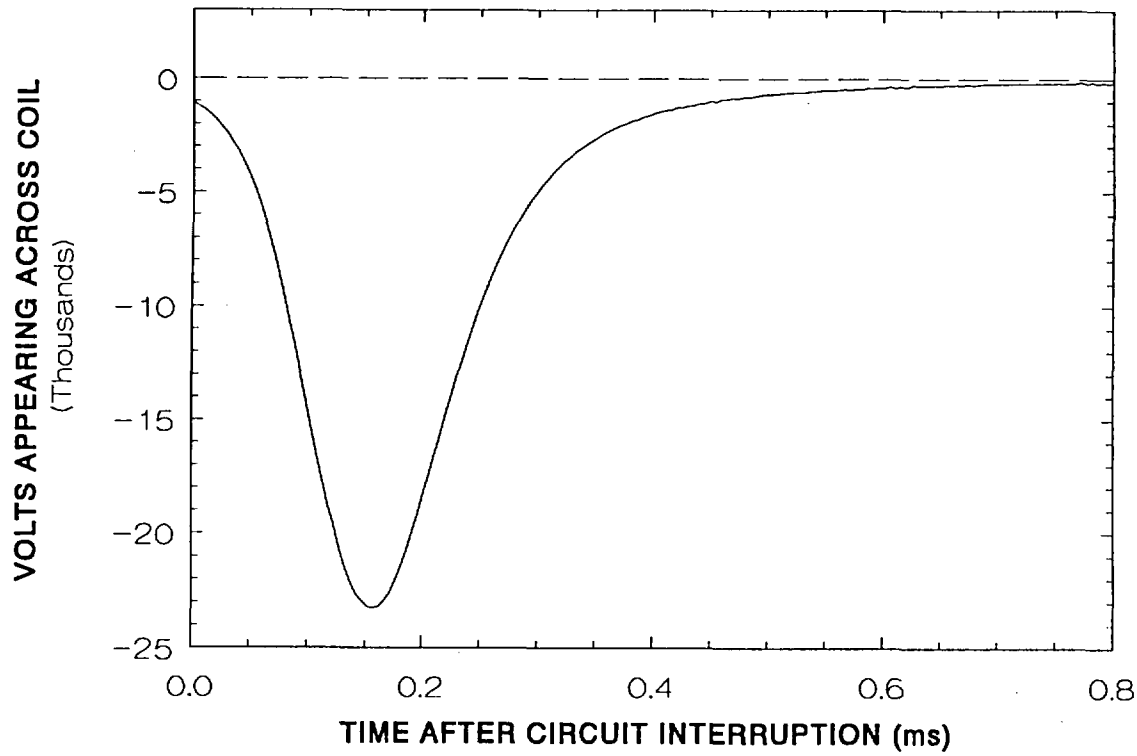

Figure 2.21 Large "flyback" voltages generated when current to 125-V dc-powered SOV "C" was interrupted abruptly. [A mercury-wetted contact relay was employed to obtain clean, extremely rapid circuit-breaking action (with no contact bounce). The test circuit is shown in Figure 2.22.]

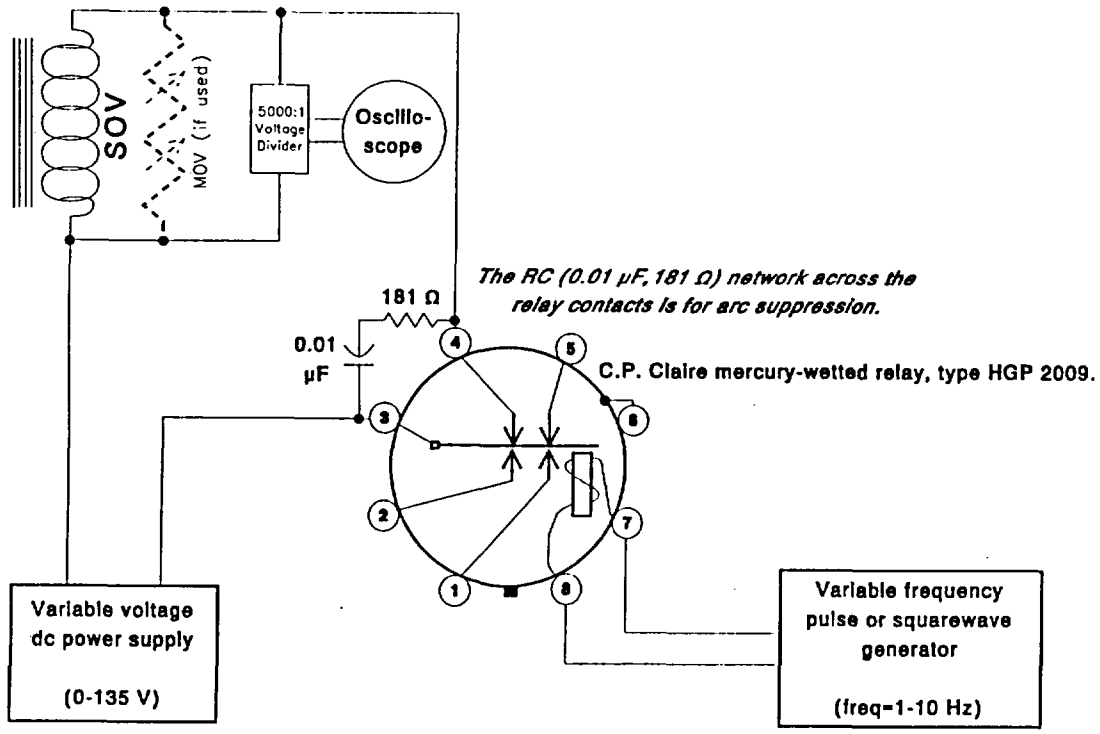

Figure 2.22 Circuit used for measuring transients generated by interruption of coil excitation to a dc-powered SOV.

- **Transient suppression devices are readily available.** Inexpensive metal-oxide varistors (MOVs) can be placed across the coil leads to effectively absorb the energy released by the sudden collapse of the solenoid's magnetic field upon turnoff. [See Figures 2.23(a) and 2.23(b), in comparison to Figure 2.21.] The magnitude of the high-voltage transient produced upon deenergizing the SOV is thereby greatly reduced (e.g., ~600 V rather than ~23,000 V), although the transient's duration is correspondingly extended (e.g., ~20 ms rather than ~0.8 ms). However, the positiveness and rapidity of solenoid release are not noticeably affected by the presence of the transient-suppressing device. (Tests demonstrated an ability to cycle an MOV-protected SOV at a rate of at least 5 actuations per second.) Therefore, no major change in SOV operating characteristics would be expected to result from the addition of such a protective device.* The extent to which transient suppression devices are used for SOV coil protection in U.S. nuclear power plants is unknown to the author.

- **Potentially damaging voltage differences are not as great as they might at first appear.** The voltage differences appearing between adjacent turns and even between successive coil layers are only a small fraction of the total inductive surge voltage appearing across the coil terminals as a result of magnetic field collapse. Industry sources** state that although turn-to-turn short circuits can occur as a result of imperfections in the lacquer insulation coating the copper coil wire, it is quite rare that this causes any problem, because the turn-to-turn voltages are too small to jump the interconductor air gap. It is also stated that layer-to-layer short circuits are practically unheard of because most coil manufacturers place additional dielectric material between successive coil layers during the winding process.**

- **Circuit interruption is likely to be slower in practice.** The manual switch or relay normally employed in nuclear plants will probably not break the circuit as rapidly as the mercury-wetted contact relay used in these laboratory tests; therefore, the flyback voltage generated in practice is unlikely to be as high as that shown in Figure 2.21.

- **Dc SOVs are tolerant of shorted turns.** The previously cited industry sources state that shorted turns present a serious operational problem only for ac-powered SOVs, whereas the production of a large flyback voltage upon circuit interruption is a characteristic of dc-powered SOVs. (Ac-powered SOVs have magnetic fields that continually change polarity, and circuit interruption occurs at a random point with respect to the phase of the 60-Hz power line.)

  Changing our point of view, it is conceivable that the inductive surge phenomenon can be turned to advantage as a means for measuring certain critical solenoid coil electrical parameters that would probably be affected by shorted turns, insulation breakdown, and similar degradations. Following up on work performed by others for NASA,[14] this possibility was investigated by examining the free oscillation ("ring-down") behavior obtained upon deenergization of two bare solenoid coils of identical construction—one undamaged and the other having ~176 of its ~3042 original turns shorted out as a result of having undergone severe EQ tests.* A mercury-wetted contact relay was used to provide a clean circuit interruption, but to avoid the occurrence of dissipative phenomena (e.g., saturation losses in the core iron), only 30 Vdc was applied to the coil instead of the normal operating voltage of 125 Vdc. The undamaged coil was observed to behave like a damped oscillator when deenergized from this lower voltage (Figure 2.24), whereas the waveform produced by the coil with shorted turns was highly asymmetric and died out very rapidly (Figure 2.25).

  Some insight into the marked differences between these two ring-down traces can be obtained by examining the solenoid's lumped equivalent circuit (Figure 2.26). Basically, the inductance of the coil, L, plus some inevitable series resistance, R_L, are seen to be shunted by the distributed (turn-to-turn and layer-to-layer) capacitance of the solenoid, C. In principle, there is also some series resistance, R_{c1},

*This conclusion is in agreement with the authors of ref. 1, who state (on p. 26) "[Although] testing has shown that the operation of a relay actuated by a coil with surge suppression usually takes twice as long as one without this protective feature. . .generally this time delay is small enough not to be a practical concern in control circuits."

**Telephone discussion, John Shank and Frank Fry (ASCO) with Robert Kryter (ORNL), November 17, 1988.

*These coils were loaned to us by John Shank and Frank Fry of ASCO, Florham Park, New Jersey.

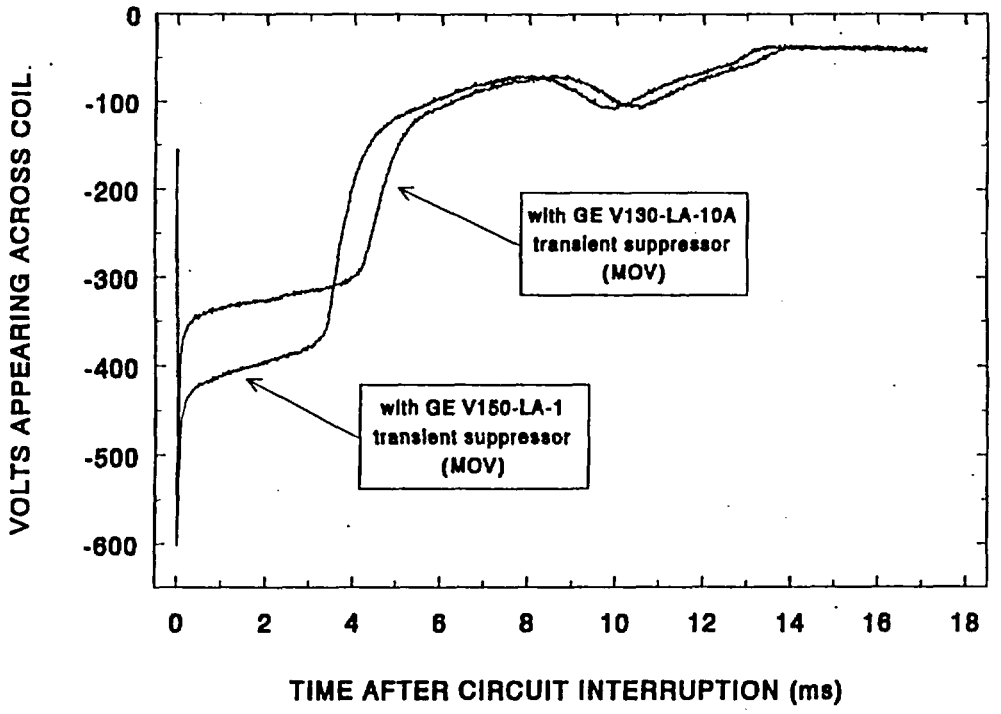

Figure 2.23(a) Same SOV and experimental setup as for Fig. 2.21, except that two varieties of transient-suppressing metal-oxide varistors were placed directly across the terminals of SOV "C" to absorb the energy released by the coil's collapsing magnetic field. (The voltage decay characteristics of the two types of suppressor are essentially the same for times greater than 6 ms. The experimental setup is the same as for Fig. 2.21.)

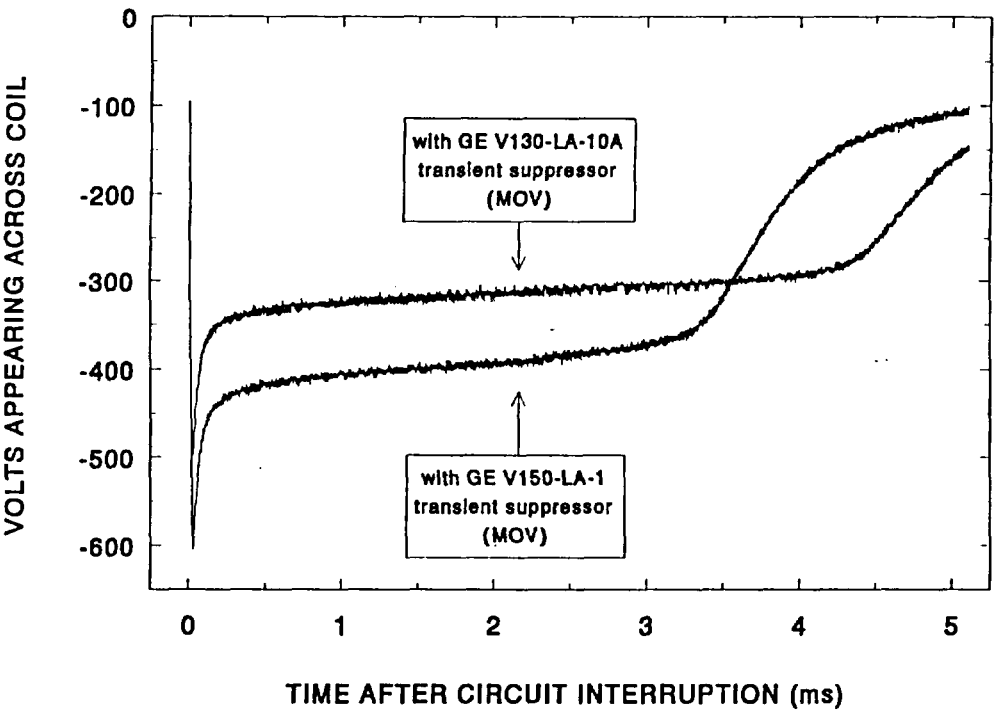

Figure 2.23(b) Time expansion of the early period illustrated in Fig. 2.23(a), showing limitation of peak transient voltage to ~500 V by the 10-A suppressor (upper curve) and to ~600 V by the 1-A suppressor (lower curve). (The suppressor with the higher current rating achieves its somewhat better peak limiting at the expense of slower voltage decay.)

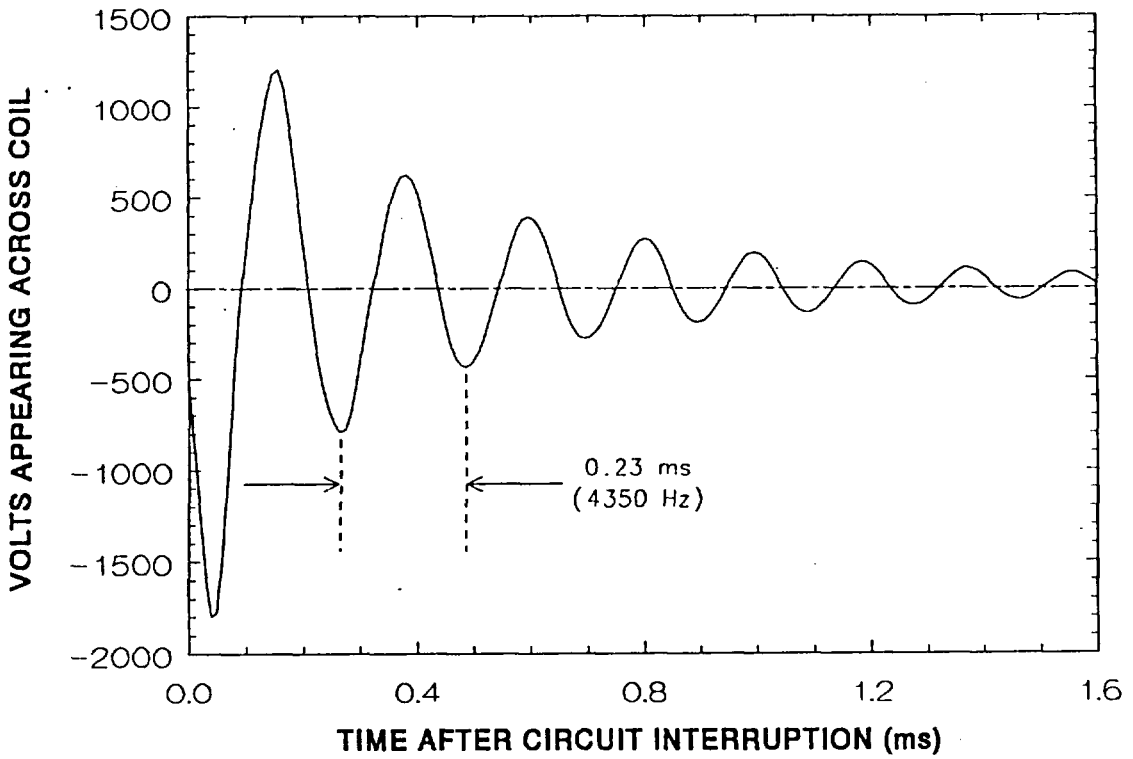

Figure 2.24 The solenoid coil with no shorted turns behaves like a classical damped oscillator when deenergized from 30 Vdc by a wetted-contact relay.

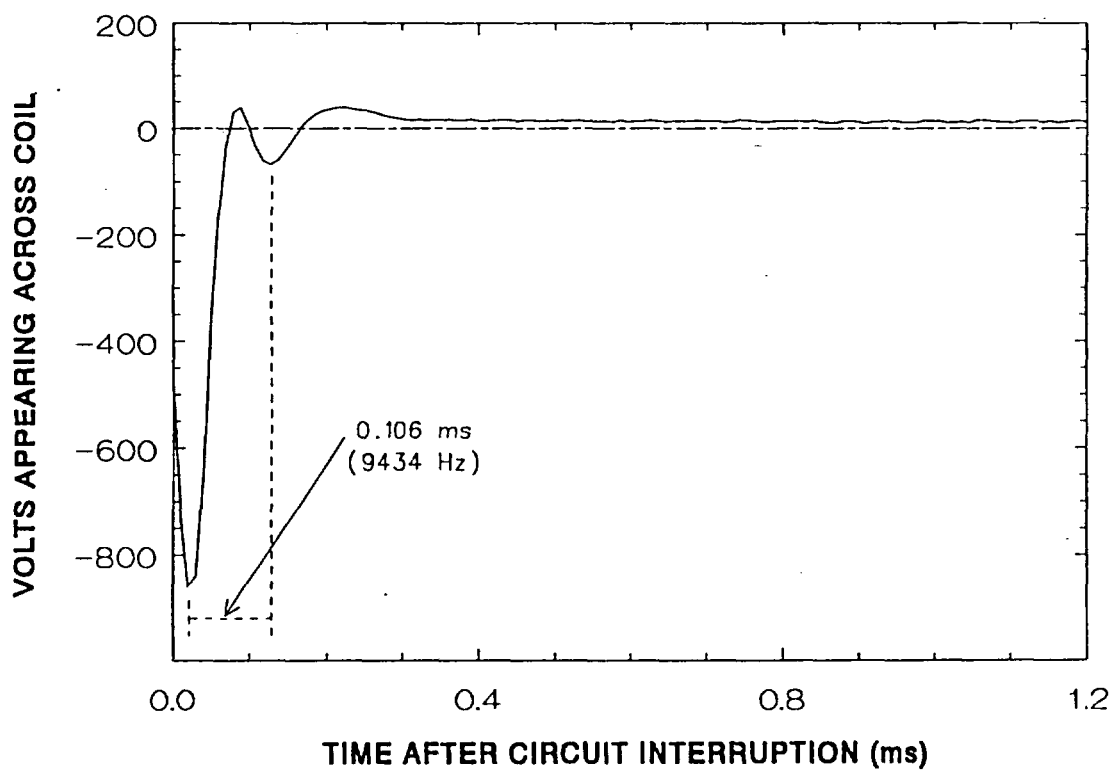

Figure 2.25 The solenoid coil having ~176 of its ~3042 turns shorted behaves quite differently from its healthy counterpart when deenergized from 30 Vdc by a wetted-contact relay.

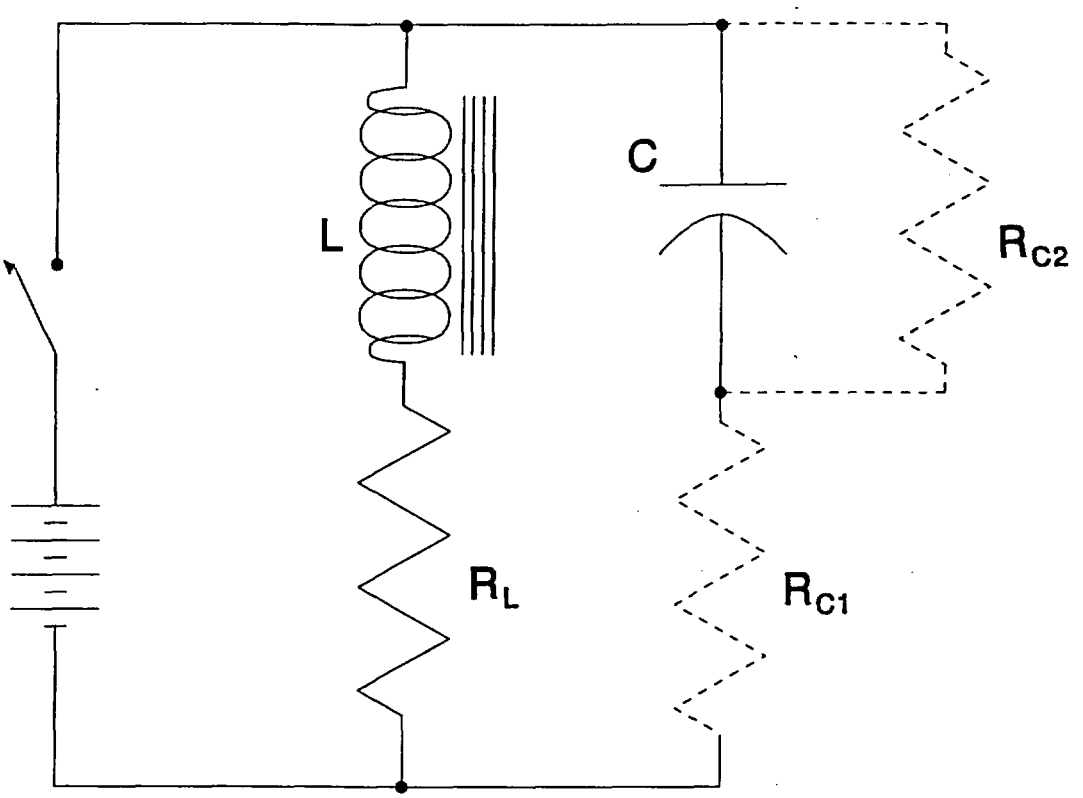

Figure 2.26 Equivalent circuit for an SOV. (As a first approximation, the possible presence of parasitic resistances R_{c1} and R_{c2} may be ignored for simplicity of mathematical analysis.)

associated with the coil's distributed capacitance, but this is probably small in value and can therefore be ignored in first approximation. Likewise, in principle there is also some shunt resistance, R_{c2}, associated with the coil's distributed capacitance, but it is probably very large in value and can therefore be ignored in first approximation. With these simplifying assumptions, the free-oscillation resonance frequency, f_r, for the series/parallel combination of L, R_L, and C is found to be[15] given by

$$f_r = \frac{1}{2\pi}\sqrt{\frac{1}{LC} - \frac{R_L^2}{4L^2}} \quad . \tag{7}$$

Because we can easily measure f_r, L, and R_L, it is convenient to rearrange Eq. (7) and solve for the unknown parallel distributed capacitance, C:

$$C = \frac{4L}{4(Lf_r 2\pi)^2 + R_L^2} \quad , \tag{8}$$

where C is in farads, R_L in ohms, f_r in hertz, and L in henrys. Applying Eq. (8) to transient data obtained on several solenoid coils, both bare and fully assembled (with plunger present and placed inside the protective coil housing), yields estimates of distributed parallel capacitance in the range of 150 to 210 pF (for bare coils) and 30 to 45 pF (for fully assembled SOVs).

Two observations may be drawn immediately from this equivalent circuit analysis:

- The natural resonance frequency associated with circuit interruptions of SOVs (i.e., the ring-down frequency) depends on the value of the inherent distributed capacitance of the solenoid coil that appears in parallel, electrically, with the coil's inductance. Because the numerical value of this distributed capacitance is likely to change substantially if the coil develops faults such as shorted turns or layer-to-layer insulation breakdown, measurement of natural resonant frequency would appear at first glance to be an excellent means of detecting SOV coil electrical faults (as borne out by the strikingly different characteristics of Figures 2.24 and 2.25).

- However, because the capacitance of the electrical cable connecting the SOV to its power source (which may approach a value of tens of nF in practice) also appears in parallel with the SOV coil,

this cable capacitance is likely to completely overshadow the distributed capacitance of the coil alone (which is about 50 pF) and thereby fix the ring-down characteristics of the in-situ SOV, regardless of the true condition of the solenoid coil.

Although providing general insight, the simplified equivalent circuit analysis presented does not appear to explain adequately the marked differences between the ring-down data obtained for the normal SOV solenoid coil (Figure 2.24) vs the SOV coil known to have ~6% of its original turns shorted (Figure 2.25).* First of all, if one calculates the approximate distributed capacitance for the normal and faulted coils from deexcitation transient data using Eq. (8), substantially the same values (210 pF for the normal coil vs 215 pF for the faulted coil) are obtained in both cases.** This finding is contrary to the seemingly reasonable assumption that the presence of shorted turns would alter the coil's distributed capacitance, C. (Perhaps this assumption is true for layer-to-layer but not for turn-to-turn faults; we have no idea which type of fault is present in the defective coil, which is of molded construction and therefore cannot be unwound or examined visually without destroying it.) Secondly, we must deal with the apparent contradiction that although the extremely rapid damping (or die-away) of the faulted coil's transient can be explained in terms of the simplified equivalent circuit model only by an increase in the parameter

$$\alpha = R_L / 2L \tag{9}$$

—because the magnitude of α establishes the rate at which the oscillatory transient dies away with time[15]

$$V(t) = \frac{V_0}{2\pi f_r L} e^{-\alpha t} \sin(2\pi f_r t) \tag{10}$$

—no such large increase in α is actually measurable with a low-excitation-voltage impedance bridge for the defective coil as opposed to the normal one:

$$\alpha_{\text{defective}} = \frac{97.0\ \Omega}{(2)(100.2\ \text{mH})} = 484\ s^{-1}\ , \tag{11}$$

whereas

$$\alpha_{\text{normal}} = \frac{100.4\ \Omega}{(2)(113.9\ \text{mH})} = 441\ s^{-1}\ . \tag{12}$$

In fact, other than the vastly different free-oscillation characteristics, about the only electrical properties that are significantly different for the faulted and unfaulted coils (Table 2.5) are the in-phase component of impedance, Re(Z), measured at an excitation frequency of 1000 Hz (231.2 vs 103.8 Ω), and the closely related quality factor, Q, also measured at 1000 Hz (2.7 vs 6.9).

We have no explanation for the discrepancies described; they are presented for completeness and in the hope that some more knowledgeable reader may be able to use these results to obtain a better understanding of the phenomena involved. Perhaps the lumped equivalent circuit model is just too simple to account for the changes introduced by shorted turns within the solenoid coil, or perhaps the shorts are not "hard"; that is, their presence is unmeasurable at the low levels of excitation applied by the impedance bridge and detectable only when the coil is subjected to high-voltage transients.

In summary, it is clear that additional research will be needed to advance the understanding of the various electrical phenomena that occur in coils having defective windings before a practical SOV coil diagnostic system can be devised, should it be decided that one is truly needed. Results also show that it may be impractical to perform coil diagnosis in situ from a distant location using any sort of measurement technique based on free oscillation upon deexcitation, because the capacitance of the power leads connecting the valve to its power source may be several times larger than the distributed capacitance of the coil itself (thereby clouding interpretation of the measurement). However, if the coil power leads can be accessed directly (with the capacitive burden of the cable removed), the flyback transient characteristics may provide a far more sensitive indication of coil insulation breakdown than does simple change in dc resistance.

Note also that if transient suppression devices (MOVs) were used consistently to protect dc-powered SOVs, a major contributor to solenoid coil failure would be eliminated, leaving only operation at excessive temperatures (and perhaps radiation damage in a very few plant locations) as a significant stressor for coil insulation.

*Telephone discussion, John Shank and Frank Fry (ASCO) with Robert Kryter (ORNL), November 17, 1988.

**The data used to estimate C are not those shown in Figures 2.24 and 2.25, since the latter data were obtained at 30 Vdc where R-C relay contact protection is required, thereby making the test results more difficult to interpret. The transient curves used to estimate C were obtained without relay contact protection at 10 Vdc, where resonant frequencies of ~34 kHz were observed.

Table 2.5. Room-temperature electrical properties of faulted and normal bare coils

Property	Coil 17 (3042 eff. turns before, 2866 eff. turns after EQ tests)	Coil 18 (3039 eff. turns before and after EQ tests)[a]
R_{dc}	97.0 Ω	100.4 Ω
Re(Z) (5 Hz)	97.66	101.13
Im(Z) (5 Hz)	3.09	3.32
Re(Z) (60 Hz)	98.05	101.02
Im(Z) (60 Hz)	40.02	42.92
Re(Z) (1 kHz)	231.2	103.8
Im(Z) (1 kHz)	629.8	715.7
L (5 Hz)	98.4 mH	105.8 mH
Q (5 Hz)	0	0
L (60 Hz)	106.15 mH	113.86 mH
Q (60 Hz)	0.4	0.4
L (1 kHz)	100.22	113.92 mH
Q (1 kHz)	2.7	6.9

[a]EQ—environmental qualification.

2.6 Other Methods Examined or Proposed

[Degradations or malfunctions addressed: mechanical looseness or binding and valve leakage caused by worn, degraded, or improper parts or the presence of foreign materials inside the valve]

Four additional potentially useful monitoring and diagnostic measurement techniques identified for study midway through this investigation were

- analysis of the detailed time "signature" of inrushing current that produces SOV actuation;
- detection of the presence of humming or chattering of the plunger assembly within ac-powered SOVs (indicative of mechanical wear) using either frequency analysis of the coil current signal or an acoustic sensor placed in close proximity to the valve;
- verification of complete and normal SOV opening and closure (including the detection of valve leakage) based on the acoustic "signature" sensed by a miniature microphone placed in close proximity to the SOV; and
- inference of plunger position within the valve body based on the magnetic field strength external to the SOV as sensed by a Hall effect device placed on the valve exterior.

In principle, these techniques should permit the detection of worn or improper parts and extraneous materials, valve misassembly, degraded elastomers, and misalignment of the solenoid core. Although the purely electrical techniques would require no special sensors to be fitted to the valve, affixing an acoustic or magnetic sensor to the valve would make possible as well the detection of through-valve and external leakage of process fluid, the identification of plunger mechanical problems, and positive verification of plunger movement.

These first two measurement techniques were examined briefly but were soon abandoned as unpromising. The signature of the inrush current accompanying normal SOV switch-on had been studied earlier by Meininger and Weir with somewhat inconclusive results.[16] Their data analysis had focused almost exclusively on the frequency domain (where they were unable to demonstrate marked sensitivity to the presence of valve problems), so we naturally turned to further exploration of waveform properties in time. However, after acquiring the inrushing-current data shown in Figure 2.16 (demonstrating by the variable impedance properties of an ac-powered SOV that its plunger movement is very rapid—complete in ~20 ms following the application of power—and therefore difficult to track electrically) and performing a few additional inrushing-current tests on dc-powered SOVs with no positive results, it was decided not to pursue this idea further.

The technique of identifying looseness and vibration by the detection of perturbations to the coil current waveform [presumed to result from the humming or chattering of SOV internals at the frequency of the magnetization reversals (60 Hz) or its harmonics] was also examined without much success. Current waveforms typical of both normal and loosely assembled (i.e., audibly buzzing) valves are shown in Figure 2.27; very little difference can be seen,* indicating that feedback of the audible mechanical vibration into the time-dependent current drawn by the solenoid is almost nonexistent. This conclusion is reinforced by the spectra of these waveforms (Figure 2.28)—both assembly conditions are characterized by the presence of strong odd harmonics (n = 1,3,5. . .) of the 60-Hz fundamental but, except for a slightly higher current amplitude** when the valve is correctly assembled, the spectra are substantially identical—in particular, no new frequencies [with the possible exception of the appearance of even harmonics (n = 2,4. . .)] appear to arise as a result of the buzzing internal parts. Given these unpromising results, detailed analysis of coil current waveform as a means of detecting looseness and vibration in ac-powered SOVs was not pursued further. However, this is not to imply that a miniature acoustic sensor placed on or near the valve would have a similar difficulty in detecting excessive internal vibration; in fact, judging from the clearly audible low-frequency buzzing produced by loosely assembled valves, such a locally positioned sensor would probably be quite effective in detection of wear or misassembly. Of course, the extra complexities of add-on instrumentation may affect the practicality of such an approach, but the basic principle seems to be sound.

The latter two measurement techniques listed at the beginning of this section were never actually tried owing to the pressure of time and programmatic limitations. However, others have reported considerable success with the use of a miniature microphone placed near the SOV to sense, through differences in time- and frequency-domain signatures, incomplete opening and closure of SOVs used in a BWR control-rod-drive scram system.[17]

It seems reasonable to assume that similar information could be derived using a Hall effect device placed on or near the SOV to detect magnetic field changes accompanying correct execution of plunger stroke, as an alternative to monitoring the acoustic signature characteristic of correct valve opening and closure. Hall effect devices are tiny and thereby provide good spatial resolution but, being solid-state devices, they are not known for their robustness in high-temperature, radiation-containing environments. However, their usefulness in this application merits study if further research is performed in this area.

Finally, there would be added benefit if the findings of this SOV investigation could be applied and utilized creatively, wherever practical, in surveillance and testing programs directed at safety-related electrical components of nuclear power plants other than SOVs.

*The two waveforms have been time-shifted slightly to facilitate shape comparison.

**This causes the mean value of the spectral ratio plotted in Figure 2.28(c) to be >1, which is consistent with the greater peak amplitude seen in Figure 2.27.

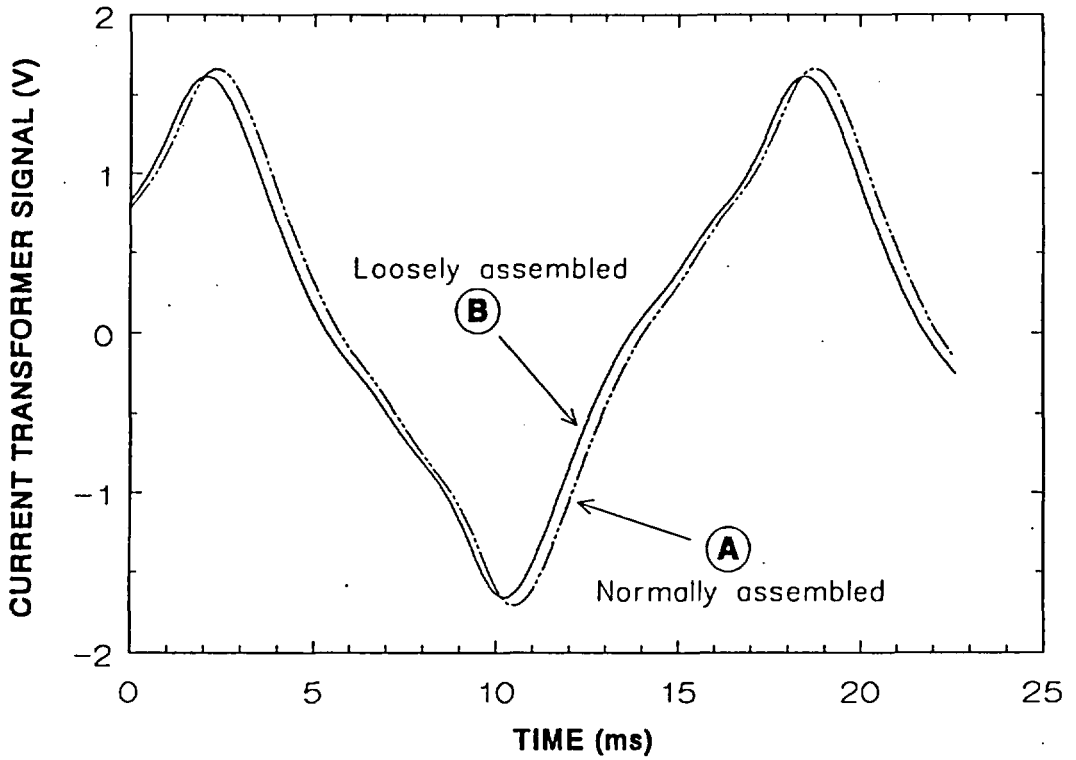

Figure 2.27 Coil current time waveforms for a 60-Hz ac-powered SOV. (A: normally assembled, no audible buzzing; B: loosely assembled, loud buzzing indicating vibration of internal parts. The waveforms are distorted because an iron-cored current transformer was used to acquire the data without breaking into the circuit.)

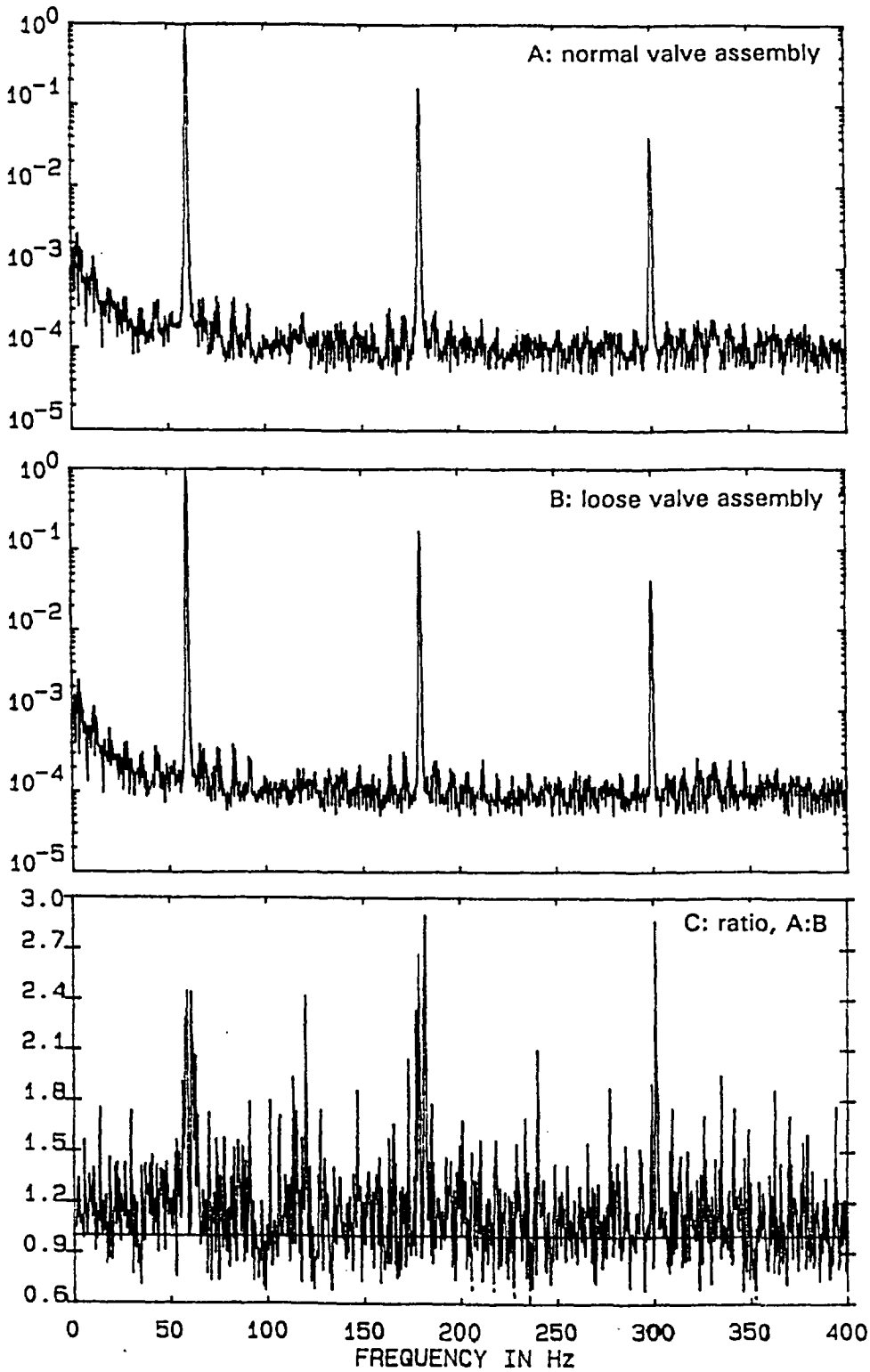

Figure 2.28 Coil current frequency spectra derived from the waveforms shown in Fig. 2.27. (A: normally assembled SOV, no audible buzzing; B: loosely assembled SOV, loud buzzing indicating vibration of internal parts; C: line-by-line ratio, spectrum A divided by spectrum B.)

3. CLOSING REMARKS AND RECOMMENDATIONS

Because our review of the technical literature did not reveal any degradation-monitoring techniques (either presently in widespread industrial use or under development) that are oriented specifically to SOVs, this Phase II study was necessarily more inventive than evaluative in nature. However, the work has revealed a number of SOV-monitoring methods based on electrical properties that are potentially useful for ascertaining operational readiness through the measurement of degradation-sensitive performance parameters that may be trended over component life. In so doing, early indications of poor performance that may foreshadow more serious malfunctions or failures of these devices can be obtained, thus aiding in the scheduling of maintenance activities or timely valve replacement.

The four techniques receiving the most attention were

- measurement of coil mean temperature during operation by in situ measurement of coil electrical dc resistance or ac impedance, combined with an experimentally established temperature coefficient of resistivity for the copper winding (i.e., the same principle as a resistance thermometer);
- indication of plunger movement upon application of ac power, plunger static position within the solenoid coil, and freedom of plunger movement within the guide tube by means of measurement of coil ac impedance (inductance) changes resulting from movement of the iron plunger relative to the coil;
- detection of mechanical binding by tracking changes in the electric current (or voltage) at the SOV critical bistable (pull-in and dropout) points, because these define conditions of balance between electrical (magnetic), spring (restoring), and friction forces within the SOV assembly; and
- detection of shorted turns or insulation breakdown within the solenoid coil based on the characteristics of the "flyback" transient generated when a dc SOV is deenergized abruptly.

Two other techniques were examined briefly and then abandoned because initial results showed little promise for eventual development into effective degradation detection and diagnosis tools. They were

- detection of mechanical binding by analysis of the detailed time "signature" of inrushing current that accompanies initial plunger movement upon application of electrical power to the SOV, and
- indication of mechanical looseness (resulting from wear of internal valve parts, improper assembly, or replacement with incorrect internal parts) by electrical detection of the presence of humming or wear-producing chattering of the plunger assembly within ac-powered SOVs, using frequency-domain analysis of the coil current signal.

Strengths shared by most of these monitoring techniques include the following:

- The measured parameters have been demonstrated to be sensitive to historically important modes and causes of SOV failure.
- Most of the measurement techniques employed are minimally disruptive to plant operations.
- The diagnostic tests can be performed at a location remote from the SOV with no attendant degradation in sensitivity.
- The SOV can often be made to serve as its own sensor, thereby eliminating the need for additional instrumentation and signal wires.

Weaknesses of the examined monitoring techniques must also be acknowledged and include the following:

- Those techniques requiring a momentary change of valve state or short-term substitution of a special electrical power supply are disruptive to plant operations.
- The monitoring techniques described may not cover all conceivable types of aging-related degradation and may not be universally applicable to SOVs of all type, size, and construction.

Also, as a result of programmatic priorities and limited resources, some planned tests whose results might have yielded additional insights were never performed but are

recommended for serious consideration in any future investigation in this area. Among these are

- further study of the reproducibility of SOV pull-in and dropout critical points and their sensitivity to realistic, progressively worsening problems. Compare baseline measurements with those obtained after introducing different sources and degrees of mechanical binding to the valve (using thread sealant, lubricating compound used to aid the assembly of internal valve parts, metal or paint chips, etc., in combination with heat). Try introducing internal contamination more naturally by repeated cycling of valves held at elevated temperature while connected to an oil-contaminated compressed air supply.

- further study of the coil impedance change accompanying plunger motion. Determine the sensitivity with which the following can be verified electrically: (1) obstructions (i.e., dirt, metal slivers and paint chips) that restrict total plunger travel and (2) permanently indented or chemically degraded (i.e., gummy) elastometric valve seats.

A major criticism that can be leveled at the overall investigation is that it does not go far enough—that is, that the monitoring techniques studied were demonstrated only in a controlled laboratory environment, using a small population of unaged SOVs of substantially similar construction and a limited number of implanted (rather than naturally occurring) defects. Accordingly, it is recommended that in a future study,

- performance-monitoring techniques be field-tested using a larger population of both new and naturally aged SOVs that would be likely to display one or more varieties of degraded performance, and

- techniques be refined and adapted as is necessary to permit their use in a real plant environment (for example, devise a means for applying a dc interrogation signal to an ac-powered SOV so that its temperature could be measured accurately even in a normally energized state, or devise a means for ascertaining free plunger movement upon SOV turn-on without need for a special ramped-voltage power supply).

Finally, there would be added benefit if the findings of this SOV investigation could be applied and utilized creatively, wherever practical, in surveillance and testing programs directed at safety-related electrical components of nuclear power plants other than SOVs.

4. PUBLICATIONS RESULTING FROM THIS WORK

1. Kryter, R. C., "Assessment of Nonintrusive Methods for Monitoring the Operational Readiness of Solenoid-Operated Valves," *Proceedings of the 16th Water Reactor Safety Information Meeting, October 24–27, 1988, Gaithersburg, Maryland,* NUREG/CP-0097, Vol. 3, March 1989.

2. Kryter, R. C., "Nonintrusive Methods for Monitoring the Operational Readiness of Solenoid-Operated Valves," *Nucl. Eng. Des.* 118, 409–17 (1990).

3. Kryter, R. C., "A Nonintrusive Method for Measuring the Operating Temperature of a Solenoid-Operated Valve," p. II-3-3-1 in *Guide for Monitoring Equipment Environments During Nuclear Plant Operation,* NP-7399, proceedings of the EPRI Workshop on Monitoring Equipment Environments During Nuclear Plant Operation, April 10–11, 1990, Baltimore, Maryland, Electric Power Research Institute, Palo Alto, California, June 1991.

REFERENCES

1. Bacanskas, V. P., G. C. Roberts, and G. J. Toman, "Aging and Service Wear of Solenoid-Operated Valves Used in Safety Systems of Nuclear Power Plants, Vol. 1: Operating Experience and Failure Identifications," NUREG/CR-4819, Vol. 1, March 1987.

2. Ornstein, H. L., "Operating Experience Feedback Report—Solenoid-Operated Valve Problems," NUREG-1275, Vol. 6, February 1991.

3. Verna, B. J., "Commendable Operator Performance and Solenoid-Operated Valve Problems," *Nucl. News*, 32–33 (July 1991).

4. Ref. 2, Sect. 8.1, p. 32, and Sect. 8.2, p. 32.

5. Institute of Electrical and Electronics Engineers, "Evaluation of Maintenance and Related Practices for Solenoid Operated Valves in Nuclear Power Generating Stations," 89TH0248-5 PWR, New York, March 1991.

6. Arrhenius, S., Z. *Physik. Chem.*, 4, 226 (1899). Available in public technical libraries. Simplified descriptions of the so-called Arrhenius Law may be found in most university-level physical chemistry textbooks (e.g., Laidler, K. J., *Chemical Kinetics*, 2nd ed., McGraw-Hill, New York, 1965, pp. 50–54; also Frost, A. A., and R. G. Pearson, *Kinetics and Mechanism*, 2nd ed., Wiley, New York, 1961, pp. 22–25).

7. Institute of Electrical and Electronics Engineers, Inc., "IEEE Standard for Qualifying Class IE Equipment for Nuclear Power Generating Stations," IEEE 323-1974, New York, September 1983.

8. Institute of Electrical and Electronics Engineers, Inc., "IEEE Standard for Qualification of Safety-Related Valve Actuators," IEEE 382-1985, New York, 1985.

9. Bacanskas, V. P., G. J. Toman, and S. P. Carfagno, "Aging and Qualification Research on Solenoid Operated Valves," NUREG/CR-5141, August 1988, Sect. 6.4, p. 31.

10. Chemical Rubber Publishing Company, *Handbook of Chemistry and Physics*, 37th ed., Cleveland, Ohio, Sept. 1, 1955, pp. 2355–61.

11. Henney, K., ed., *Radio Engineering Handbook*, 5th ed., McGraw-Hill, New York, 1959, Chap. 5, p. 11.

12. Ref. 2, Sects. 4, 5.2.3, and 5.2.4.

13. Ref. 11, Chap. 1, p. 105.

14. George C. Marshall Space Flight Center, "Pulse coil tester," MFS-29301, *NASA Tech Briefs*, Huntsville, Alabama, March 1988.

15. Ref. 11, Chap. 5, pp. 18–21.

16. Meininger, R. D., and T. J. Weir, "Development of a Testing and Analysis Methodology to Determine the Functional Condition of Solenoid-Operated Valves," NUREG/CR-5008, September 1987.

17. McElroy, J. W., "BWR Control Rod Drive Scram Pilot Valve Monitoring System," *Proceedings of EPRI Conference 'Incipient Failure Detection for Power Plants,' October 10–12, 1984, Orlando, Florida*, Electric Power Research Institute, Palo Alto, California.

APPENDIX A

DC RESISTANCES OF NINE TEST VALVES OVER THE TEMPERATURE RANGE OF 20 TO 165°C

The nine fully assembled SOVs used in this study (Table 2.1) were placed simultaneously in a thermostatically controlled, electrically heated oven whose interior temperature could be held constant (to within ~±1°C) at any desired value from ambient to 165°C, the highest temperature we believe likely to be achieved by SOV self-heating alone (i.e., ignoring the possibility of fire or a steam leak). The electrical leads from the solenoids were passed through a hole at the top of the oven, which was then sealed with thermal insulation. The oven temperature was read externally from a mercury-filled capillary stem thermometer protruding into the oven cavity and in close proximity to the valves.

After each temperature change, resistance measurements were delayed for a minimum of one hour in order to ensure isothermal conditions within the valve bodies and coils. Measurements were made with a digital electronic ohmmeter of ~0.1% repeatability that employed a low excitation level (1.5 V) so as to minimize heat deposition within the coil as a result of the measurement itself, which required ~3 s to perform on each valve.

The test results are shown in Figures A.1 through A.9, where coil dc resistance is plotted against oven (and therefore coil) temperature on linear scales.

The following observations and conclusions were drawn from these measurements:

1. The variation of dc resistance, R_{dc}, with temperature over the range of interest to this study (20 to 165°C) is almost exactly linear (i.e., the coefficient of correlation = 0.9997 or better for all nine SOVs). Thus, R_{dc} is a highly accurate indicator of coil mean temperature, as long as the resistivity of the copper winding remains constant with thermal cycling and the passage of time.

2. The magnitude of the temperature coefficient of coil resistance is sufficiently large to permit accurate temperature inference using resistance-measuring equipment of only modest accuracy:

   $$\left|\text{(change in } R_{dc})/°C\right| \approx 0.3 - 0.4\% \text{ at } 20°C$$

   $$\left|\text{(change in } R_{dc})/°C\right| \approx 0.27 - 0.35\% \text{ at } 70°C$$

   Thus, if measurements were to be made with industrial-grade equipment accurate to within only 2 to 3% of reading, inferred coil temperature would nonetheless be accurate to about ±10°C (assuming that the temperature coefficient of resistance is known to somewhat greater accuracy, presumably through laboratory measurements). Such temperature accuracy is probably quite sufficient for purposes of component life prediction.

3. The measured value of the temperature coefficient of resistance compares favorably with the magnitude predicted by typical handbook values of ρ and α for annealed copper:[1]

   Resistivity (ρ) of pure annealed Cu at 20°C = 1.692 E-6 $\Omega \cdot$ cm

   Temperature coefficient of resistivity (α) of pure annealed Cu over the range 0 to 100°C = 0.00433 E-6 $\Omega \cdot$ cm/°C.

   $$\text{Therefore, } \left|(\Delta\rho/\rho)\right| = \frac{0.00433}{1.692} \Rightarrow 0.256\%/°C \text{ at } 20°C \ .$$

REFERENCE

1. Chemical Rubber Publishing Company, *Handbook of Chemistry and Physics*, 37th ed., Cleveland, Ohio, Sept. 1, 1955, pp. 2355–61.

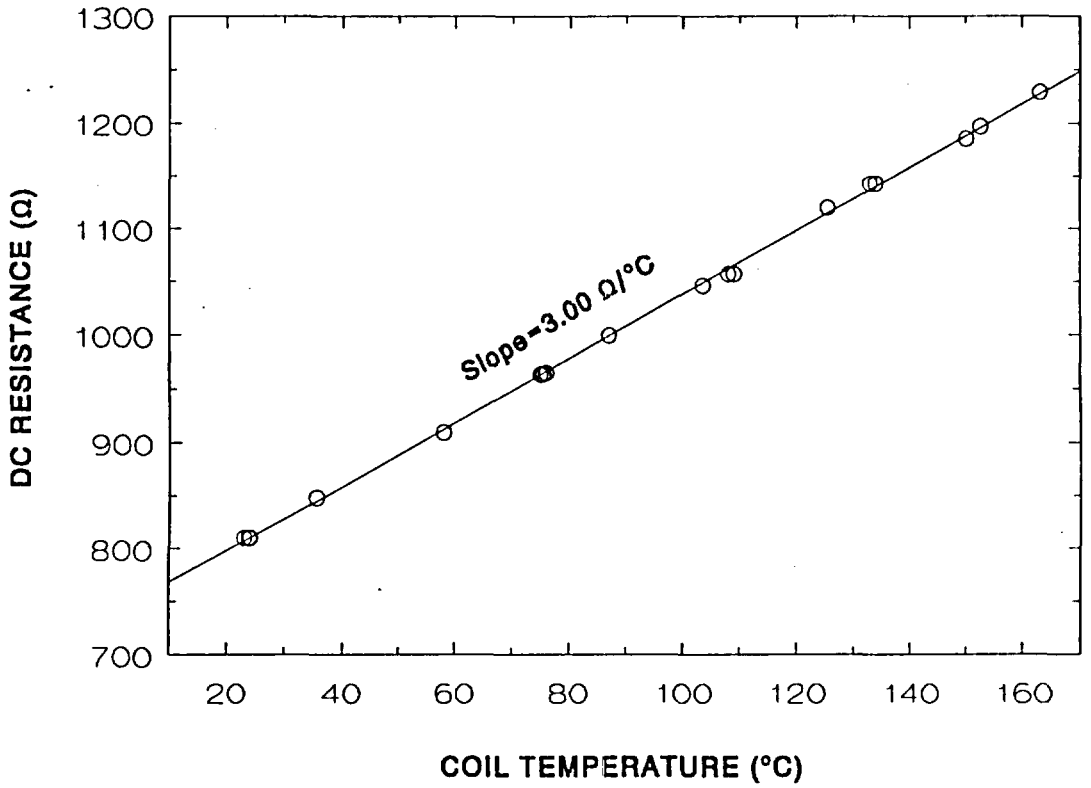

Figure A.1 Dc resistance vs temperature: SOV "A."

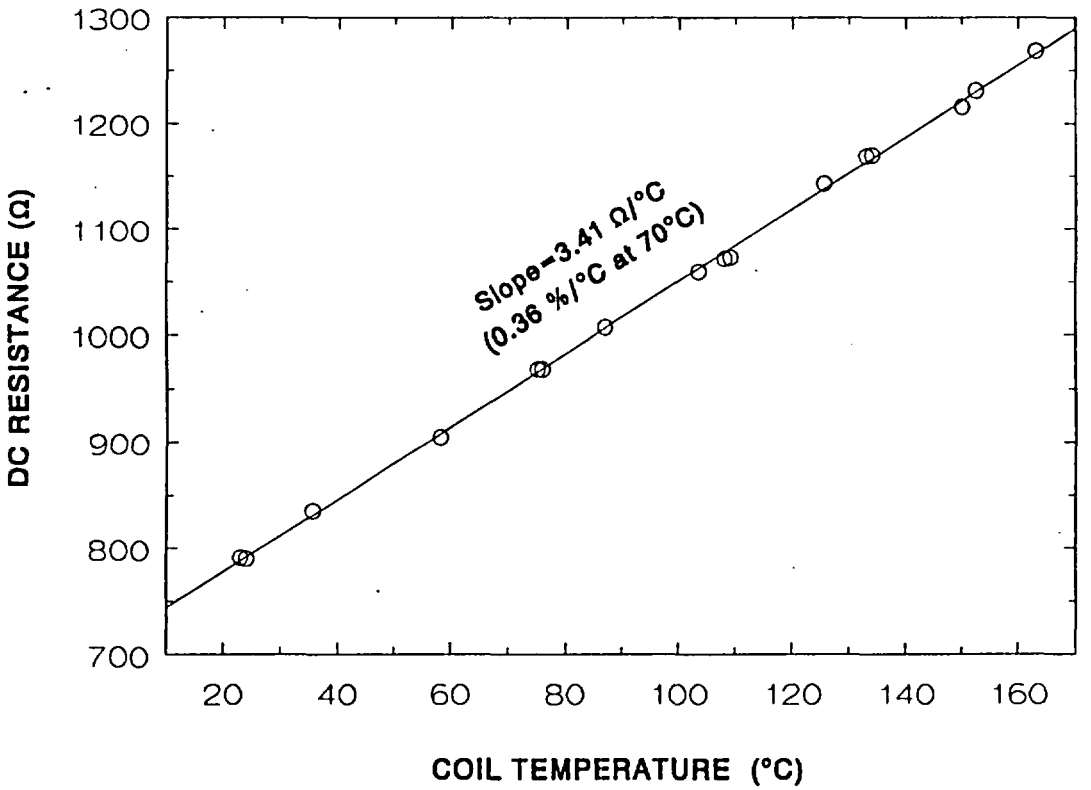

Figure A.2 Dc resistance vs temperature: SOV "B."

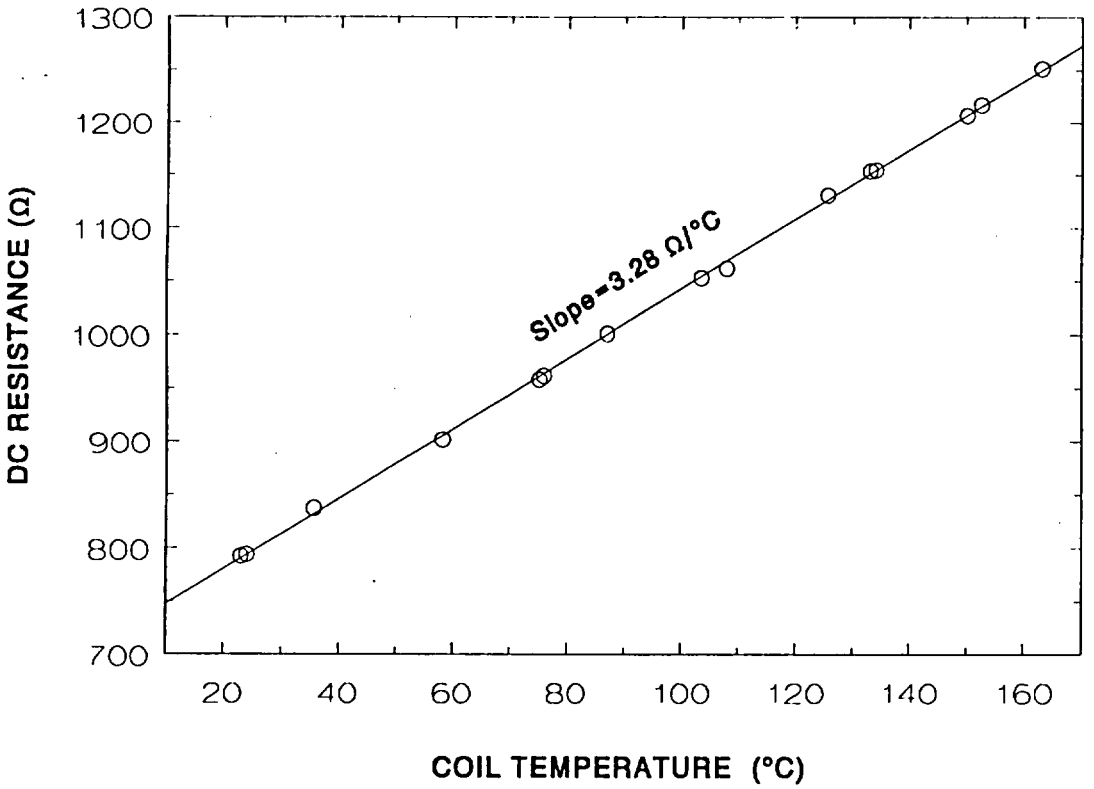

Figure A.3 Dc resistance vs temperature: SOV "C."

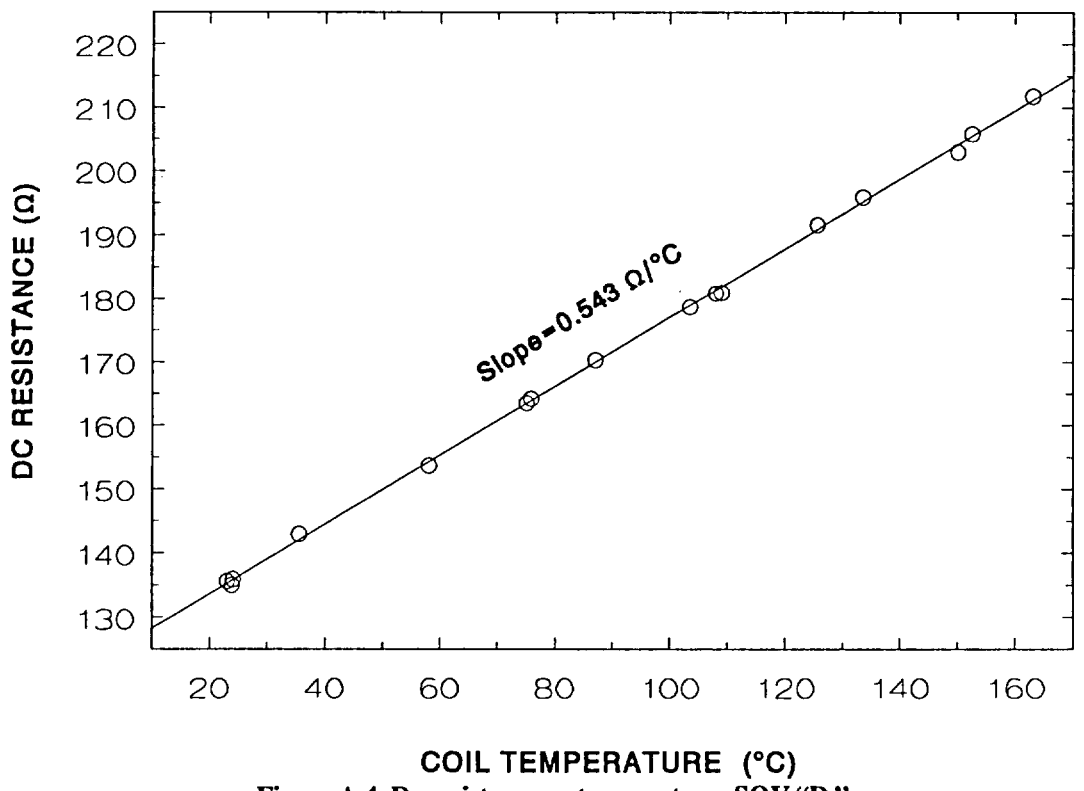

Figure A.4 Dc resistance vs temperature: SOV "D."

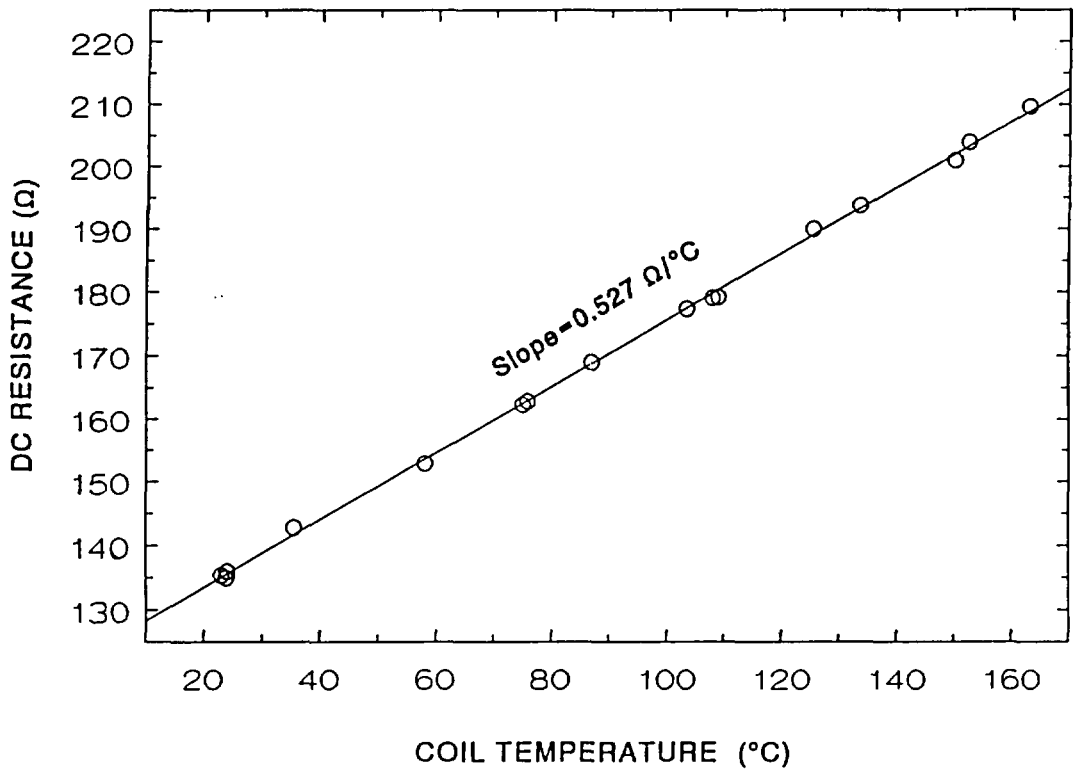

Figure A.5 Dc resistance vs temperature: SOV "E."

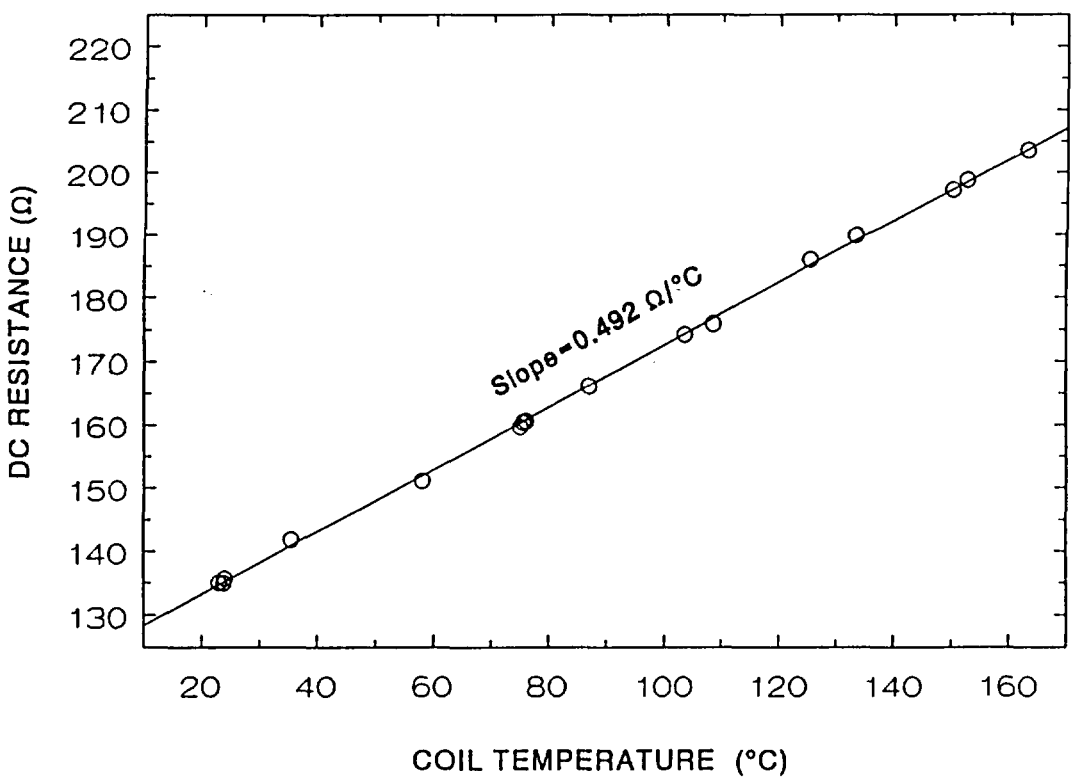

Figure A.6 Dc resistance vs temperature: SOV "F."

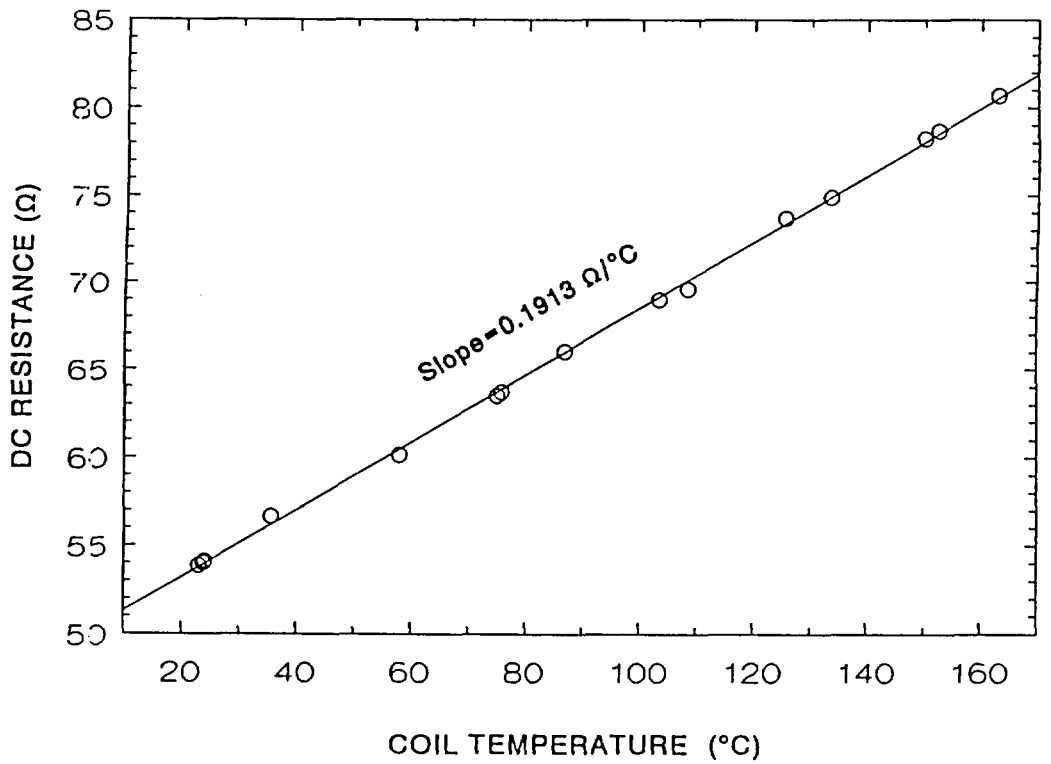

Figure A.7 Dc resistance vs temperature: SOV "G."

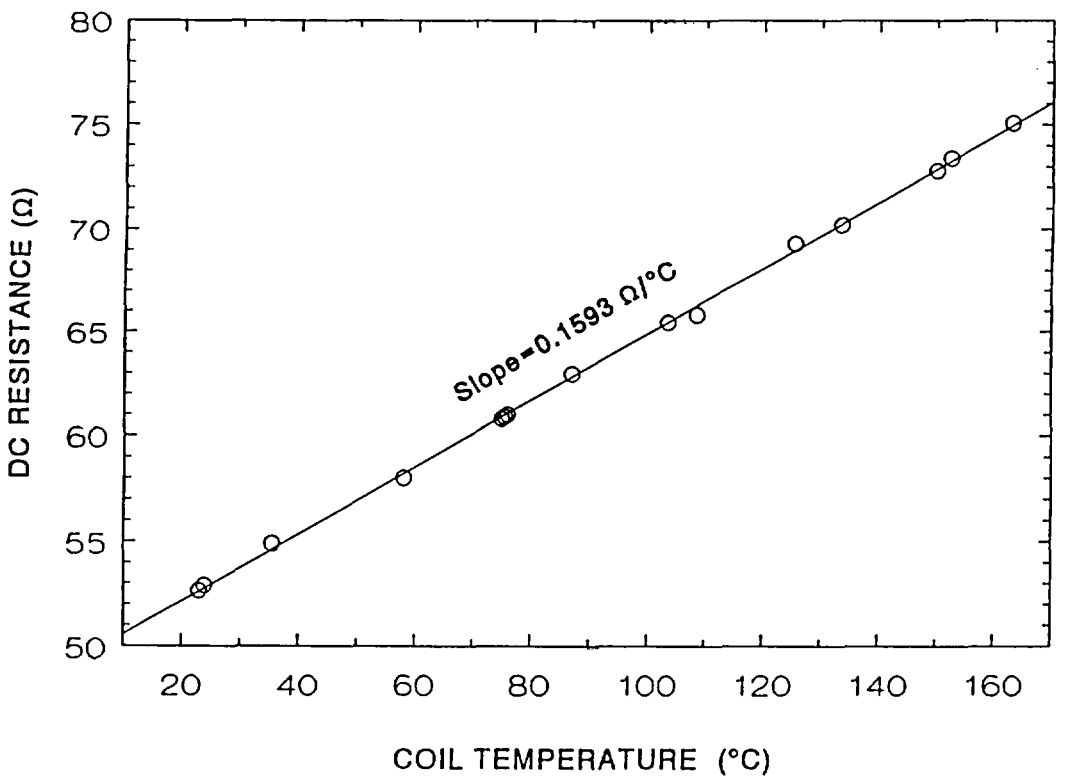

Figure A.8 Dc resistance vs temperature: SOV "H."

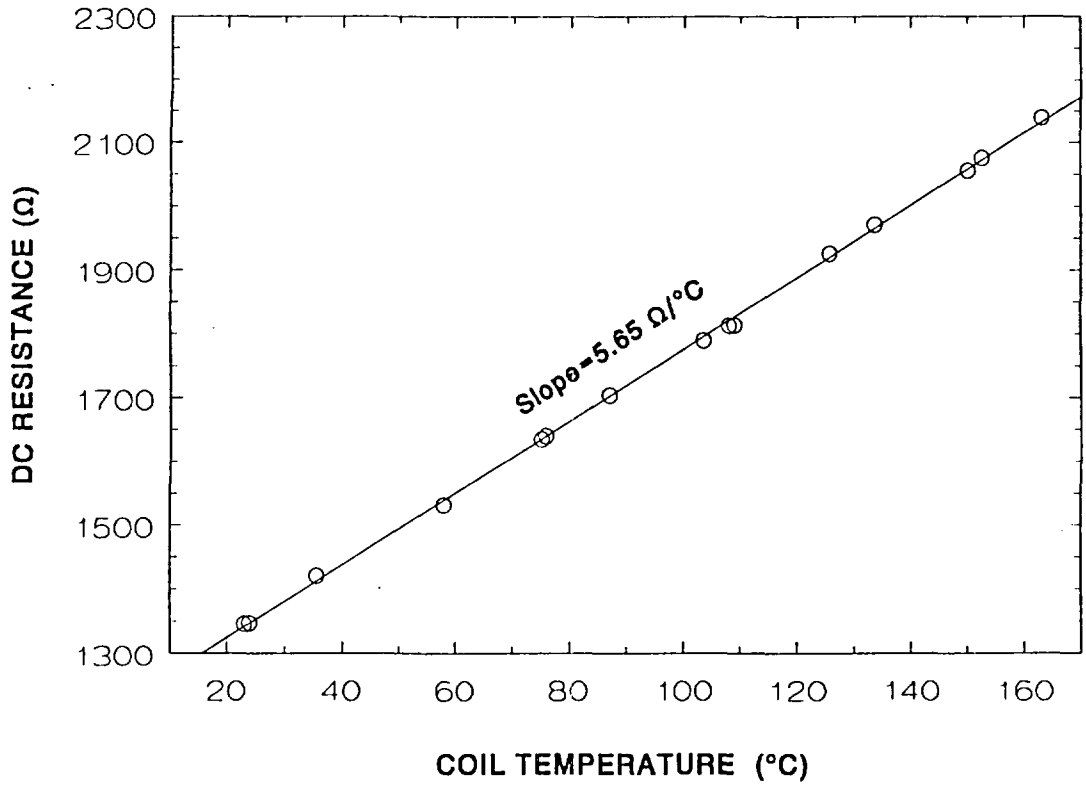

Figure A.9 Dc resistance vs temperature: SOV "L"

APPENDIX B

AC IMPEDANCES OF FIVE SELECTED TEST VALVES OVER THE TEMPERATURE RANGE OF 20 TO 155°C AT THREE WIDELY SEPARATED FREQUENCIES: 5, 60, AND 500 Hz

Using exactly the same setup and procedures as described in Appendix A for dc resistance measurements, ac impedances were measured for five fully assembled SOVs (i.e., "A", "C", "E", "G", and "I") as a function of temperature at three fixed excitation frequencies.* To minimize self-heating, the measurements were performed at a low level of excitation (1.1 V_{rms}) using a Hewlett-Packard model 4192A low-frequency impedance analyzer. The five SOVs were selected to be representative of various types of physical construction (e.g., solenoid coil, valve body, plunger/guide tube arrangement) and electrical design (i.e., ac and dc operation).

The results of these tests are shown in Figures B.1 through B.15, where the real (in-phase), imaginary (quadrature), and vector magnitude (absolute value) representations of the complex impedance are plotted against oven (and therefore coil) temperature on linear scales. Also shown for reference is the dc resistance (shown by a dashed line), which should be equivalent to the ac impedance extrapolated to zero frequency.

The following conclusions and observations were drawn from these data:

1. As would be expected, the complex impedance at an excitation frequency of 5 Hz is nearly all real [i.e., the imaginary component, Im(Z), is comparatively small], and the real component, Re(Z), is very nearly equal to R_{dc}. Also, both Re(Z) and R_{dc} display the same temperature coefficient (i.e., the same magnitude of positive slope with increasing temperature). In addition, the imaginary component of the impedance is essentially independent of temperature at 5 Hz.

2. Both Re(Z) and $|Z|$ display highly linear dependencies on temperature. At an excitation frequency of 5 Hz, they also have essentially the same slope.

3. Coils designed for 125 Vdc operation (i.e., "A", "C", and "I") display quite similar variation of impedance with temperature and frequency as those designed for 117 Vac operation (i.e., "E" and "G"), although the actual impedances are much greater for the dc coils, because they are wound with many more turns of wire than the coils intended for operation at 60 Hz ac.

4. Re(Z) is ~50% larger than R_{dc} at 60-Hz excitation frequency (and 5 to 10 times larger at 500 Hz) but continues to show excellent linearity with temperature and almost as large a temperature coefficient (expressed as ohms per degree C) as R_{dc}. However, since Re(Z) > R_{dc} at frequencies higher than 60 Hz, the percentage change in value per degree C (which provides a yardstick of difficulty in performing a measurement) is less (namely, ~0.1 to 0.3%/°C) for Re(Z) at these frequencies than for R_{dc}, although still in the range of field measurement practicability.

5. At excitation frequencies of 60 and 500 Hz, Im(Z) is no longer independent of temperature, but the magnitude of the temperature coefficient of this quadrature component of impedance is significantly smaller than the temperature coefficients associated with R_{dc} and Re(Z).

6. As a result of observations 4 and 5 above, the change (expressed as a percent of value) per degree C is considerably smaller at 60 or 500 Hz for $|Z|$ than for either Re(Z) or R_{dc}. This is unfortunate from a standpoint of field measurement, because $|Z|$ is the quantity most easily measured, being merely the ratio of the root-mean-square voltage applied to the coil (V_{rms}) to the root-mean-square current drawn by the coil (I_{rms}). Therefore, obtaining a temperature estimate accurate to ±10°C would require measurements of V_{rms} and I_{rms} (yielding $|Z|$) to accuracies considerably better than ±1% if the coil's temperature coefficient is only 0.1% of value per degree C. Note that such measurement accuracy is 2 to 4 times greater than would be required of an R_{dc} measurement yielding the same ±10°C uncertainty in coil temperature, because of the larger temperature coefficient associated with R_{dc}.

*With the exception of 60 Hz—which was selected, of course, because it is the frequency of the power mains throughout the United States—the selection of the other two test frequencies was arbitrary. However, 5 and 500 Hz represent reasonable lower and upper limits for test signals that would be practical to apply to plant wiring.

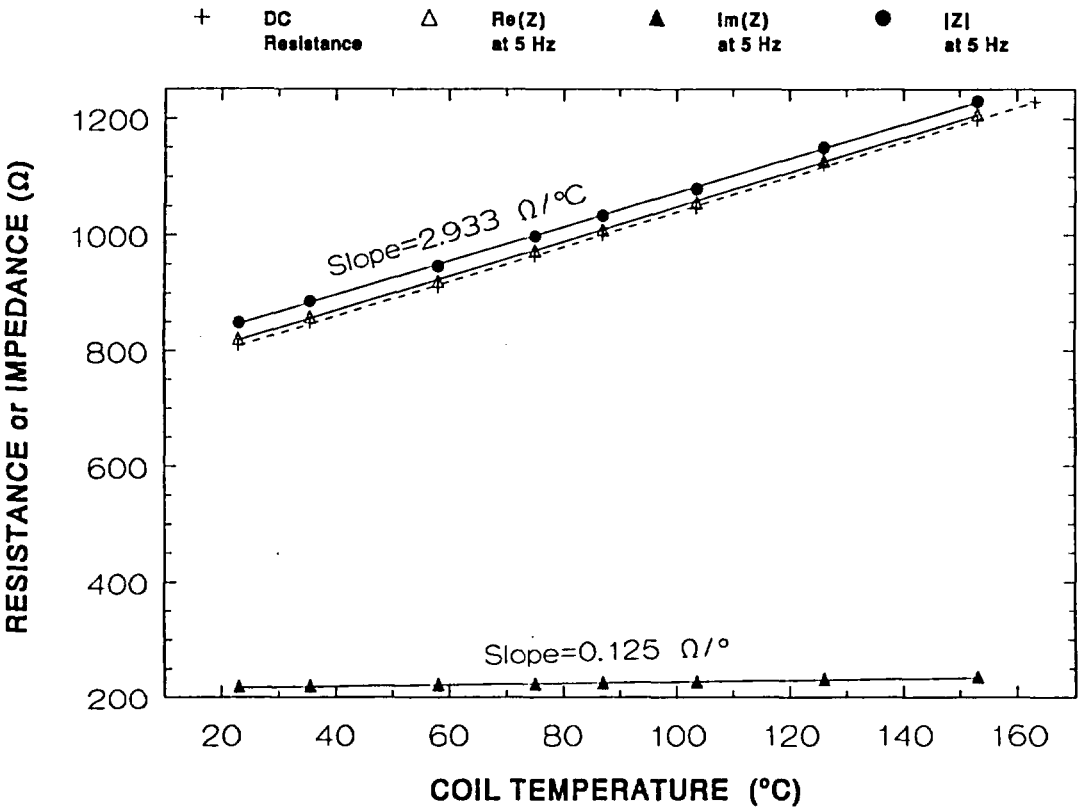

Figure B.1 Dc resistance, 5-Hz impedance vs temperature: SOV "A."

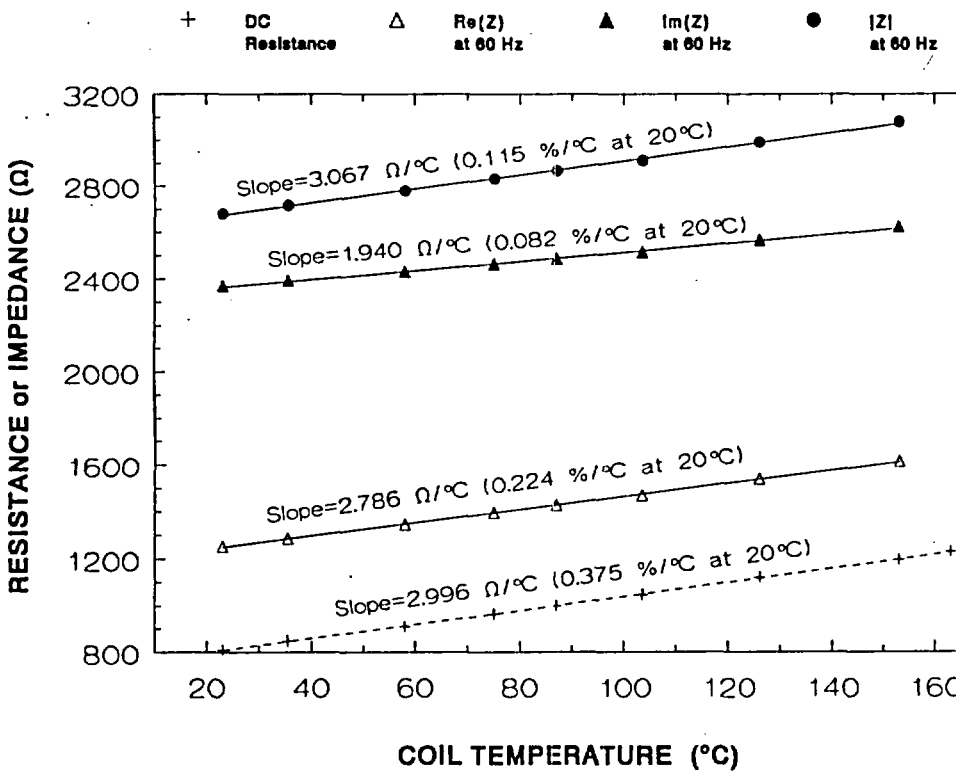

Figure B.2 Dc resistance, 60-Hz impedance vs temperature: SOV "A."

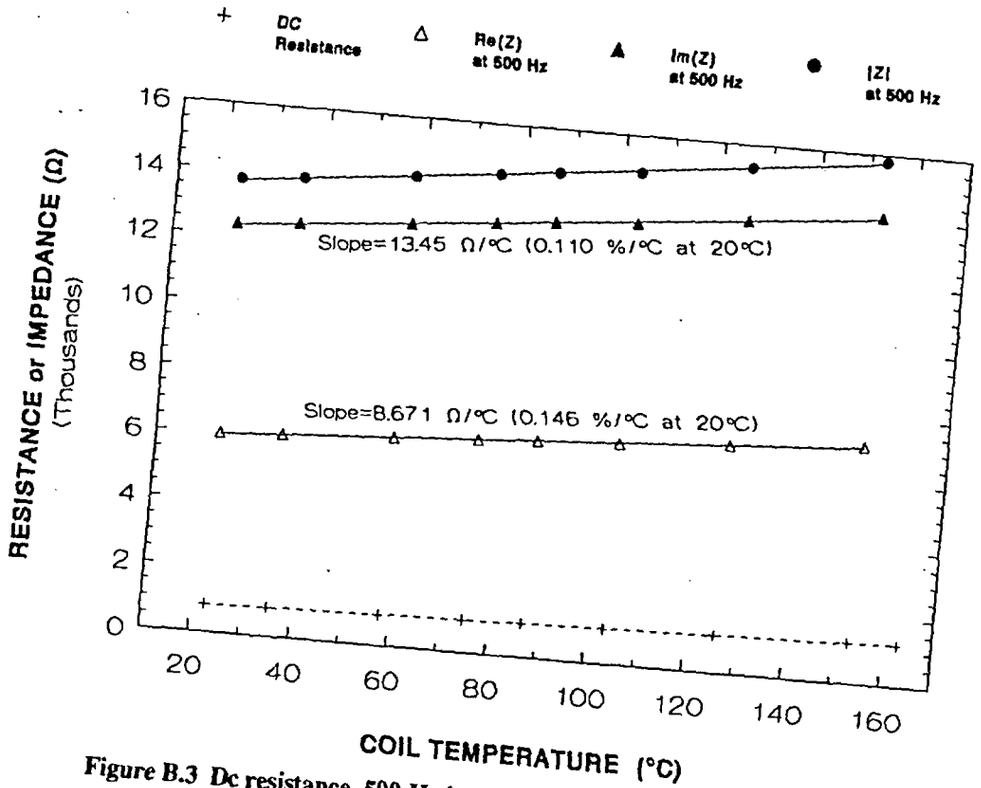

Figure B.3 Dc resistance, 500-Hz impedance vs temperature: SOV "A."

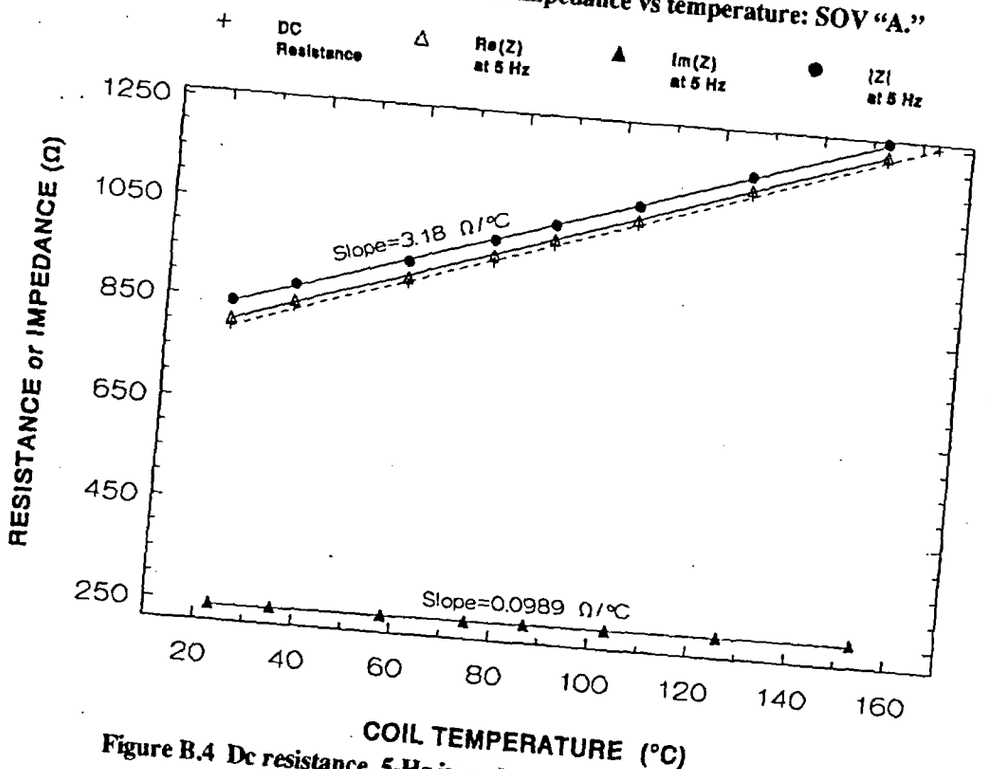

Figure B.4 Dc resistance, 5-Hz impedance vs temperature: SOV "C."

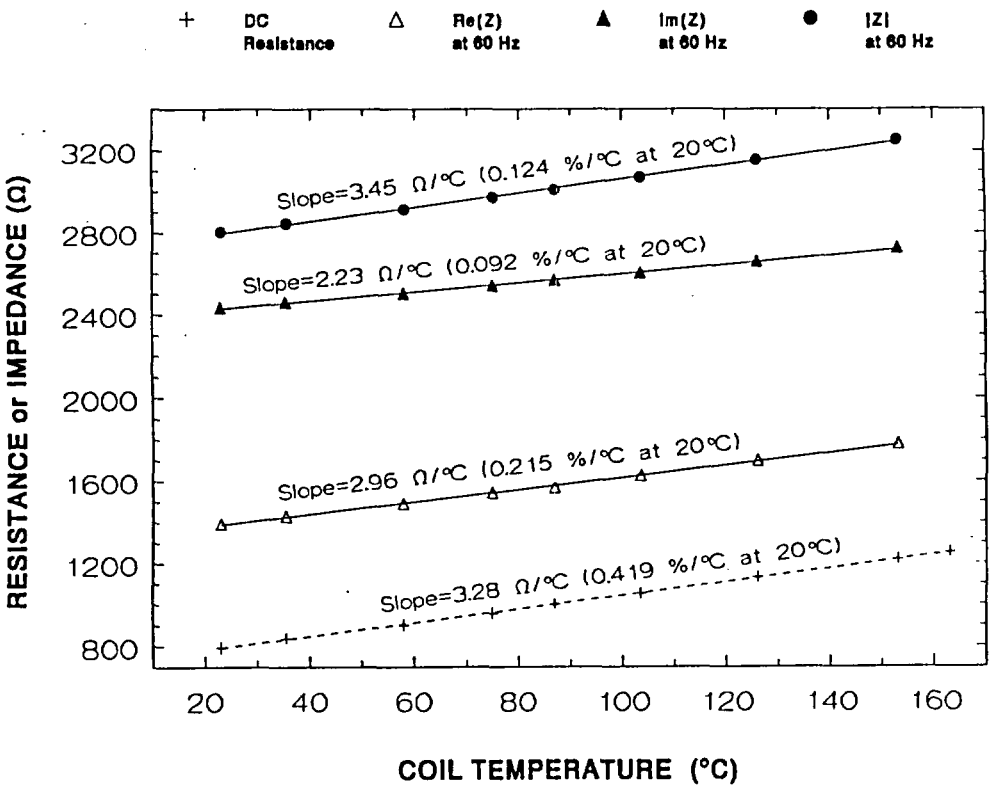

Figure B.5 Dc resistance, 60-Hz impedance vs temperature: SOV "C."

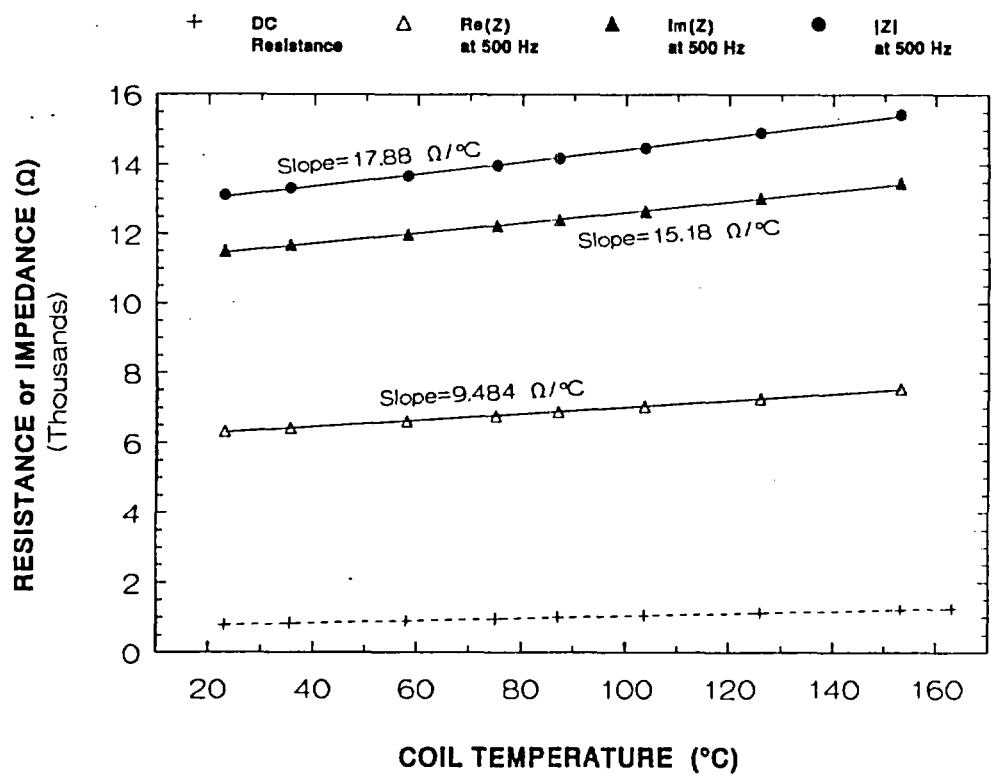

Figure B.6 Dc resistance, 500-Hz impedance vs temperature: SOV "C."

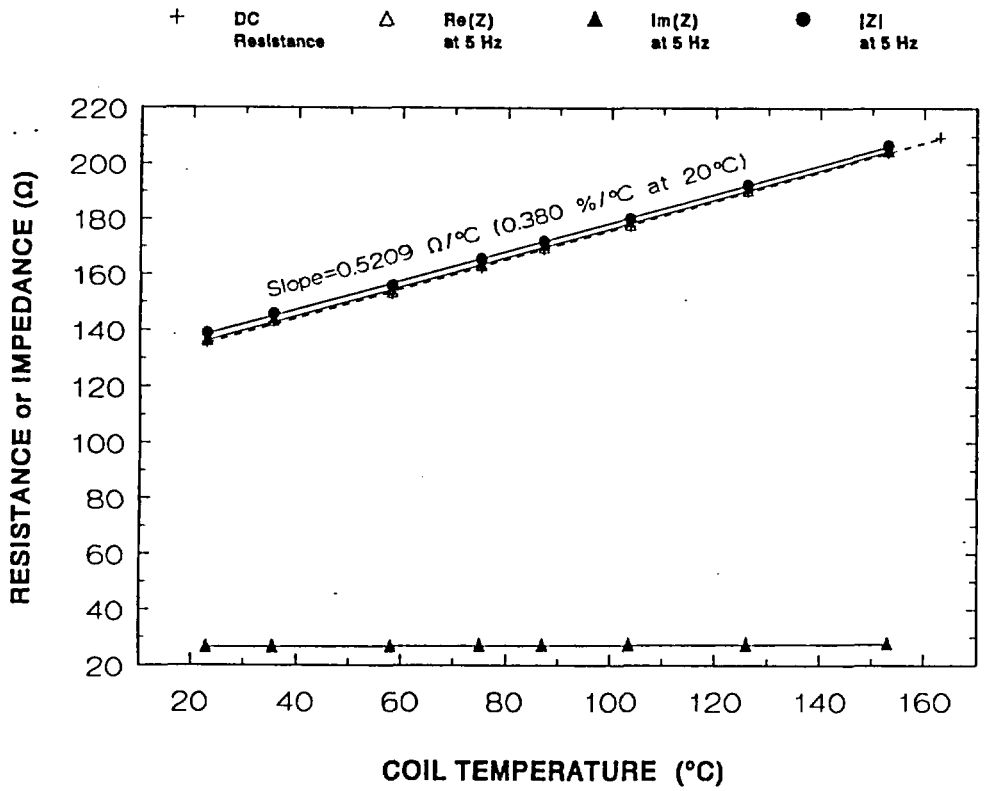

Figure B.7 Dc resistance, 5-Hz impedance vs temperature: SOV "E."

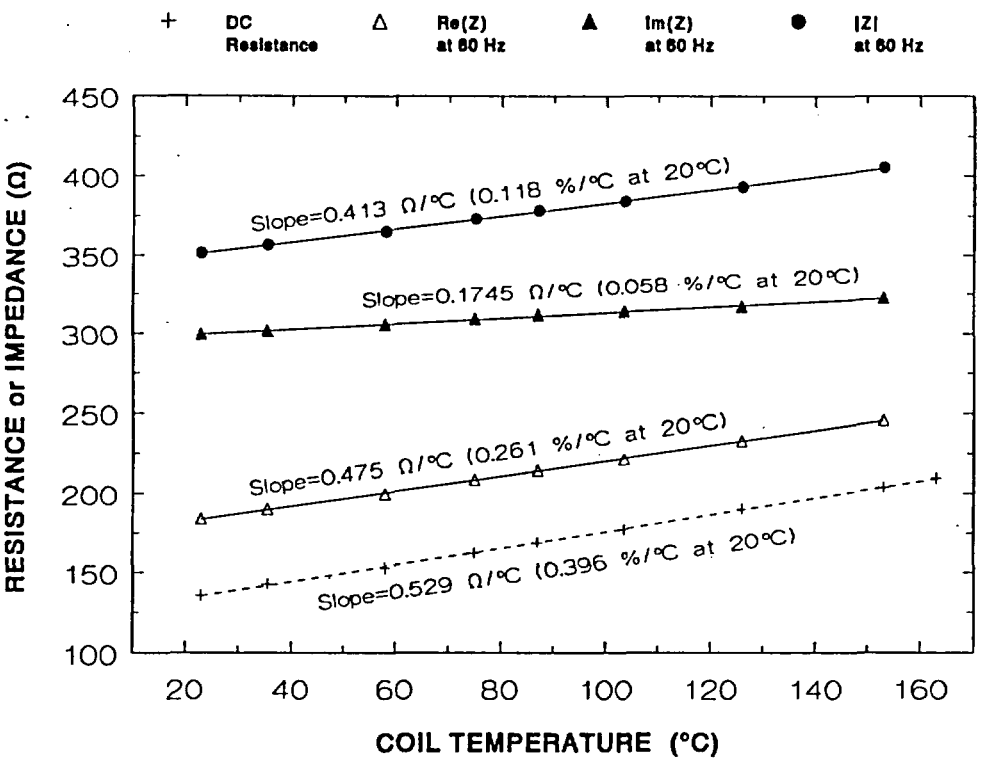

Figure B.8 Dc resistance, 60-Hz impedance vs temperature: SOV "E."

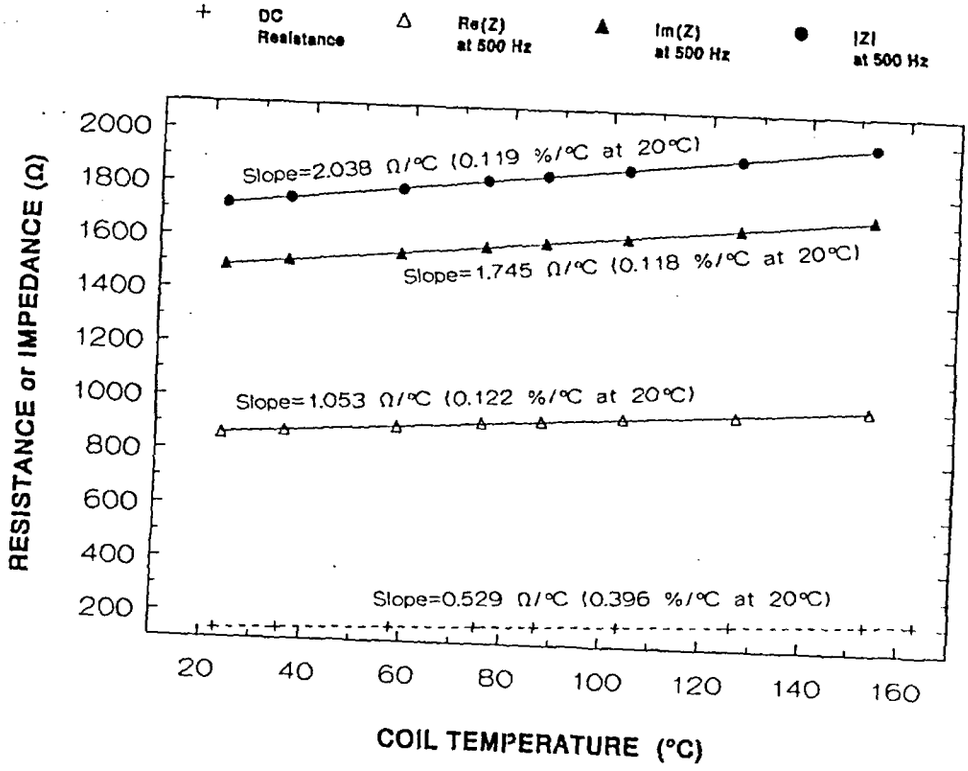

Figure B.9 Dc resistance, 500-Hz impedance vs temperature: SOV "E."

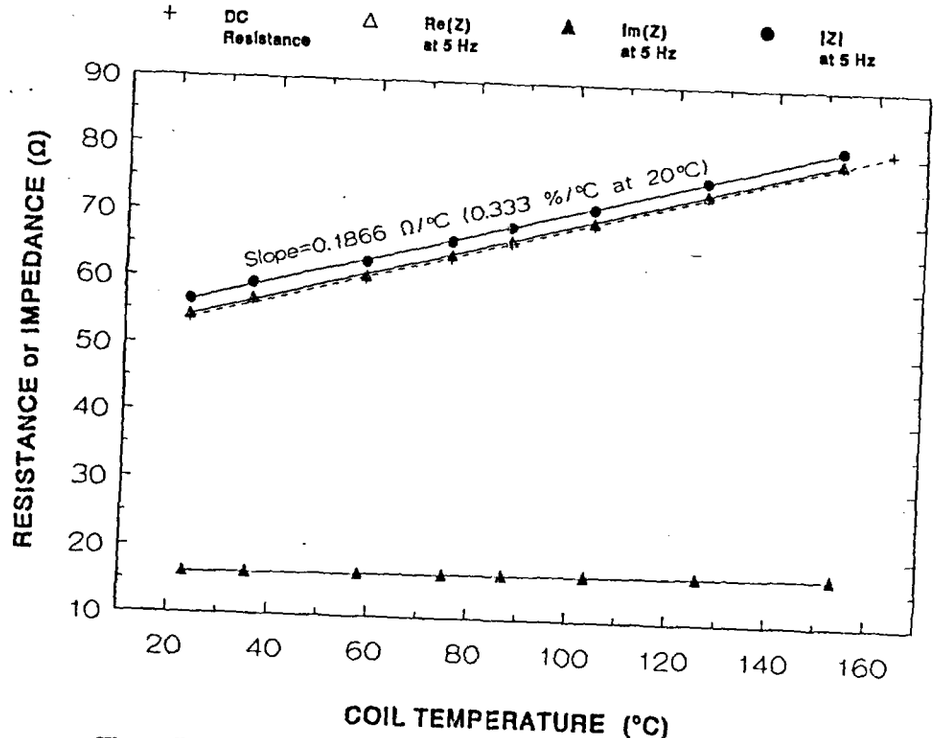

Figure B.10 Dc resistance, 5-Hz impedance vs temperature: SOV "G."

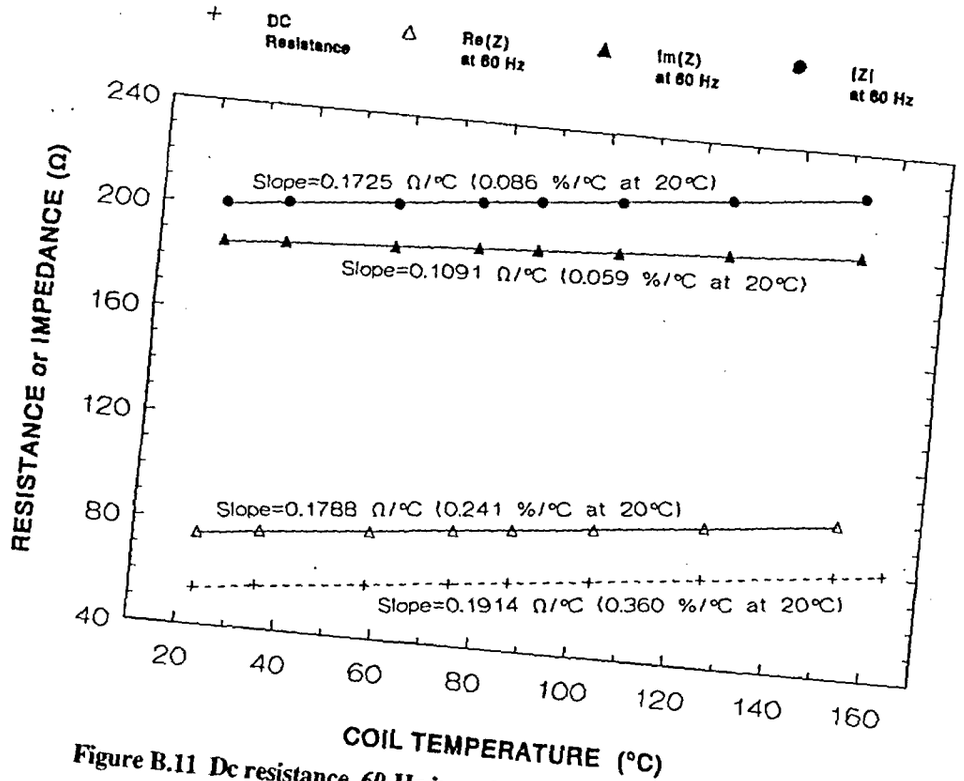

Figure B.11 Dc resistance, 60-Hz impedance vs temperature: SOV "G."

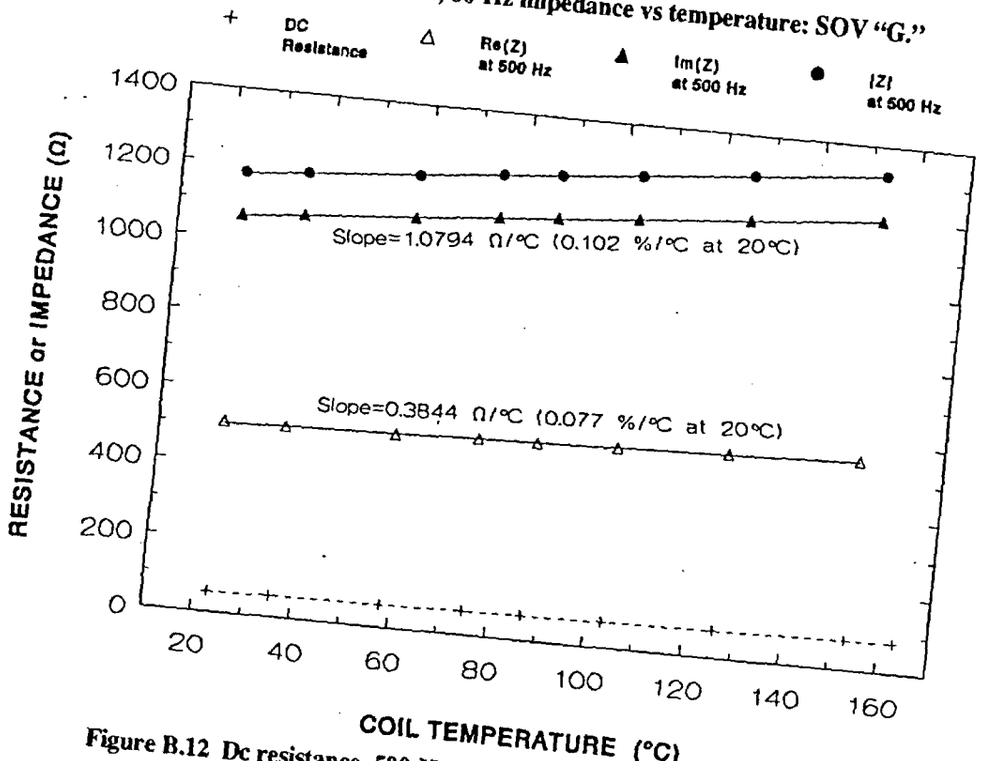

Figure B.12 Dc resistance, 500-Hz impedance vs temperature: SOV "G."

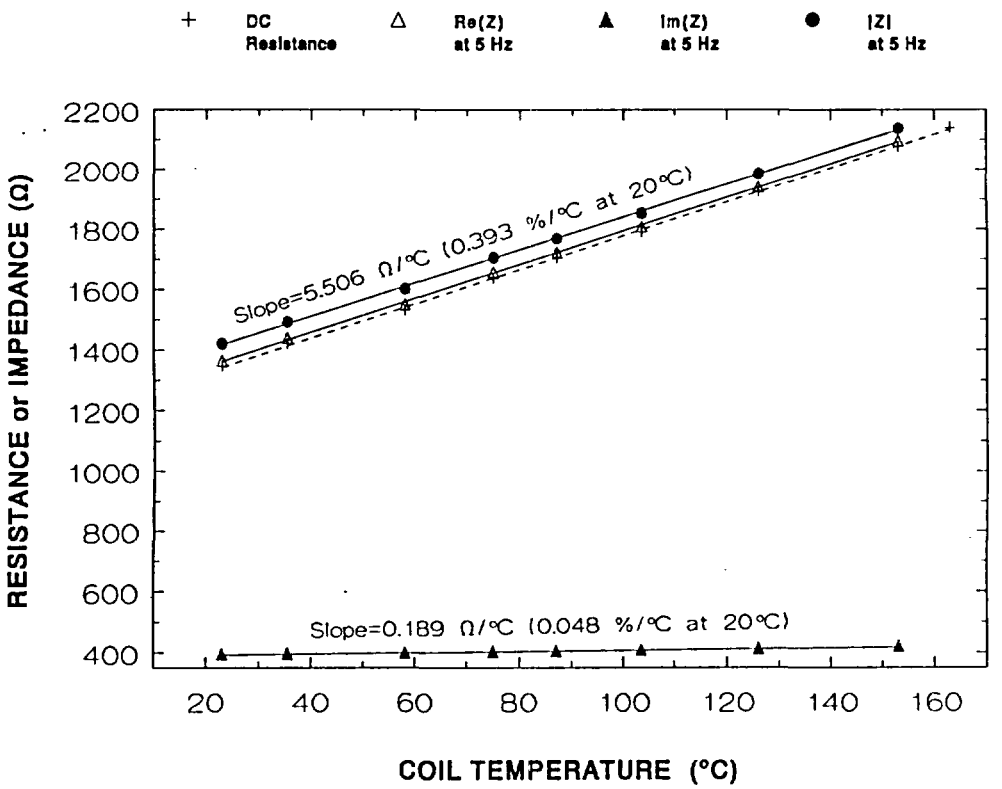

Figure B.13 Dc resistance, 5-Hz impedance vs temperature: SOV "L"

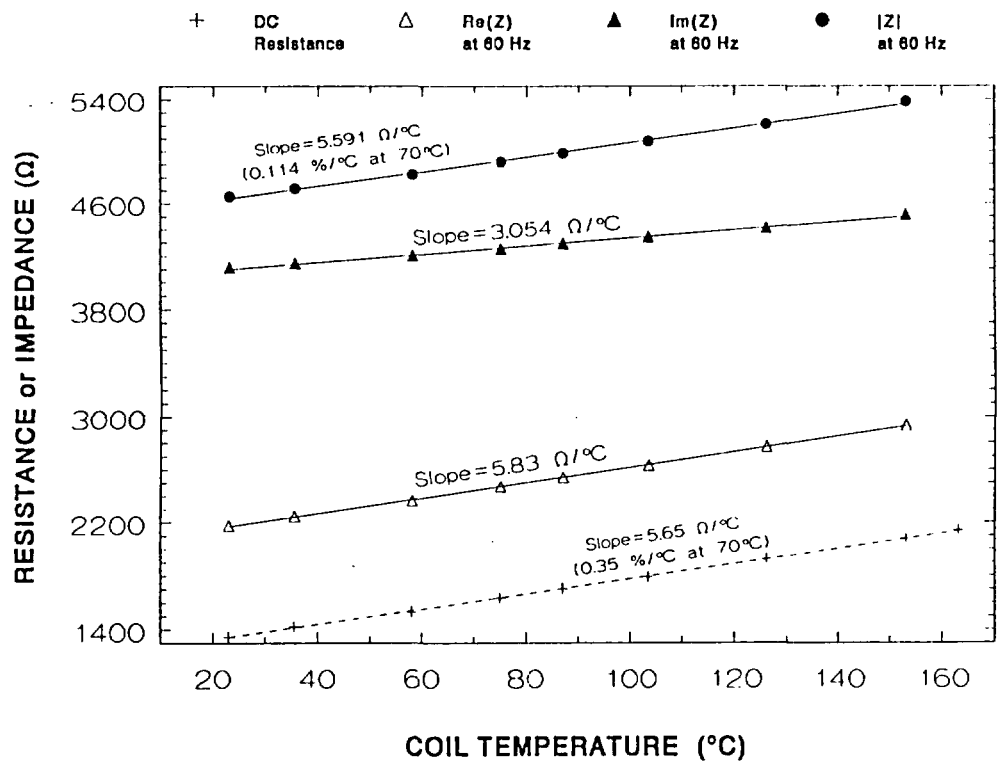

Figure B.14 Dc resistance, 60-Hz impedance vs temperature: SOV "L"

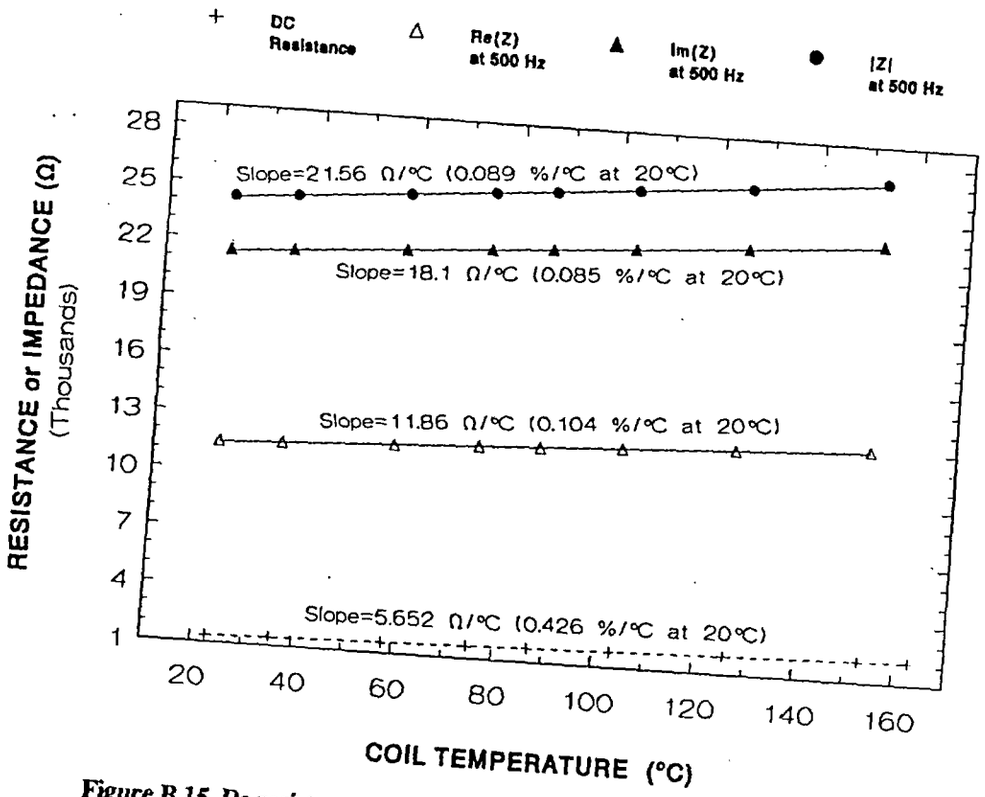

Figure B.15 Dc resistance, 500-Hz impedance vs temperature: SOV "I."

APPENDIX C

AC INDUCTANCES (L) AND QUALITY FACTORS (Q) OF FIVE SELECTED TEST VALVES OVER THE TEMPERATURE RANGE OF 20 TO 155°C AT THREE WIDELY SEPARATED FREQUENCIES: 5, 60, AND 500 HZ

As an adjunct to the measurement of the ac impedances of five of the fully assembled test SOVs (i.e., "A", "C", "E", "G", and "I") as a function of temperature at three fixed excitation frequencies (Appendix B), inductances and quality factors (defined as the ratio of inductive reactance to effective resistance) were also measured at a low level of excitation (1.1 V_{rms}) using a different operating mode of the same impedance analyzer. These measurements were performed primarily to see if either L or Q were quantities suitable for ascertaining coil temperature. The test procedures were the same as described in Appendices A and B, and consisted of placing the assembled SOVs in a temperature-controlled oven.

The test results are displayed in Figures C.1 through C.10, where the real quantities L and Q are plotted against oven (and therefore coil) temperature on linear scales. The three excitation frequencies chosen were again 5, 60, and 500 Hz.*

The following conclusions and observations were drawn from these data:

1. Inductance of the fully assembled SOVs increases quite linearly with temperature over the range of interest (20 to 155°C), but the temperature coefficient is not large when expressed as a percentage of value, being typically 0.03 to 0.13% of value per degree C. This number is a factor of 2 to 4 smaller than the percent-of-value temperature coefficients typically measured for Re(Z) or R_{dc} (see Appendix B).

2. The temperature coefficient of L for these SOVs, expressed as a percent change of value per degree C, is larger at higher than at lower frequencies. This is attributable to the diminished value of the inductance at higher excitation frequencies, coupled with an absolute slope (mH per degree C) that varies little with frequency.

3. Inductance typically drops by almost a factor of 2 as the excitation frequency rises from 5 to 500 Hz, but solenoid coils designed for ac operation (i.e., "E" and "G") retain a larger fraction of their low-frequency inductances at 60 Hz than do coils intended for dc operation (i.e., "A", "C", and "I").

4. SOVs intended for dc excitation typically have ten to twenty times the inductance at any frequency of interest to this study (i.e., <500 Hz) compared with SOVs intended for ac excitation at about the same voltage. This is attributable to the far greater number of turns of wire in the coils designed for dc operation as compared with their ac counterparts.

5. Quality factor decreases slightly with increasing temperature for most of the SOVs tested (valve "G" at 500 Hz excitation is an exception), but the linearity of the relationship is not exceptionally good. The Q of all the solenoids shows a marked increase with frequency of excitation (particularly in the intervals of 5 to 60 Hz); this is attributable to the rapid increase of inductive reactance with frequency (see Appendix D) compared with the much slower increase of effective resistance with frequency.

6. Inductance is a much better indicator of solenoid temperature than quality factor, but as a result of the relatively small magnitude of the temperature coefficient of inductance and the relatively poor linearity of the Q vs temperature relationship, neither L nor Q appears to be as well suited to temperature indication as R_{dc} or Re(Z). However, inductance measured at 500-Hz excitation frequency may be at least as good an indicator of coil temperature as the absolute value of the impedance, $|Z|$, although the instrumentation necessary to perform the L measurement is considerably more complicated than the simple V_{rms} and I_{rms} measurements needed to compute $|Z|$ at 60 Hz. Also, measurement of L at 500 Hz would require disruption of normal 60-Hz power to the SOV, whereas the measurement of $|Z|$ can be accomplished nonperturbatively.

*With the exception of 60 Hz—which was selected, of course, because it is the frequency of the power mains throughout the United States—the selection of the other two test frequencies was arbitrary. However, 5 and 500 Hz represent reasonable lower and upper limits for test signals that would be practical to apply to plant wiring.

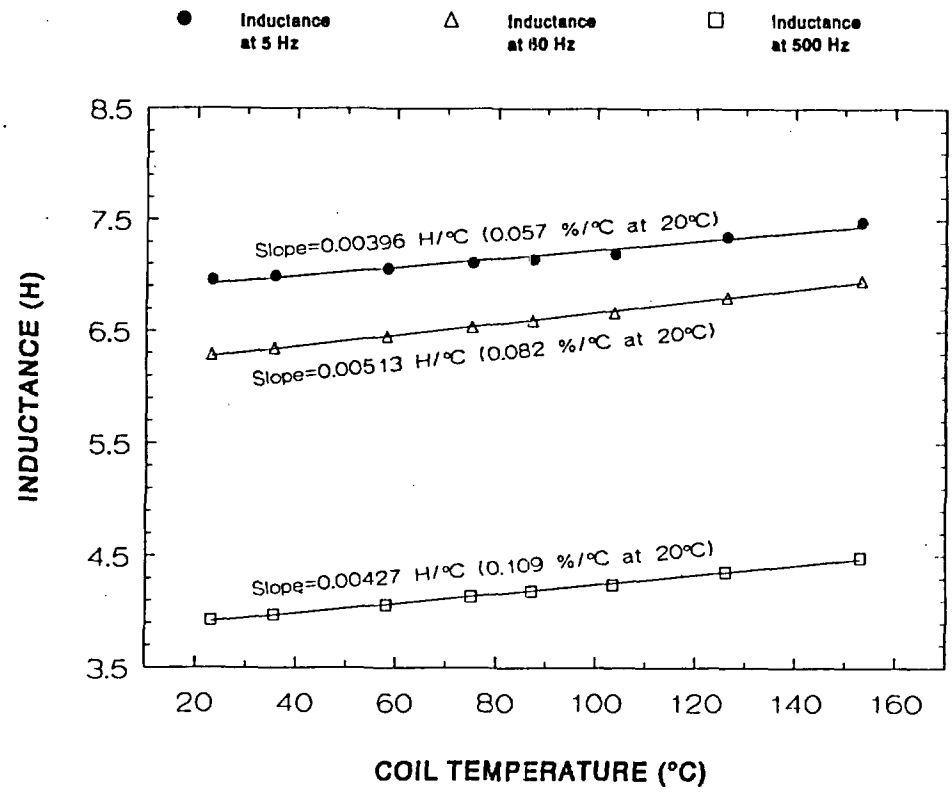

Figure C.1 Inductance vs temperature at three excitation frequencies: SOV "A."

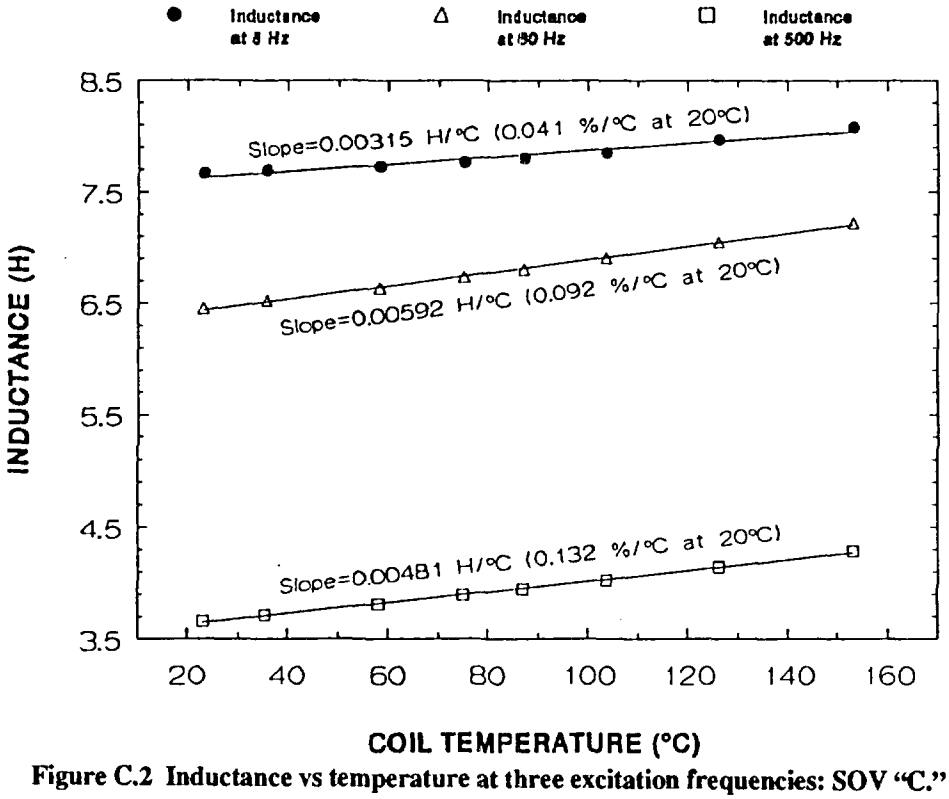

Figure C.2 Inductance vs temperature at three excitation frequencies: SOV "C."

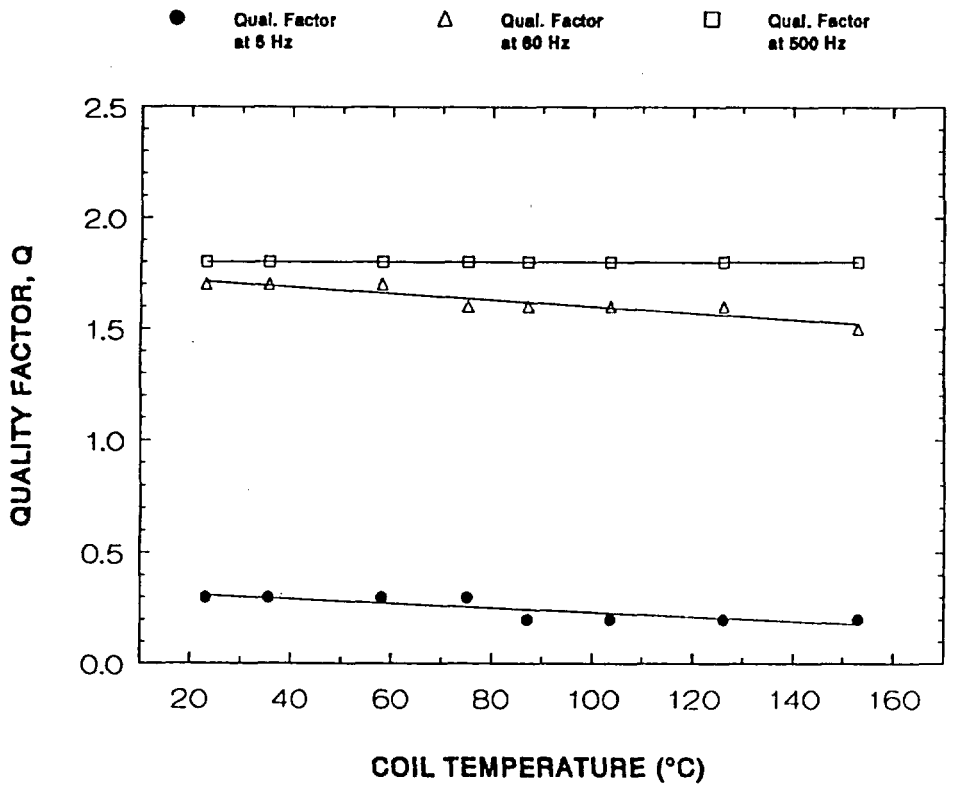

Figure C.7 Quality factor vs temperature at three excitation frequencies: SOV "C."

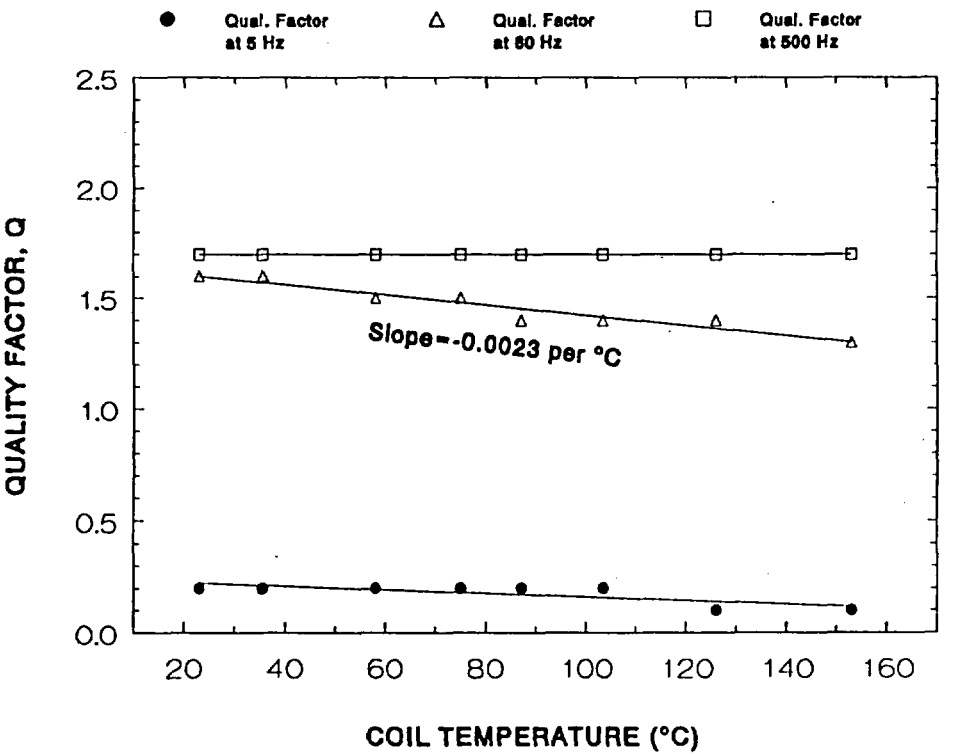

Figure C.8 Quality factor vs temperature at three excitation frequencies: SOV "E."

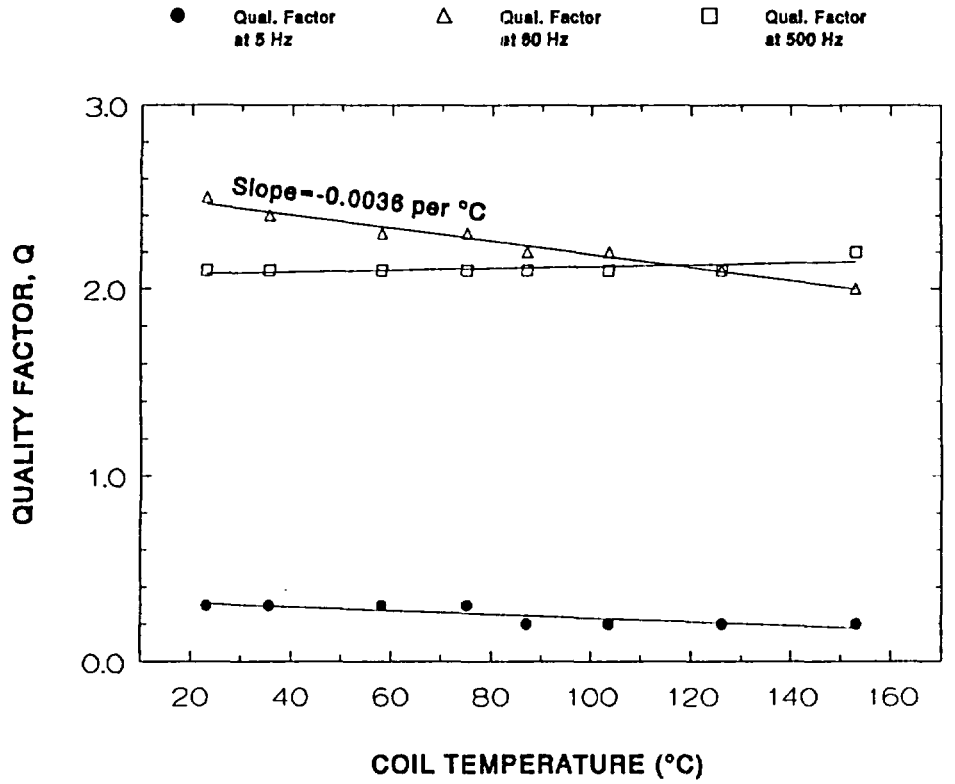

Figure C.9 Quality factor vs temperature at three excitation frequencies: SOV "G."

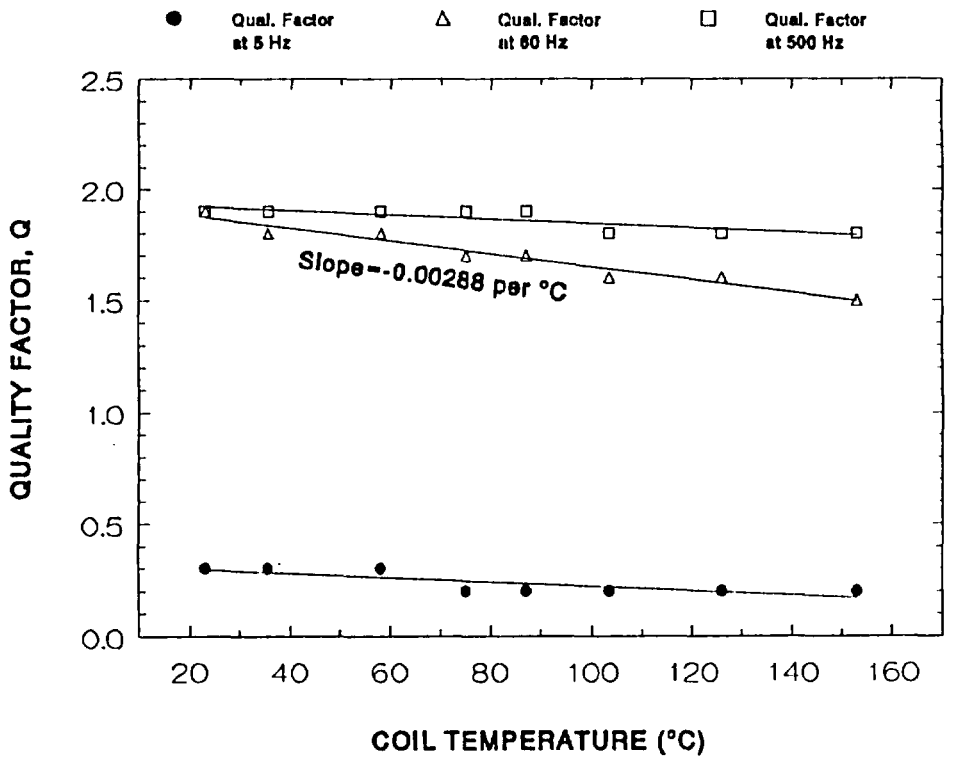

Figure C.10 Quality factor vs temperature at three excitation frequencies: SOV "I."

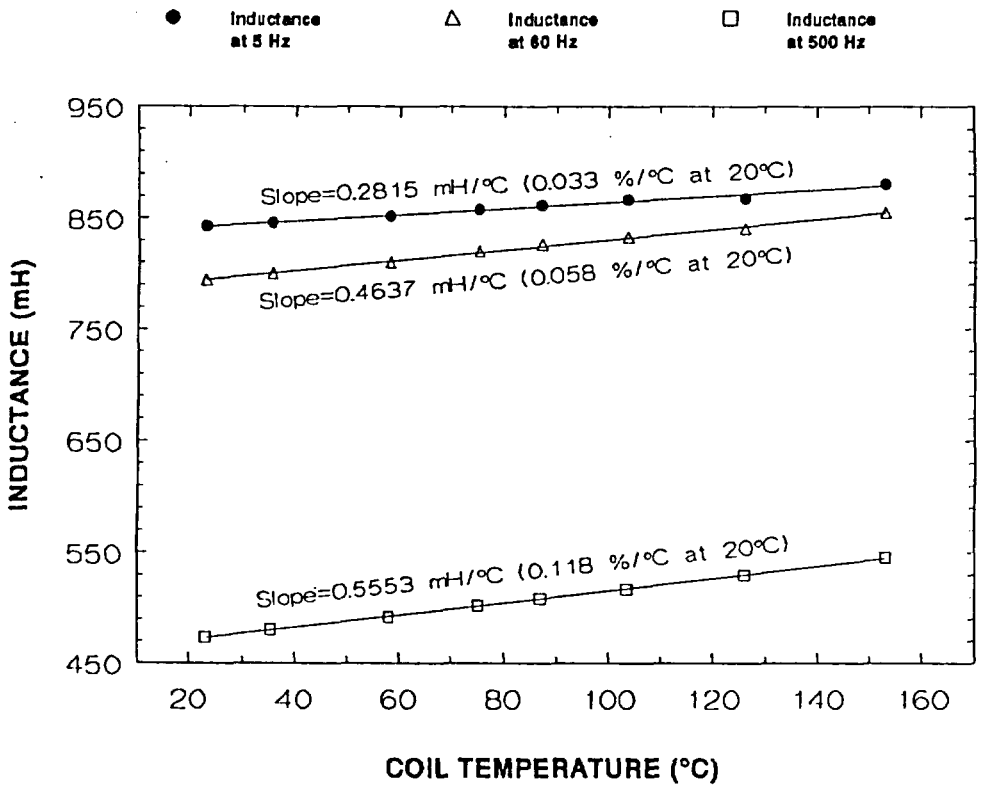

Figure C.3 Inductance vs temperature at three excitation frequencies: SOV "E."

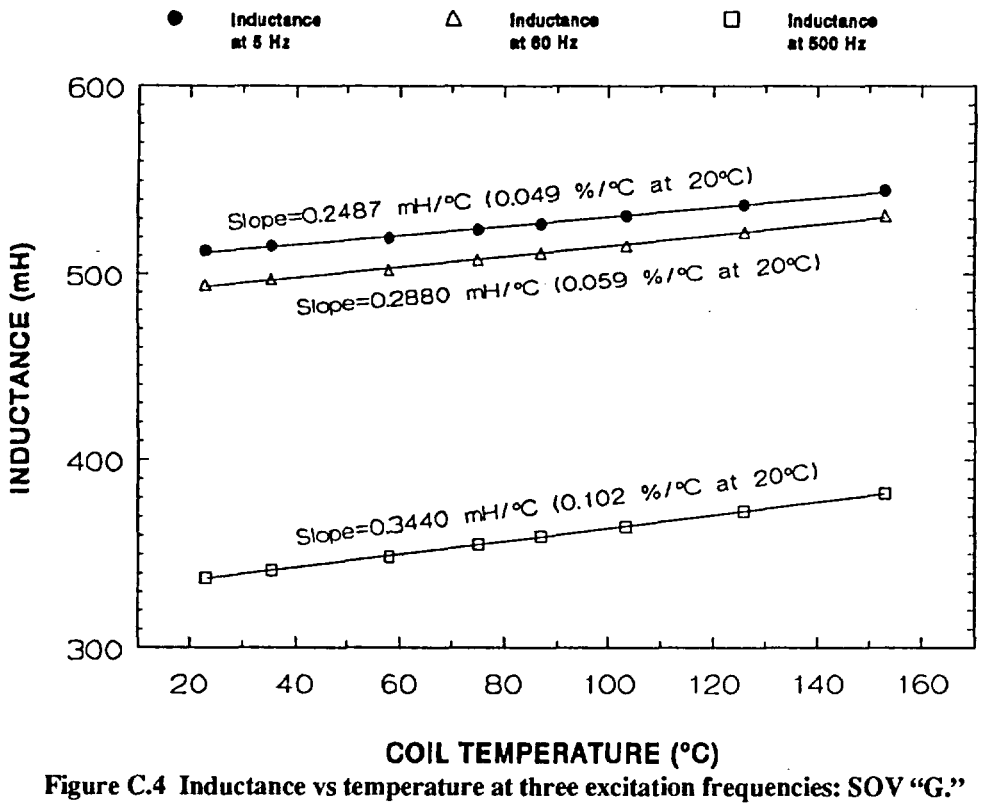

Figure C.4 Inductance vs temperature at three excitation frequencies: SOV "G."

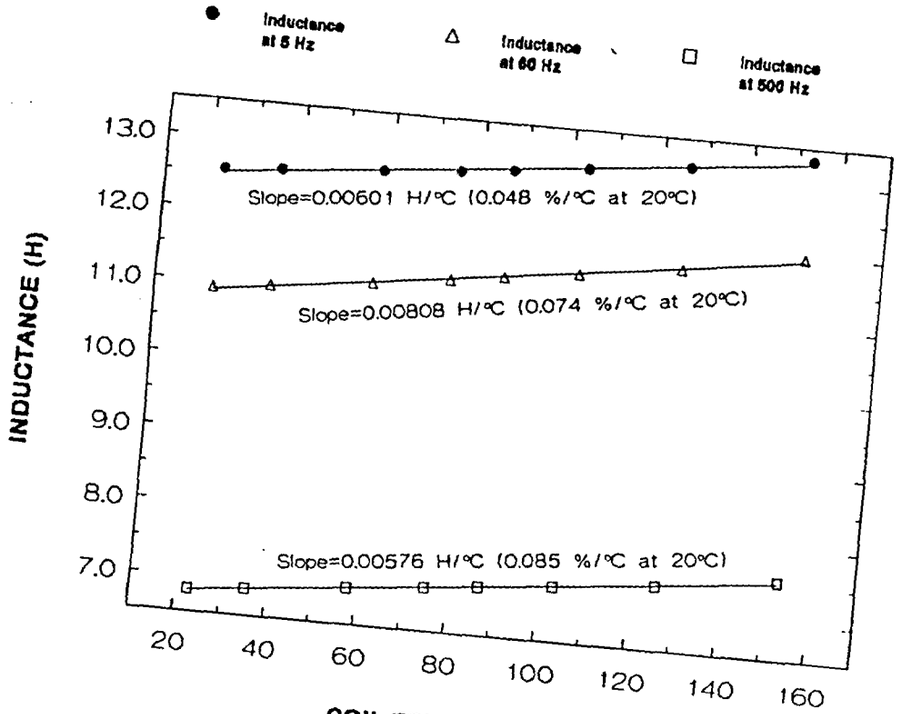

Figure C.5 Inductance vs temperature at three excitation frequencies: SOV "L"

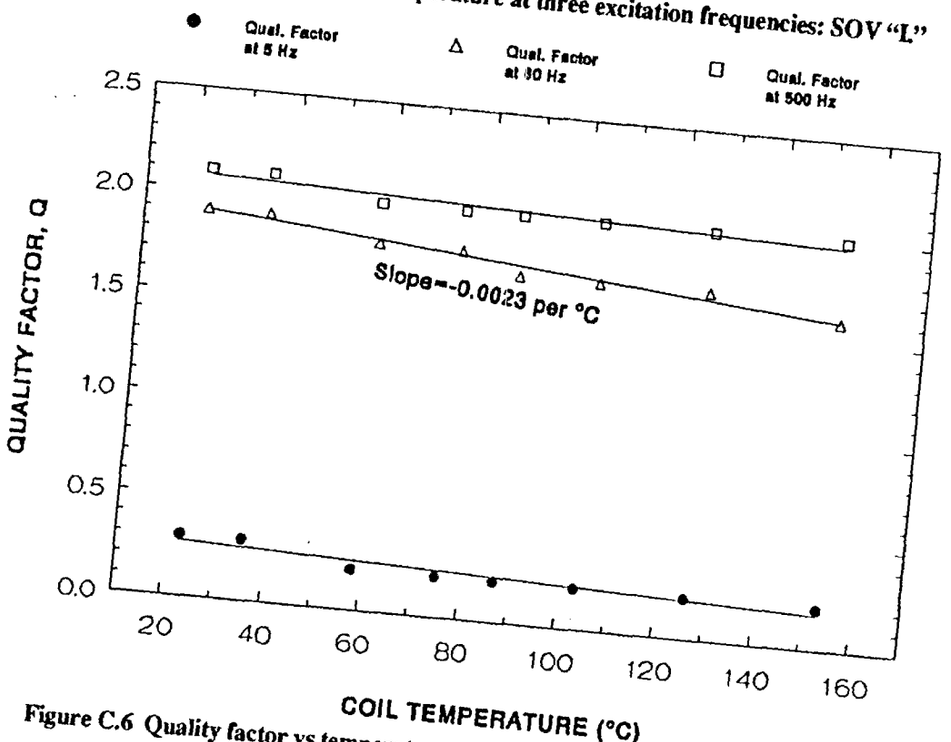

Figure C.6 Quality factor vs temperature at three excitation frequencies: SOV "A."

APPENDIX D

FREQUENCY DEPENDENCE OF IMPEDANCE FOR DC- AND AC-POWERED SOLENOID COILS

As a follow-up to the unexpected finding (see Appendix B) that Re(Z) is ~50% larger than R_{dc} at 60-Hz excitation frequency (and 5 to 10 times larger at 500 Hz), a more detailed investigation of the frequency dependence of impedance and inductance was conducted for a few selected solenoid coils. All measurements were made at room temperature (23°C) and at a low level of excitation (1.1 V_{rms}), using a Hewlett-Packard model 4192A low-frequency impedance analyzer, so the SOVs were in their rest (unpowered) state. SOVs "A", "D", and "G" were tested in a normally assembled condition, whereas the solenoid coils of SOVs "C", "E", "G", and "I" were measured bare (i.e., removed from the SOV housing and devoid of plunger and guide tube).

The measurement results are shown in Figures D.1 through D.5, where the real (in-phase), imaginary (quadrature-phase), and vector sum (absolute value) of impedance, $|\mathbf{Z}|$, and the inductance, L, are plotted against frequency on linear scales. Unless otherwise stated, the solid curves have no theoretical significance; their function is merely to join the measured data points smoothly so that the trend is easily seen.

The following observations and conclusions were drawn from these measurements:

1. Fully assembled SOVs designed for dc operation (i.e., "A", "C", and "I") have impedance vs frequency characteristics that are similar to SOVs designed for ac operation (i.e., "D", "E", and "G"), even though the impedance is typically ten times greater for the dc coils as a result of the larger number of turns used in winding the dc solenoids.

2. The real (in-phase) component of the complex solenoid impedance is not independent of frequency (as one might expect for a nearly ideal inductor—that is, an ideal inductor plus some series resistance) and is always greater than the dc resistance, although Re(Z) approaches R_{dc} as the frequency of excitation approaches zero. This was at first thought to be attributable to "skin effect," but data obtained on bare coils (Figures D.4 and D.5) later revealed that the noted behavior is due to a combination of eddy current losses in the copper winding and hysteresis losses in the iron plunger and guide tube present in the fully assembled SOV.

3. The imaginary (reactive) component of the complex solenoid impedance does not grow linearly with frequency, as one would expect for an ideal inductor. It is thought that the downward curvature (negative second derivative with respect to frequency) seen in Figures D.1 through D.3 is attributable to the presence of distributed stray parallel (i.e., turn-to-turn) capacitance, the reactance of which tends to partially cancel the inductive reactance of opposite algebraic sign.

4. As a result of observations 2 and 3 above, the magnitude of the complex impedance of fully assembled SOVs is seen to increase fairly linearly with frequency over the range of 0 to 120 Hz, although this relationship is of no particular value to the study at hand.

5. The inductances of the bare solenoid coils (Figures D.4 and D.5) were found to be almost independent of excitation frequency (the expected result for an air-cored coil), whereas $|\mathbf{Z}|$ for the bare coils plots nicely as a second-order polynomial in frequency—that is, $|\mathbf{Z}| = a_0 + a_1 f + a_2 f^2$. The existence of the f^2 term strongly suggests that eddy-current losses in the copper coil winding are responsible for this nonideal behavior, since such losses are known to grow as the second power of frequency.[1]

6. The presence of permeable iron within the bare solenoid coil significantly increases its impedance (e.g., at 200-Hz excitation frequency, $|\mathbf{Z}|$ of the bare coil "G" was found to increase from 104 Ω to 575 Ω as a result of threading the coil onto the guide tube/plunger assembly).

REFERENCE

1. Webber, F. G., and R. L. Sanford, "Inductance; Magnetic Materials," p. 3-2 in Henney, K., ed., *Radio Engineering Handbook*, 5th ed., McGraw-Hill, New York, 1959.

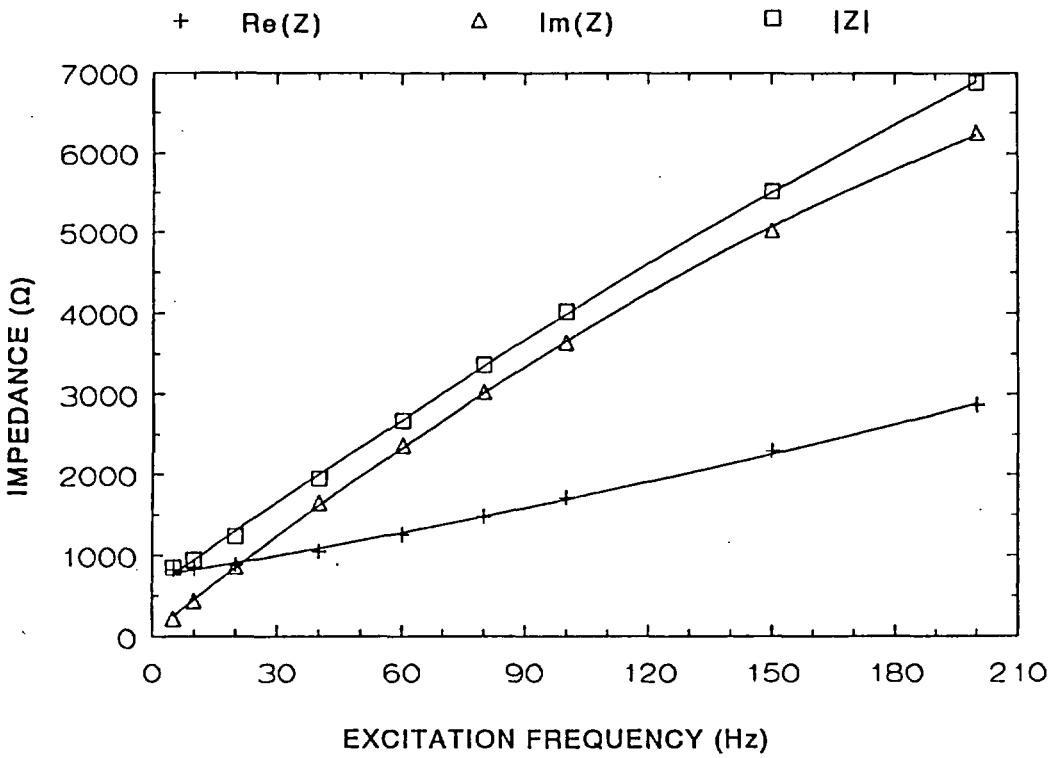

Figure D.1 Variation of impedance components with excitation frequency: SOV "A."

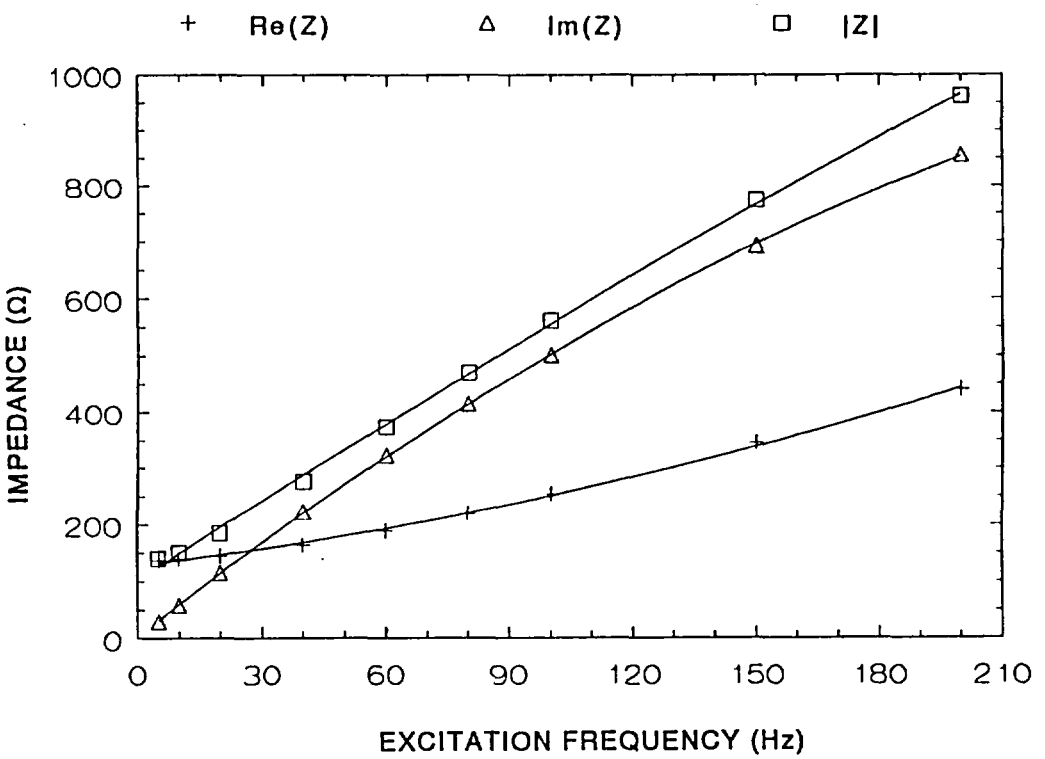

Figure D.2 Variation of impedance components with excitation frequency: SOV "D."

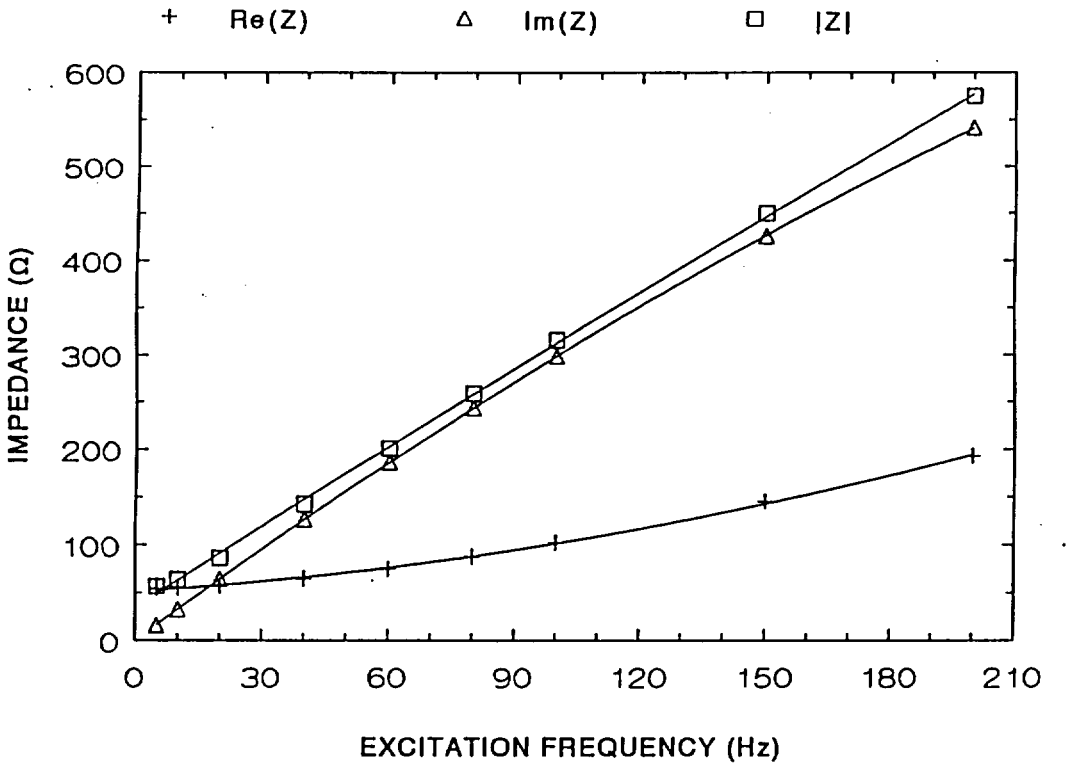

Figure D.3 Variation of impedance components with excitation frequency: SOV "G."

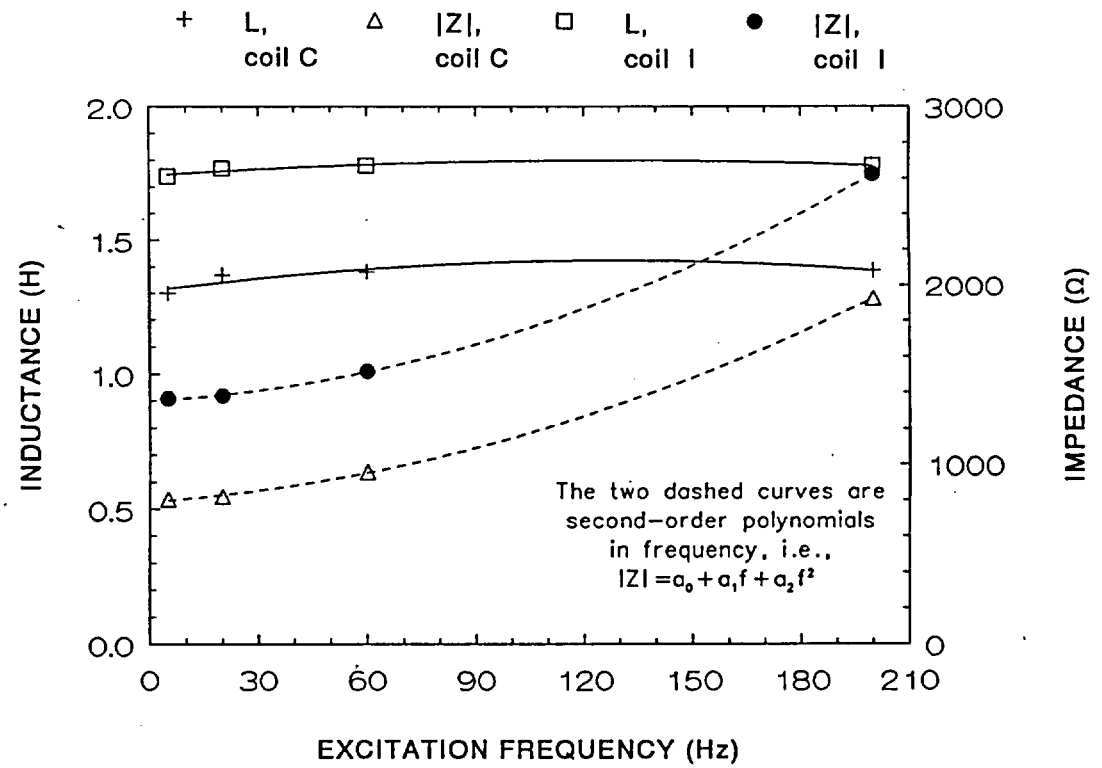

Figure D.4 Variation of inductance and impedance with frequency: bare solenoid coils "C" and "I."

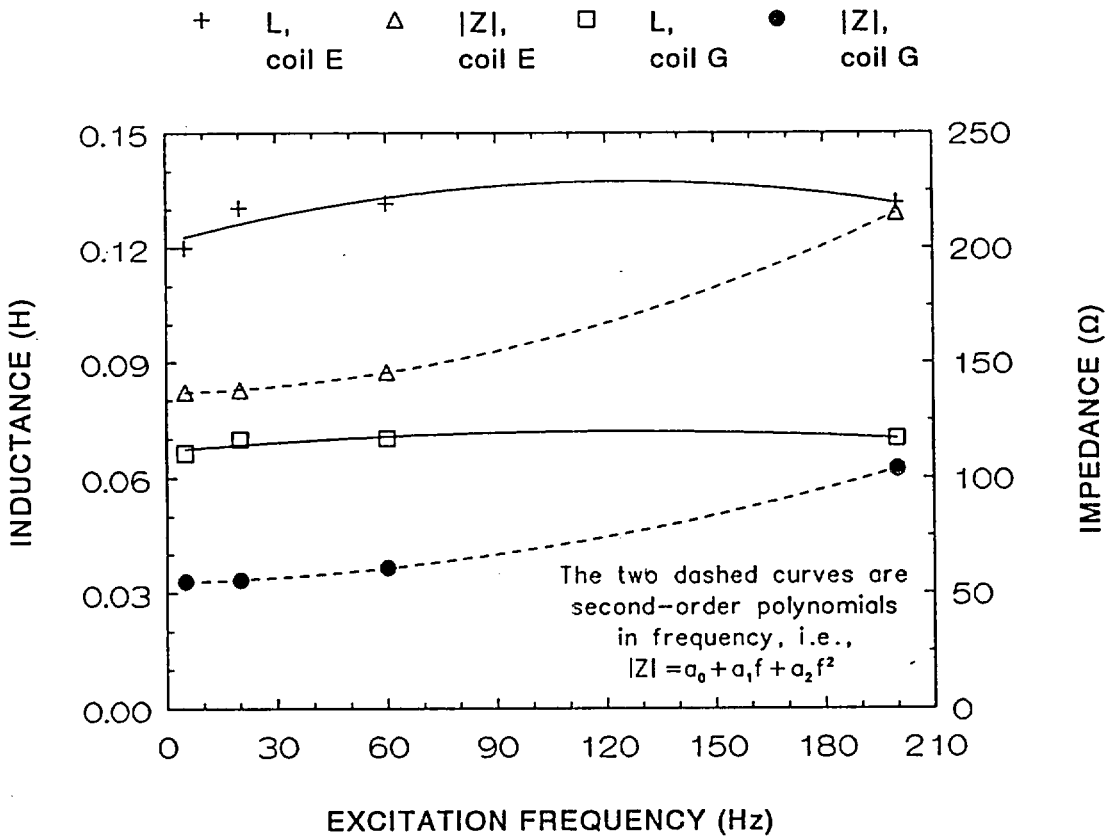

Figure D.5 Variation of inductance and impedance with frequency: bare solenoid coils "E" and "G."

APPENDIX E

VARIATION OF COIL RESISTANCE AND IMPEDANCE WITH APPLIED VOLTAGE

Appendices A, B, C, and D establish the variation of several of the important electrical characteristics of SOVs as a result of changes in temperature and frequency of excitation. In all cases, however, the measurements represent small-signal properties, since the level of excitation applied by the measuring instrument (a digital ohmmeter or an impedance analyzer) was only about 1 V. We now address the large-signal behavior of two especially important electrical characteristics of SOVs—dc resistance and ac impedance at normal power line frequency (60 Hz).

Table E.1 shows measurements obtained from four different instruments applied to SOV "D" at room temperature. (Ac measurements were performed at 60 Hz exclusively.) The nearly 3:1 difference between R_{dc} and $|Z|$ as measured by the Hewlett–Packard model 4192A impedance analyzer is understandable in terms of the data presented in Appendix B, but the source of the almost 2:1 difference in $|Z|$ measured at high vs low excitation is not readily apparent. The instrumentation was vindicated by measuring a nonreactive load of about the same ohmic value as SOV "D" (four nominal 3500-Ω resistors connected in parallel so as to yield a combined resistance of approximately 850 Ω). Table E.2 shows that the results obtained using the same measurement techniques on the resistor as had been used on the SOV are in substantial agreement, so a different explanation for the low- vs high-excitation discrepancy must be sought.

The key to this mystery is the realization that SOV "D" was in its "rest" (open) state for the first two measurements of Table E.1, whereas it was in its "energized" (closed) state for the third and fourth measurements, the primary difference being the position of the iron-cored plunger within the solenoid coil. Electrical engineers will recognize that the presence of magnetically permeable iron in or near the coil will dramatically affect the inductance (and therefore the impedance) of a solenoid, and also that the magnitudes of certain magnetic and electrical loss mechanisms that are present only with ac are strongly dependent on the level of magnetization, which in turn depends on the level of electrical excitation. These effects are illustrated in Figures E.1 and E.2.

Figure E.1 was obtained by gradually increasing the dc potential applied to SOV "D" while simultaneously measuring the voltage across and the current through the SOV coil in order that the SOV's dc resistance, R_{dc}, could be calculated by application of Ohm's law: $R_{dc} = V_{dc}/I_{dc}$. The SOV was observed to change state (from open to closed) at about 14 V_{dc},* but the computed resistance is seen to be essentially unaffected by this state change or, in fact, by the application of additional excitation voltage.

Figure E.2 was generated in the same manner as the previous figure except that 60-Hz ac (rather than dc) excitation was employed. In marked contrast to the dc results, the magnitude of the ac impedance, $|Z| = V_{rms}/I_{rms}$, is seen to vary by almost a factor of 3 as the voltage applied to the SOV is increased from zero to 135 V_{rms}. Three distinct regions are identifiable in the figure: (1) a low-voltage region in which magnetic flux linkages among coil turns and between the coil and the plunger continually build (causing increased electrical impedance as a result of increased inductance), a process which eventually saturates, thereby yielding a plateau throughout which $|Z|$ is essentially independent of excitation voltage; (2) an abrupt, almost 2:1 increase in impedance resulting from the retraction of the SOV plunger into the solenoid coil as the valve changes state; and (3) a rapid decline in $|Z|$ as parasitic effects (i.e., eddy currents in the coil copper; hysteresis losses in the iron of the plunger) cause inductance to be reduced as solenoid excitation is further increased.

The following observations and conclusions were drawn from these data:

1. The value measured for dc resistance is, for all practical purposes, independent of the level of excitation** as well as the valve state [open or closed (i.e., plunger withdrawn or retracted into the solenoid coil)].

*This valve actuation voltage is very low because SOV "D" was designed for ac rather than dc operation; therefore, it has relatively few turns in its solenoid coil and a rather low dc resistance (135 Ω), which causes it to draw a relatively large amount of current (100 mA) at this low voltage.

**It is assumed that measurements are performed in a matter of seconds in order that coil temperature is not raised significantly owing to the deposition of heat within the coil (resistive power loss = I^2R).

Table E.1. Dc resistance/ac impedance of SOV "D" at 23°C

Instrument used	Technique	Quantity obtained	Result (Ω)
Dc ohmmeter	Direct reading	Low-excitation R_{dc}	135.5
Impedance analyzer	Direct reading	Low-excitation $\|Z\|$	374.1
Rms voltmeter and ammeter	V_{rms}/I_{rms}	High-excitation (112 V_{rms}) $\|Z\|$	648.1
True rms electronic module	V_{rms}/I_{rms}	High-excitation (112 V_{rms}) $\|Z\|$	645.9

Table E.2. Dc resistance/ac impedance of 850-Ω resistor

Instrument used	Technique	Quantity obtained	Result (Ω)
Dc ohmmeter	Direct reading	Low-excitation R_{dc}	846
Impedance analyzer	Direct reading	Low-excitation $\|Z\|$	848
Rms voltmeter and ammeter	V_{rms}/I_{rms}	High-excitation (112 V) $\|Z\|$	833
True rms electronic module	V_{rms}/I_{rms}	High-excitation (112 V) $\|Z\|$	879

2. In contrast, the value measured for ac impedance depends strongly on both (a) the valve state (because inductance is materially increased when the iron plunger is drawn into the solenoid) and (b) the level of ac excitation (since parasitic mechanisms decrease inductance at higher levels of applied voltage after the plunger is drawn into the solenoid, while at very low applied voltage mutual inductance may be unsaturated).

3. Observations 1 and 2 above indicate that if ac impedance measurements (as opposed to dc resistance measurements) are to provide correct indications of coil temperature, they must be made at known electromechanical conditions (i.e., at a known valve state and level of excitation). It may, for example, be necessary to standardize the voltage applied to the SOV or, if this is impractical, to correct the impedance measured at nonstandard operating voltage to what would have been obtained at an established standard excitation.

4. The strong dependence of $|Z|$ on the position of the plunger within the solenoid may provide a diverse and possibly sensitive means for ascertaining valve position, especially under unusual (e.g., accident) conditions where valve position may not be determinable by other means.

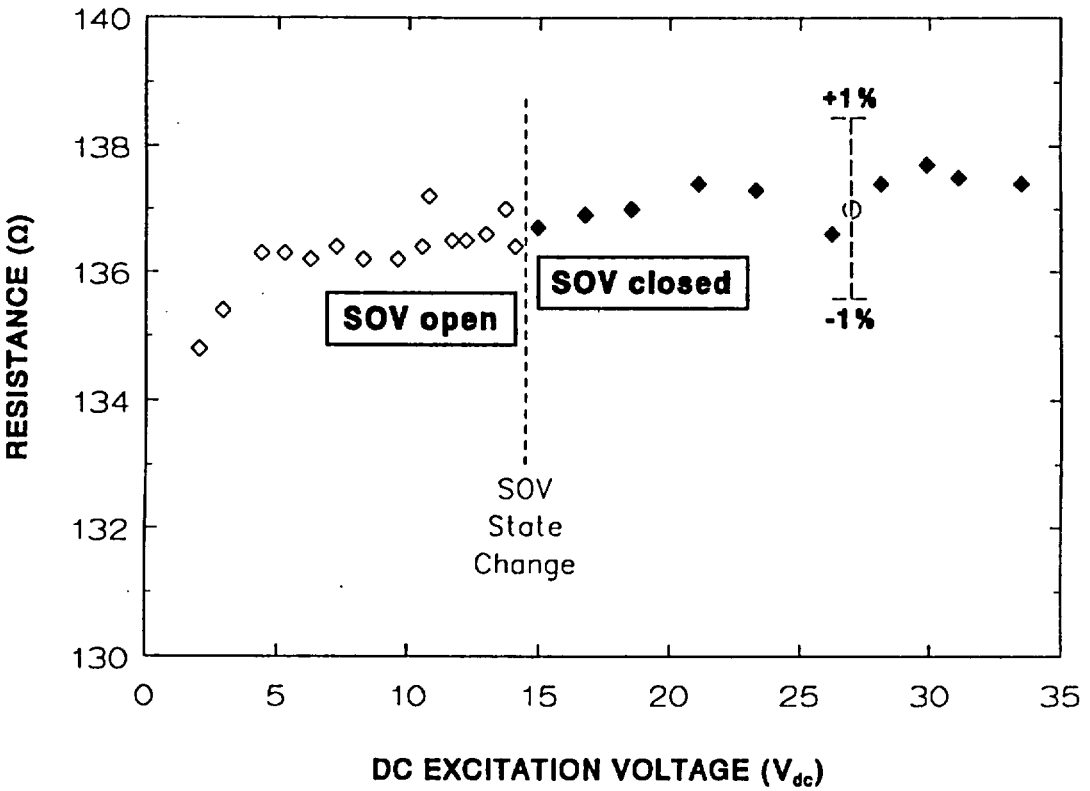

Figure E.1 Dc resistance vs level of excitation: SOV "D."

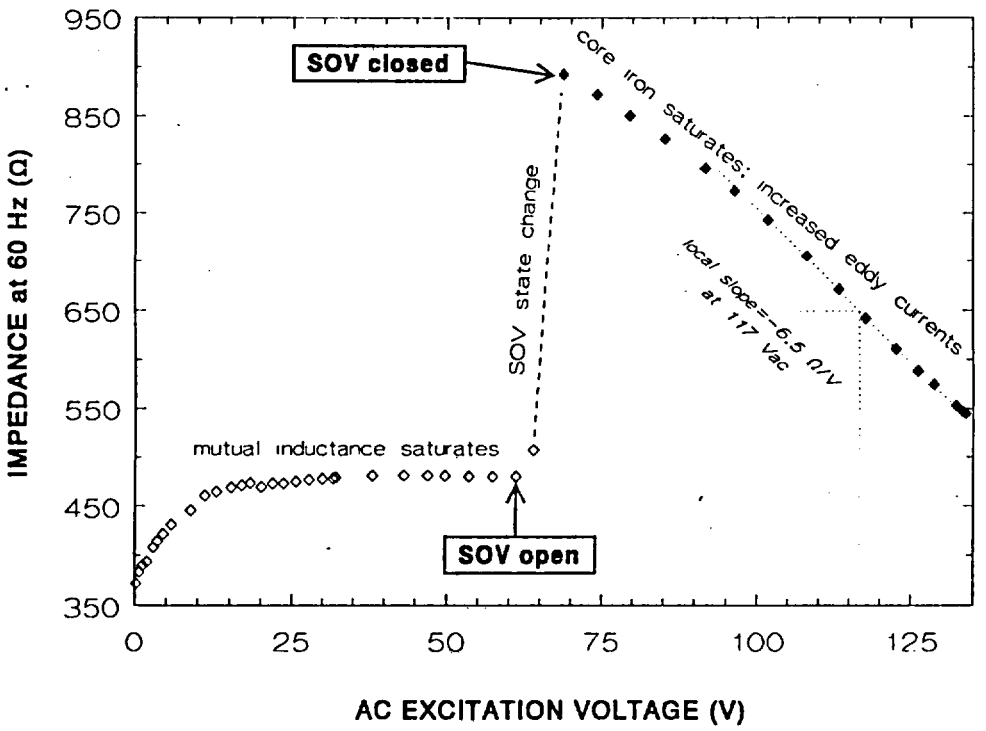

Figure E.2 Ac impedance vs level of excitation: SOV "D."

APPENDIX F

VERIFICATION OF ABSOLUTE TEMPERATURE CALIBRATION BY APPROACH-TO-ISOTHERMAL-CONDITION TESTS

The rather large differences (>40°C) between temperatures derived from SOV coil resistance measurements and those measured at the coil periphery with a stem thermometer (see Sect. 2.2.1.1 and Figure 2.5) created a need to prove that there was no systematic error in measuring temperature by the electrical method. Measurements made in a thermostatically controlled oven (Appendix A) had shown no problem, so what was different about the open-air environment of the laboratory bench? It was reasoned that open-air measurements would never yield correspondence between the electrically derived coil temperatures (which are inherently volume-averaged) and the mercury-in-glass temperatures (which are point measurements at the coil's outer radius), since the inevitability of a thermal gradient between the inner source of heat (~14 W of power deposited within the coil) and the outer convective heat transfer surface of the coil—combined with thermal resistance at the point of thermometer contact with the coil—would ensure that the external readings would always lie well below any internal readings made while the coil was being heated from within.

To test this hypothesis, a more-nearly-isothermal test environment was created by placing a dc-powered SOV ("B") in a thick-walled styrofoam insulating enclosure, passing the electrical leads and the stem thermometer through holes in the side of the enclosure, and filling the remaining empty volume of the box with styrofoam "peanut hulls" so as to minimize convective air circulation within.

Initially, full electrical power was applied to the valve for a period of some tens of minutes in order to bring the SOV and its surrounding stagnant airspace up to a temperature well above room ambient (24.6°C, at which temperature the solenoid had an electrical resistance of 793.9 Ω).* Electrical power was then reduced to a "holding" level necessary to overcome inevitable heat losses through the enclosure walls in order that approximate thermal equilibrium could be attained. This essentially steady-state situation is illustrated by the initial 2.5 h of Figure F.1, where the temperature indicated by the stem thermometer is seen to be on the order of 92 to 100°C, while the temperature derived from coil resistance is on the order of 123 to 130°C. The fact that, even under these well-insulated conditions, there existed an unchanging ΔT of ~30°C between the two slowly rising readings indicates that the thermal resistance of the coil-potting compound is fairly high, and therefore a strong radial thermal gradient within the coil is unavoidable so long as the coil is powered.

Therefore, at $t = 2.5$ h the electrical "holding" power was removed. Over the succeeding 32 min the mercury thermometer reading dropped ~22°C and the resistance-derived temperature plummeted by ~49°C (Figure F.1) as the SOV continued to dissipate heat to its surroundings. After an additional 8 min the two indicated temperatures differed by only 1.5°C, even though the entire SOV was still quite hot (~75°C). This approach-to-isothermal test provides convincing evidence that, under the right conditions, temperatures inferred from coil resistance will be in good agreement with temperatures indicated by a glass stem thermometer or thermocouple placed in contact with the coil's outer surface.

Further confirmation is provided by the data plotted in Figure F.2, which illustrates two additional approach-to-isothermal tests in which SOV "B" was allowed to cool (unpowered) within the insulated enclosure after having been brought to an elevated temperature by application of normal electrical power (125 V_{dc}). In the first test (left side of graph) the two temperature indications came to within 2.1°C of agreement at an SOV temperature of ~92°C in about 16 min after termination of coil heating. In the second test (right side of graph) even better agreement (<0.5°C) was obtained after a longer period (~30 min) in the unpowered state allowed valve temperatures to fall even further (45 to 50°C) but nevertheless remain well above normal ambient.

In summary, the apparent temperature discrepancies noted in Sect. 2.2.1.1 are not indicative of a calibration problem or a systematic measurement error but rather result from a combination of relatively high thermal resistance at the stem thermometer–coil contact point and the existence of a

*For SOV "B," $T(t) = R(t) - 793.9\ \Omega/3.4095\ \Omega/°C + 24.6$, where $T(t)$ is the time-dependent temperature in °C, $R(t)$ is the coil dc resistance in ohms, and the temperature coefficient of resistance is taken from the slope of Figure A.2.

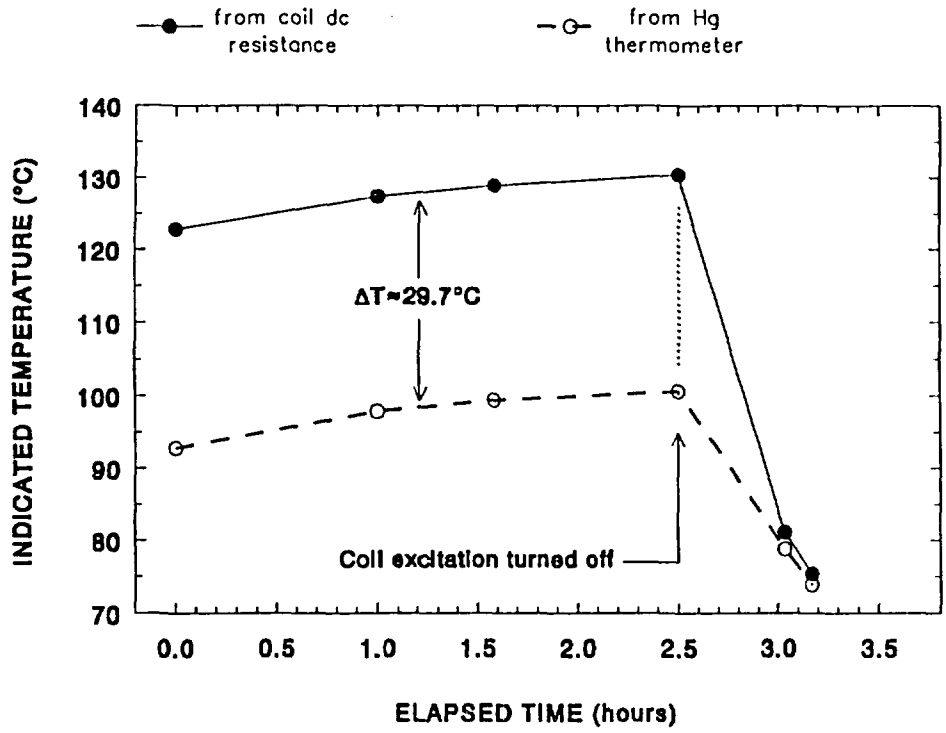

Figure F.1 Comparison of temperature derived from coil resistance to that indicated by a thermometer external to the coil under (1) essentially equilibrium (electrically powered) and (2) transient (electrically unpowered) thermal conditions. (For the initial 2.5 h of the test, ~98 Vdc was applied to the SOV to approximately balance its heat losses to the environment.)

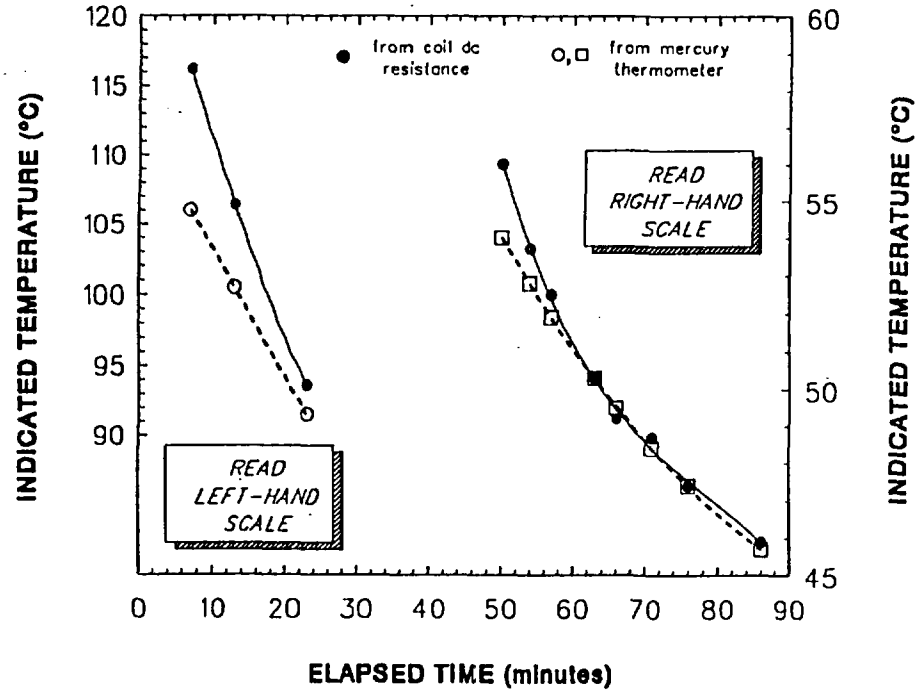

Figure F.2 Two more approach-to-isothermal-condition tests for SOV "B" placed in a thermally well insulated container. (For a prior period, the valve was brought to an elevated temperature by application of normal electrical power to the solenoid coil; electrical excitation was terminated at $t = 7$ min.)

large radial temperature gradient within the potted solenoid coil when the latter is electrically energized. The important implications of this finding to real plant measurements are that (1) coil-resistance-derived temperature inferences should provide more realistic figures for the prediction of coil life than would be obtained from a nonimbedded (i.e., surface-mounted) conventional temperature sensor, and (2) coil-resistance-derived temperatures may be too high (i.e., overly conservative) for estimating service life of temperature-sensitive SOV components other than the coil itself (e.g., valve seats, O-rings, gaskets and seals, etc.).

NUREG/CR-4819, Vol. 2
ORNL/TM-12038
Distribution Category RV

INTERNAL DISTRIBUTION

1. J. L. Anderson
2. S. J. Ball
3. R. E. Battle
4. D. A. Casada
5. N. E. Clapp, Jr.
6. R. L. Clark
7. D. F. Cox
8. B. G. Eads
9. E. C. Fox
10. D. N. Fry
11. A. C. Gehl
12. R. H. Greene
13. H. D. Haynes
14. R. A. Kisner
15. K. Korsah

16–32. R. C. Kryter

33. J. C. Moyers
34. G. A. Murphy
35. C. E. Pugh
36. C. W. Ricker
37. R. L. Shepard
38. A. Zucker
39. J. B. Ball, Advisor
40. B. Chexal, Advisor
41. T. B. Sheridan, Advisor
42. R. M. Taylor, Advisor

43–44. Central Research Library

45. Y-12 Technical Reference Section

46–47. Laboratory Records Department

48. Laboratory Records ORNL-RC
49. ORNL Patent Section
50. I&C Division Publications Office

EXTERNAL DISTRIBUTION

51. Assistant Manager for Energy Research and Development, U.S. Department of Energy, Oak Ridge Operations Office, Oak Ridge, TN 37831

52–53. Office of Scientific and Technical Information, P.O. Box 62, Oak Ridge, TN 37831

54. D. M. Eissenberg, Box 133, RD–1, Cambridge, NY 12816
55. G. Sliter, Electric Power Research Institute, P.O. Box 10412, Palo Alto, CA 94303
56. J. W. Tills, Institute for Nuclear Power Operations, 1100 Circle 75 Parkway, Atlanta, GA 30339-3064
57. M. Subudhi, Brookhaven National Laboratory, Bldg. 130, Upton, L.I., NY 11973
58. A. B. Johnson, Battelle–PNL, MS P8–10, P.O. Box 999, Richland, WA 99352
59. J. P. Vora, U.S. Nuclear Regulatory Commission, Office of Nuclear Regulatory Research, Electrical and Mechanical Engineering Branch, 5650 Nicholson Lane, Rockville, MD 20852
60. E. J. Brown, U.S. Nuclear Regulatory Commission, Office for Analysis and Evaluation of Operational Data, Reactor Operations Analysis Branch, MS 2104, Maryland National Bank Building, 7735 Old Georgetown Road, Bethesda, MD 20814
61. C. Michelson, Advisory Committee on Reactor Safeguards, 20 Argonne Plaza, Suite 365, Oak Ridge, TN 37830

62. M. Vagins, U.S. Nuclear Regulatory Commission, Office of Nuclear Regulatory Research, Chief, Electrical and Mechanical Engineering Branch, 5650 Nicholson Lane, Rockville, MD 20852
63. W. S. Farmer, U.S. Nuclear Regulatory Commission, Office of Nuclear Regulatory Research, Electrical and Mechanical Engineering Branch, 5650 Nicholson Lane, Rockville, MD 20852
64. M. J. Jacobus, Sandia National Laboratories, P.O. Box 5800, Division 6447, Albuquerque, NM 87185
65. H. L. Magleby, Idaho National Engineering Laboratory, MS 2406, P.O. Box 1625, Idaho Falls, ID 83415
66. Scott Newberry, U.S. Nuclear Regulatory Commission, NRR/SICB, MS 7E12, 1 White Flint North, 11555 Rockville Pike, Rockville, MD 20852
67. Jerry L. Mauck, U.S. Nuclear Regulatory Commission, NRR/SICB, MS 7E12, 1 White Flint North, 11555 Rockville Pike, Rockville, MD 20852
68. Matthew Chiramal, U.S. Nuclear Regulatory Commission, NRR/SICB, MS 7E12, 1 White Flint North, 11555 Rockville Pike, Rockville, MD 20852
69. Joseph P. Joyce, U.S. Nuclear Regulatory Commission, NRR/SICB, MS 7E12, 1 White Flint North, 11555 Rockville Pike, Rockville, MD 20852
70. A. C. Thadani, U.S. Nuclear Regulatory Commission, Office of Nuclear Reactor Regulation, Division of System Technology, MS8 E2, 1 White Flint North, 11555 Rockville Pike, Rockville, MD 20852
71. H. L. Ornstein, U.S. Nuclear Regulatory Commission, Office for Analysis and Evaluation of Operational Data, Reactor Operations Analysis Branch, MS 2104, Maryland National Bank Building, 7735 Old Georgetown Road, Bethesda, MD 20814
72. V. P. Bacanskas, Gilbert/Commonwealth, Inc., P. O. Box 1498, Reading, PA 19603-1498
73. John R. Shank, Automatic Switch Co., 50 Hanover Road, Florham Park, NJ 07932
74. Phil Holzman, Strategic Technology and Resources, 195 High St., Winchester, MA 01890
75. Jack Shortt, Stone and Webster Engineering Corporation, 245 Summer St., Boston, MA 02107

76–405. Given distribution as shown in NRC category RV (10–NTIS)

NRC FORM 335 (2 89) NRCM 1102 3201 3202

U.S. NUCLEAR REGULATORY COMMISSION

BIBLIOGRAPHIC DATA SHEET

(See instructions on the reverse)

1. REPORT NUMBER (Assigned by NRC, Add Vol., Supp., Rev., and Addendum Numbers, if any.)

NUREG/CR-4819
ORNL/TM-12038
Vol. 2

2. TITLE AND SUBTITLE

Aging and Service Wear of Solenoid-Operated Valves Used in Safety Systems of Nuclear Power Plants

Evaluation of Monitoring Methods

3. DATE REPORT PUBLISHED

MONTH	YEAR
July	1992

4. FIN OR GRANT NUMBER

B0828

5. AUTHOR(S)

R. C. Kryter

6. TYPE OF REPORT

Technical

7. PERIOD COVERED (Inclusive Dates)

8. PERFORMING ORGANIZATION – NAME AND ADDRESS (If NRC, provide Division, Office or Region, U.S. Nuclear Regulatory Commission, and mailing address; if contractor, provide name and mailing address.)

Oak Ridge National Laboratory
Oak Ridge, TN 37831

9. SPONSORING ORGANIZATION – NAME AND ADDRESS (If NRC, type "Same as above"; if contractor, provide NRC Division, Office or Region, U.S. Nuclear Regulatory Commission, and mailing address.)

Division of Engineering
Office of Nuclear Regulatory Research
U.S. Nuclear Regulatory Commission
Washington, DC 20555

10. SUPPLEMENTARY NOTES

11. ABSTRACT (200 words or less)

Solenoid-operated valves (SOVs) were studied at Oak Ridge National Laboratory as part of the USNRC Nuclear Plant Aging Research (NPAR) Program. The primary objective of the study was to identify, evaluate, and recommend methods for inspection, surveillance, monitoring, and maintenance of SOVs that can help ensure their operational readiness—that is, their ability to perform required safety functions under all anticipated operating conditions, since failure of one of these small and relatively inexpensive devices could have serious consequences under certain circumstances.

An earlier (Phase I) NPAR program study described SOV failure modes and causes and identified measurable parameters thought to be linked to the progression of ever-present degradation mechanisms that may ultimately result in functional failure of the valve. Using this earlier work as a guide, the present (Phase II) study focused on devising and then demonstrating the effectiveness of techniques and equipment with which to measure performance parameters that show promise for detecting the presence and trending the progress of such degradations before they reach a critical stage.

Intrusive techniques requiring the addition of magnetic or acoustic sensors or the application of special test signals were investigated briefly, but major emphasis was placed on the examination of condition-indicating techniques that can be applied with minimal cost and impact on plant operation. These include monitoring coil mean temperature remotely by means of coil dc resistance or ac impedance, determining valve plunger position by means of coil ac impedance, verifying unrestricted SOV plunger movement by measuring current and voltage at their critical bistable (pull-in and drop-out) values, and detecting the presence of shorted turns or insulation breakdown within the solenoid coil using interrupted-current test methods. The first of these techniques, though perhaps the simplest conceptually, will likely benefit the nuclear industry most because SOVs have a history of failure in service as a result of unwitting operation at excessive temperatures.

12. KEY WORDS/DESCRIPTORS (List words or phrases that will assist researchers in locating the report.)

Aging, degradation, diagnostics, maintenance practices, monitoring methods, nuclear power plants, operating experience, solenoid-operated valves, SOV, stressors, testing

13. AVAILABILITY STATEMENT

Unlimited

14. SECURITY CLASSIFICATION

(This Page) Unclassified

(This Report) Unclassified

15. NUMBER OF PAGES

16. PRICE

THIS DOCUMENT WAS PRINTED USING RECYCLED PAPER

UNITED STATES
NUCLEAR REGULATORY COMMISSION
WASHINGTON, D.C. 20555-0001

OFFICIAL BUSINESS
PENALTY FOR PRIVATE USE, $300

SPECIAL FOURTH-CLASS RATE
POSTAGE AND FEES PAID
USNRC
PERMIT NO. G-67